SAN JOSE STATE UNIVERSITY

DEPARTMENT OF CIVIL AND ENVIRONMENTAL ENGINEERING

THE EFFECTS OF HEAT OF HYDRATION OF MASS CONCRETE FOR CAST-IN-PLACE CONCRETE PILES

By

Dr. Akthem Al-Manaseer, Professor

Ms. Najah Elias, Graduate Researcher

Mr. Alfred Kaufman, External Consultant

Mr. Ric Maggenti, Technical Advisor (CALTRANS)

Mr. Peter Lee, Project Manager (CALTRANS)

Technical Report Documentation Page

1. Report No.	2. Government Accession No.	3. Recipient's Catalog No.

4. Title and Subtitle	5. Report Date
Determining Methods to Control the Effects of Heat of Hydration and Other Concerns Associated with the Placement of Mass Concrete for Cast-in-Place Concrete Piling	June 30, 2007
	6. Performing Organization Code

7. Author(s)	8. Performing Organization Report No.
Akthem Al-Manaseer, Najah Elias	SJSU ALM - 115

9. Performing Organization Name and Address	10. Work Unit No. (TRAIS)
Department of Civil and Environmental Engineering One Washington Square San José State University San José, California 95192-0083	11. Contract or Grant No. 59A0521

12. Sponsoring Agency Name and Address	13. Type of Report and Period Covered
California Department of Transportation Engineering Service Center 1801 30th St., West Building MS 9-2/5i Sacramento, California 95816	Final Report 6/21/2006 – 6/30/2007
	14. Sponsoring Agency Code

15. Supplementary Notes

Prepared in cooperation with the State of California Department of Transportation.

16. Abstract

This report describes models, ABAQUS and Schmidt, to predict the peak temperature in the center of cast-in-place concrete piling. Five concrete piles with varying diameters and made up of fourteen concrete mixes with different percentage of fly ash are used. The temperature profiles predicted using the finite element program, ABAQUS, are compared to the temperatures predicted by the step-by-step method, ACI 207 Schmidt model. The results show that the ABAQUS model correlates better to experimental results and yields better predictions of the temperature profiles than the Schmidt model. The latter is faster to run but overestimates the peak temperature. Using the results from the ABAQUS Model, a specification can be recommended that will result in acceptable concrete for large CIDH piles that in the range of 6 to 14 feet in diameter.

17. Key Words	18. Distribution Statement
Heat of hydration, mass concrete, cast-in-place, piling	Unlimited

19. Security Classification (of this report)	20. Security Classification (of this page)	21. No. of Pages	22. Price
Unclassified	Unclassified	121 pages	

Form DOT F 1700.7 (8-72) Reproduction of completed page authorized

ABSTRACT

This report describes models, ABAQUS and Schmidt, to predict the peak temperature in the center of cast-in-place concrete piling. Five concrete piles with varying diameters and made up of fourteen concrete mixes with different percentage of fly ash are used. The temperature profiles predicted using the finite element program, ABAQUS, are compared to the temperatures predicted by the step-by-step method, ACI 207 - Schmidt model. The results show that the ABAQUS model correlates better to experimental results and yields better predictions of the temperature profiles than the Schmidt model. The latter is faster to run but overestimates the peak temperature. Using the results from the ABAQUS Model, a specification can be recommended that will result in acceptable concrete for large CIDH piles that in the range of 6 to 14 feet in diameter.

TABLE OF CONTENTS

NOMENCLATURE

A. Organizations

ACI	American Concrete Institute
ASTM	American Society for testing and Materials
CTL	Construction Technology Laboratories

B. General Abbreviations and Symbols

ν	Poisson's ratio
$\varepsilon_{transverse}$	Transverse Strain
$\varepsilon_{longitudinal}$	Longitudinal Strain
E_c	Modulus of Elasticity
ω	Unit Mass
f'_c	Ultimate Strength of a Standard Concrete Cylinder
Δt	Time Interval for Schmidt Model
Δx	Length of Schmidt Model Element
h^2	Diffusion Constant
T	Concrete Specimen Temperature
H	Heat of Hydration
Q_H	Rate of Heat Generation
c_p	Specific Heat
ρ	Concrete Density

LIST OF FIGURES

LIST OF TABLES

CHAPTER 1 INTRODUCTION

1.1 Introduction

Temperature control of heat generated from the hydration process of cement in mass concrete is necessary to ensure that cement does not have any undesirable chemical process and also to prevent cracking caused by strains resulting from differential temperatures. One undesirable chemical process results in delayed ettringite formation (DEF), which causes a material related distress or deterioration of the concrete at a later date. DEF potentially occurs when internal concrete temperature exceeds a critical value (e.g. 70°C (158°F)) during the initial hydration period. The higher the initial temperature above the threshold is the higher the probability for DEF. There are also other undesirable chemical effects from the effect of high temperature.

Two models have been used in this study to describe the heat transfer in mass concrete: the finite element model using ABAQUS program and a computer spreadsheet using the ACI 207 Schmidt model. The numerical representation of such modeling is achieved by using basic material properties like conductivity, specific heat and mass density, and the adiabatic temperature curve or rate of heat generated function of time. These methods are chosen from different methods described in Appendix A.

1.2 Scope

This study utilizes the ACI 207 Schmidt model and the ABAQUS finite element model to predict temperature rise of CIDH (cast in drilled hole) concrete piles. The analysis was conducted on piles with different diameters varying from 6 to 14 feet. The actual concrete heat measurement is obtained from the QDRUM tests.

Different types of elements are utilized in the two different models. In the ABAQUS finite element model, a three-dimensional cylinder is used to model the heat transfer utilizing type DC3D10 element. In the Schmidt model, a one-dimensional strip element is utilized to model the heat transfer analysis.

The results are used to predict the temperature profile as function of time at the center of piles.

1.3 Objective

This study was conducted with special emphasis on studying the effect of different concrete mixes to predict the heat variation for different sizes of CIDH piles. The use of different concrete mixes provides different adiabatic temperature curves and thermal properties, which gives different heat variations in CIDH piles as a function of size and time. Results obtained from both models in conjunction with the QDRUM tests were used to develop thermal specifications for CIDH concrete piles.

1.4 Project Outline

This project is described in five chapters. Chapter one covers introduction, scope and objective of the study. Chapter two discuss two different models to analyze CIDH concrete piles and describes the details of the material used in the analytical models. Chapter three presents the results obtained from the two different models. Conclusions are discussed in Chapter four. Thermal specifications for CIDH piles are described in Chapter five.

CHAPTER 2 MODELING OF CIDH CONCRETE PILES

2.1 Introduction

In order to model the CIDH concrete piles, two methods were utilized in this study: The ACI 207 Schmidt model and the ABAQUS finite element model. The Schmidt model utilizes integration process to predict temperature profiles, while the ABAQUS uses a finite element model procedure to predict temperature profiles. Using both methods, peak temperature of piles having different concrete mix properties, boundary conditions and different diameters varying between 6 to 14 feet are predicted. Peak temperature was used for a specification proposal.

2.2 Material Properties

The thermal properties of concrete used in this study are the adiabatic temperature rise measured by the Q-Drum, the specific heat, the thermal conductivity, the thermal diffusivity, and the coefficient of thermal expansion. The mechanical property of the concrete used in this study is the unit mass.

2.2.1 Temperature Rise in Concrete Elements

The thermal behavior of the concrete pile is the focus of this study. The reaction of water with cement is exothermic, and heat is generated during the hydration process. The conductivity in concrete, specific heat, shape and size of the element, and external

environment creates a temperature gradient between the center and the external parts of the concrete element.

The reaction of water with cement generates heat over an extended period of time and the rate and magnitude of the temperature in the concrete during the hardening depends on:

- The concrete mix composition.
- The geometry and the initial placing temperature of the concrete.
- The ambient temperature and other boundary conditions.

A special test, called the Q-Drum, described in Appendix B, is conducted to develop curves for adiabatic temperature rise for different cement mixes and compositions. These curves are used in the Schmidt and ABAQUS models to predict the peak temperature rise in CIDH concrete pile.

2.2.1.1 Portland Cement Types

This study uses Type I/II Portland cement, Fly Ash and admixtures to determine the temperature profile of different concrete structures.

2.2.2 Specific Heat

The specific heat or heat capacity is defined as the amount of heat required to raise the temperature of a unit mass of material by one degree. Changing the aggregate type, mixture proportions, or age of concrete have little influence on the specific heat of ordinary concrete at normal temperature.[1] The specific heat is usually affected by

temperature changes, but it is assumed to be constant in mass concrete structures. The values of the specific heat in various types of concrete are about the same, and varies between 0.22 to 0.25 Btu/lb/°F.

2.2.3 Thermal Conductivity

The thermal conductivity is defined as the rate at which heat is transmitted. It is also defined as the ratio of the heat flux to the temperature gradient. The water content, aggregate type, density, and temperature in the concrete mix influences the thermal conductivity. Typical values of thermal conductivity depends on the type of aggregates used in the concrete mix and are shown below:

- Btu/hr/ft/°F for concrete with quartzite aggregates.
- 1.7 Btu/hr/ft/°F for concrete with limestone aggregates.
- 1.2 Btu/hr/ft/°F for concrete with basalt aggregates.

2.2.4 Concrete Density

Concrete density is the unit mass of concrete per unit of space. The unit mass of concrete depends on the mix proportions, and its value varies from 145 to 160 lb/ft^3.

2.2.5 Thermal Diffusivity

The thermal diffusivity refers to the rate of temperature change in concrete. A high thermal diffusivity indicates that temperature change takes longer to occur. It is equal to the thermal conductivity divided by the product of specific heat and density. [2]

The thermal diffusivity for mass concrete is not affected substantially by temperature or age but by the aggregate type and concrete density. [3]

Typical values of thermal diffusivity for various concretes are shown below:

- 0.06 ft^2/hr for quartzite concrete.
- 0.05 ft^2/hr for limestone concrete.
- 0.03 ft^2/hr for basalt concrete.

2.2.6 Thermal Coefficient of Expansion

Concrete expands with increasing temperature and contracts with decreasing temperatures. The coefficient of thermal expansion is defined as the change in linear dimension per unit length divided by the temperature change, expressed in millionths per degree Fahrenheit. The thermal coefficient of expansion of concrete depends on the type and amount of coarse aggregate in the mass concrete. Typical values of coefficient of thermal expansion are shown below:

- Up to 8 millionths/°F for quartzite concrete.
- 3 to 5 millionths/°F for limestone and basalt concrete.

Since this study focused on peak temperature to control cracking, thermal coefficient was not important to this study.

2.2.7 Concrete Placing Temperature

The concrete placing temperature is another factor in determining the maximum temperature of a concrete mix. The initial placing temperature in this study is assumed to

be equal to 73°F for the CIDH concrete piles. A higher initial temperature results in a higher maximum temperature in the concrete due to the rate of heat of hydration. [4]

Figure 2-1 from ACI 207 shows the adiabatic temperature rise as function of age with varying placing temperature. In general, the adiabatic temperature rise increases significantly as placing temperature increases at early age.[5]

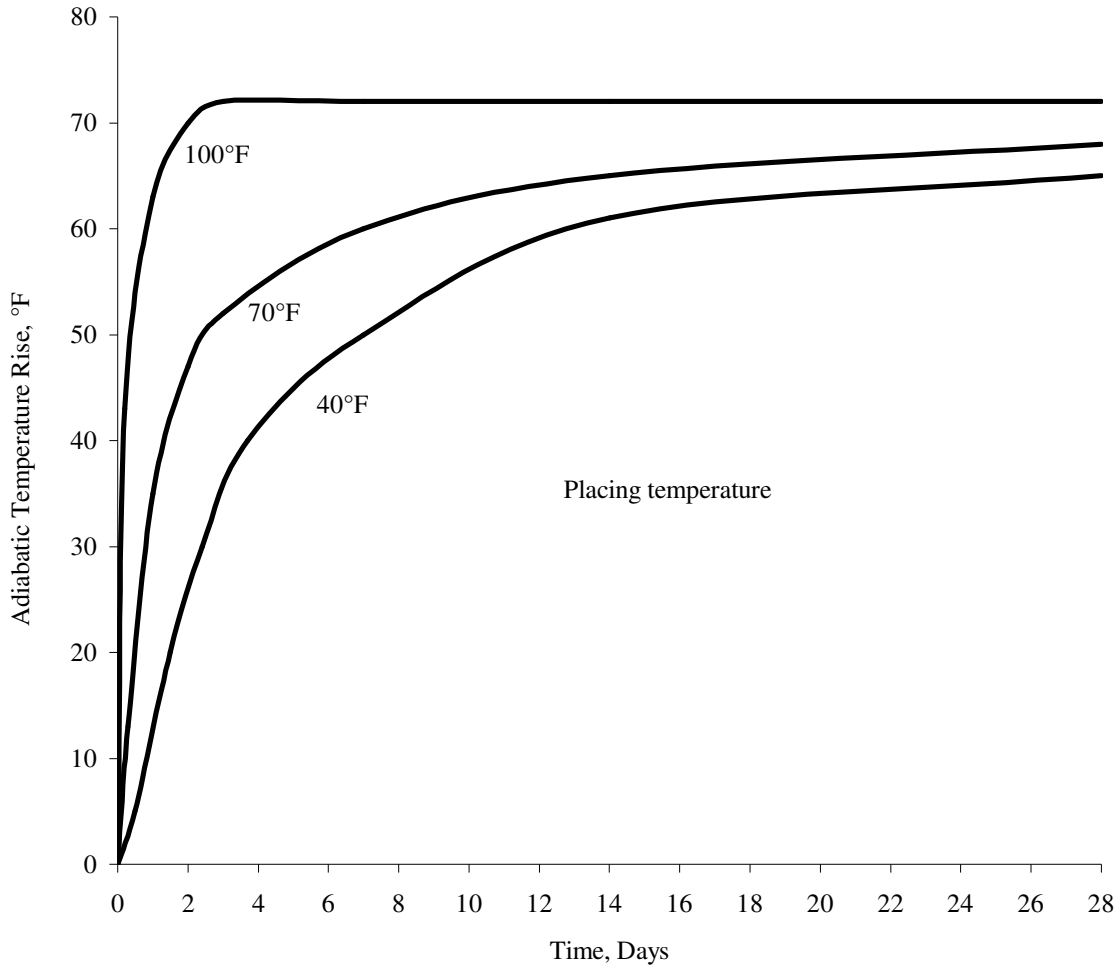

Figure 2-1 - Effect of placing temperatures of mass concrete (Type I cement 376 lb/yd^3)

2.3 Schmidt Model

2.3.1 Method Procedure

ACI 207.1R mentions that the "Schmidt's method is based on the theorem that if the body under question is considered to be divided into a number of equal elements, and if number of physical limitations are satisfied simultaneously, the temperature for a given increment at the end of an interval of time is the average of the temperature of the two neighboring elements at the beginning of that time interval." [6]

The physical relationship is:

$$\Delta t = \frac{(\Delta x)^2}{2h^2} \qquad \text{(Eq. 2.1)}$$

Where:

Δt = the time interval

Δx = the length of the element

h^2 = the diffusion constant

The computation for the temperature of any space interval at a succeeding time interval proceeds by averaging the two adjacent temperatures in the preceding time interval.[6]

2.3.2 Model Geometry and Size

The mass concrete pile is represented by one-dimensional strip, which is formed by successive one-foot long elements. The convergence to the solution occurs at a faster

rate if small pile diameters are used. For this project, five different strip representations are used:

- 6 elements for the 6-ft pile diameter.
- 8 elements for the 8-ft pile diameter.
- 10 elements for the 10-ft pile diameter.
- 12 elements for the 12-ft pile diameter.
- 14 elements for the 14-foot pile diameter.

2.3.3 Material Properties

The material properties required for the Schmidt model are the following:

- Unit mass.
- Diffusion constant.
- Adiabatic temperature rise.

2.3.4 Boundary Conditions

When concrete is placed in the field, heat is transferred to and from its surroundings. Therefore, the temperature development in the concrete structure is determined by the balance between heat generation in the concrete and heat exchange with the environment. For the Schmidt model, the rise of the surrounding temperature is equal to zero at time of placement, and its temperature starts to rise as time increases.

2.4 ABAQUS Model

2.4.1 Overview

ABAQUS is an advanced Finite Element Analysis that provides solutions for routine and sophisticated linear and nonlinear engineering problems.

A wide range of industries uses ABAQUS including aircraft manufacturers, and automobile companies, as well as national laboratories and research universities.

The ABAQUS suite consists of three products: ABAQUS/Standard, ABAQUS/Explicit and ABAQUS/CAE.[7]

2.4.2 Method Procedure

In this project, ABAQUS/CAE and ABAQUS/Standard are used. ABAQUS/CAE is divided into modules, where each module defines a logical aspect of the modeling process including the geometry, the material properties, and the mesh creation. ABAQUS/CAE generates a file containing the model. This file is then used as an input to ABAQUS/Standard, which performs the analysis, sends information back to ABAQUS/CAE to allow the monitoring of the job progress and generates an output database. Finally, using the Visualization module of ABAQUS/CAE (also known as ABAQUS/Viewer), the output database is read, and the results of the analysis are viewed.

2.4.3 Model Geometry and Size

In this study, 10-foot long cylindrical piles of diameter sizes ranging from 6 to 14 feet are analyzed. These piles are modeled using three-dimensional elements. The

element type used for modeling the piles are named depending on the element dimensionality and type of analysis, as shown in Figure 2-2.[8]

For this study, the element used is DC3D10, which is represented from the first three columns of Figure 2-2.

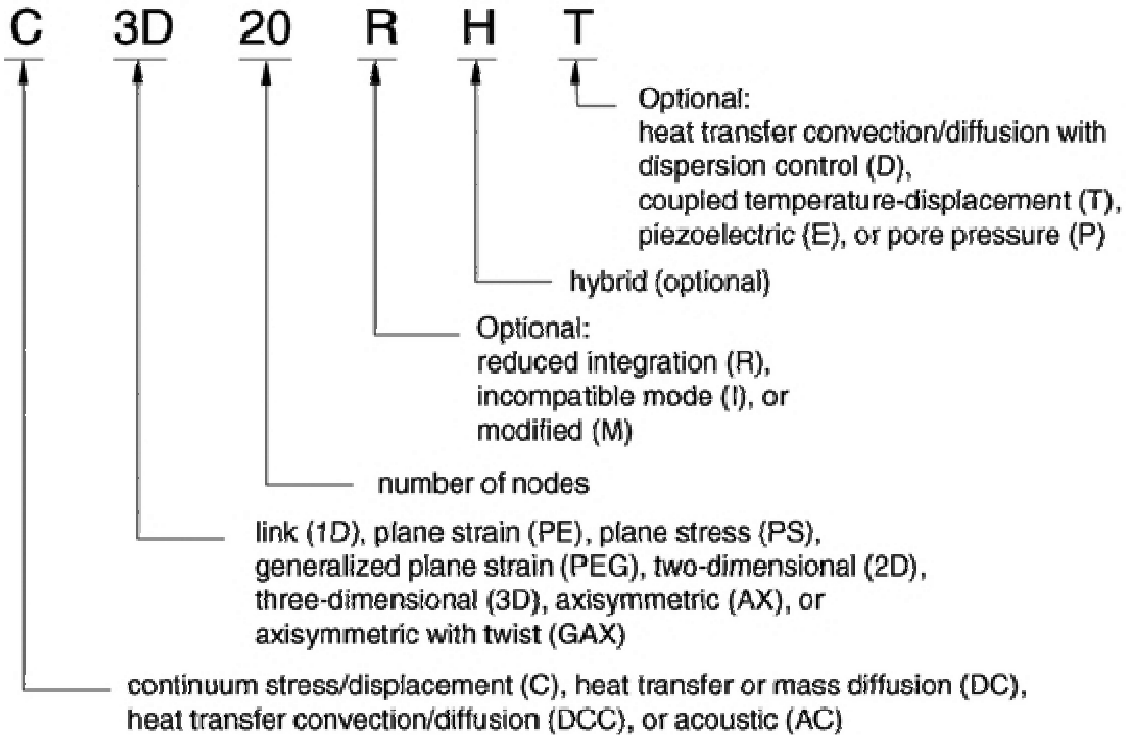

Figure 2-2 - Naming conventions for solid elements[8]

DC3D10 element is a 10-node solid quadratic heat transfer tetrahedron element. The node ordering, faces and integration points numbering of this element are shown in Figure 2-3 and Figure 2-4.[8]

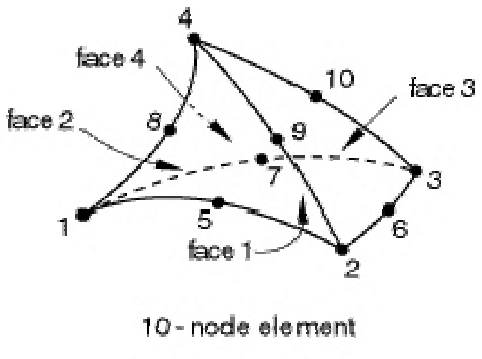

Figure 2-3 - Node ordering and face numbering on elements

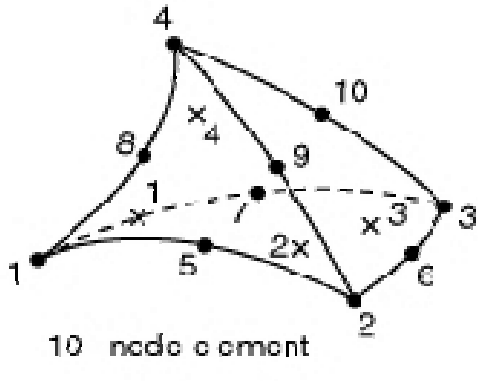

Figure 2-4 - Numbering of integration points for output

For this study, five different geometric models are developed to predict the temperature profiles in the five different CIDH concrete piles. For each model, the number of elements and nodes varies depending on the meshes and the diameter size of the different piles. Figure 2-5 shows an example of a meshing view for a 10-foot long pile. Table 2-1 shows the number of nodes and elements used in the model of each pile.

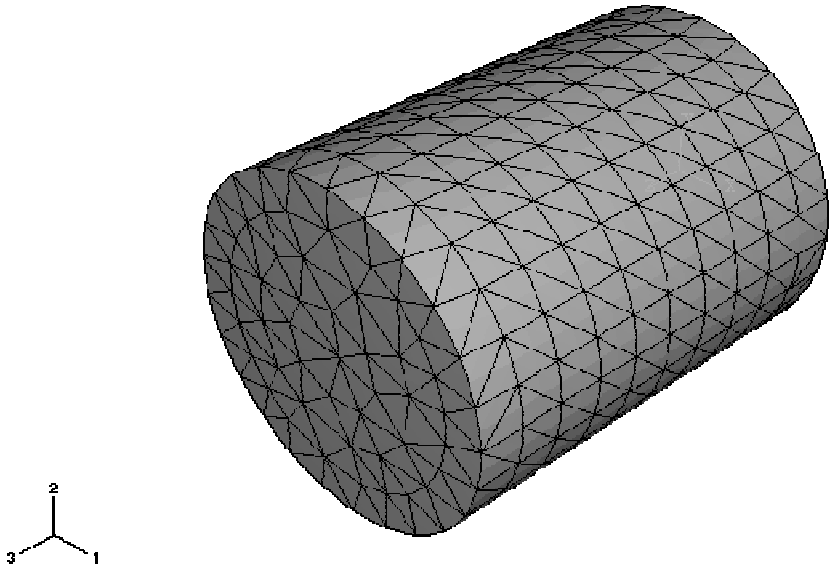

Figure 2-5 - Meshing View of 10-ft long pile – ABAQUS

Table 2-1 - Number of nodes and elements in the different models

Pile Diameter (ft)	Number of Nodes	Number of Elements
6	4190	2659
8	5164	3293
10	7632	4983
12	11494	7655
14	15024	10090

2.4.4 Material Properties

The material properties used by the ABAQUS model are the following:

- Unit mass.
- Conductivity constant.
- Coefficient of thermal expansion.
- Specific heat.
- Concrete placement temperature.
- Adiabatic temperature rise.

Since the adiabatic temperature rise cannot be input in ABAQUS, it was necessary to have the values changed to body heat flux. The adiabatic temperature rise, obtained from a Q-Drum test, is changed to body heat flux. The procedure is described next in this chapter with an example in Appendix C.

2.4.5 Adiabatic Temperature Rise as Body Heat Flux

In this study, the adiabatic temperature is changed to a load represented by a body heat flux as described next.

The heat generation and the temperature development in a concrete specimen, cured under adiabatic conditions where there is no heat transfer to the environment, can be determined from the following equation: [9]

$$\frac{dT}{dt} = \frac{Q_H}{\rho.c_p} = \frac{dH}{dt}\left(\frac{1}{\rho.c_p}\right) \qquad \text{(Eq. 2.2)}$$

Where,

T is the temperature of the concrete (°F).

ρ is the concrete density (lb/ft^3).

c_p is the specific heat of the concrete (Btu/lb/°F).

Q_H is the rate of heat generation (Btu/hr/ft^3).

H is the heat of hydration of the concrete (Btu/ft^3).

From the above equation, the body heat flux $\frac{dH}{dt}$ can be calculated as:

$$\frac{dH}{dt} = \frac{dT}{dt} (\rho.c_p) \qquad \text{(Eq. 2.3)}$$

Using the $\frac{dH}{dt}$ equation shown above, the body heat flux is calculated then utilized as an input in a tabular form for ABAQUS.

In summary, the steps involved in calculating the body heat flux are the following:

1. Read the adiabatic temperature rise function of time from the Q-Drum test.
2. Calculate the adiabatic temperature rise between two successive periods of time. (dT)
3. Calculate the heat of hydration from the previous equation. (dH)
4. Calculate the time difference between two periods. (dt)

5. Calculate the body flux by dividing the heat of hydration by the time difference between the two periods of time $\frac{dH}{dt}$.

6. Input the body heat flux as load in the ABAQUS program to analyze the heat transfer in the model.

2.4.6 Boundary Conditions

The temperature development in the concrete pile is determined by the balance between heat generation in the concrete and heat exchange with the environment. For the ABAQUS model, the boundary conditions are the temperature of the surrounding where the pile is inserted. In this study, this temperature for CIDH concrete piles is assumed to be constant and equal to 55 °F.

CHAPTER 3 RESULTS AND DISCUSSION

3.1 Introduction

In this chapter, the Schmidt and the finite element models are utilized to predict the peak temperatures reached by different mass concrete piles using different diameters, and concrete mix composition. Temperatures versus time curves, obtained from the finite element analysis using ABAQUS, are compared to the Schmidt model.

A comparative study between experimental values and analytical prediction of a one-meter cube was also performed to calibrate the model.

3.2 One-Meter Cube Analysis

In order to test the accuracy of the models, experimental data from a one-meter concrete cube was compared to values predicted from the Schmidt and finite element model. The experimental data on the cube is obtained from a previous test conducted by CALTRANS.[10]

The concrete properties of the one-meter cube and environmental conditions were given to the researchers without the actual field measurements. The researchers were asked to use the given information and generate a temperature curve for this concrete sample under the conditions given. This temperature curve was then later compared to the actual field measurements to check the accuracy of the model.

3.2.1 Schmidt Model

The one-cubic-meter sample consists of several one–dimensional vertical strip model. The strip is divided into 0.1-meter (0.33 ft) long elements as shown in Figure 3-1.

Bottom element	0.1 m	0.1 m	0.1 m	0.1 m	0.1 m	0.1 m	0.1 m	0.1 m	Top element

Figure 3-1 – One-Dimensional strip utilized in the Schmidt model for one-meter cube

3.2.2 Material Properties for One-Meter Cube using Schmidt

Three material properties are used in the Schmidt model: The adiabatic temperature rise, the density, and the diffusion constant. The adiabatic temperature rise versus time for the center of the one-cubic meter sample is obtained from experimental data from reference 10 and shown in Figure 3-2. The unit mass and diffusion coefficient constants are assumed as follows:

- Unit mass: $\rho = 2240$ Kg/m^3 (140 pcf).
- Diffusion coefficient: $h^2 = 0.1$ m^2/day (1ft^2/day).

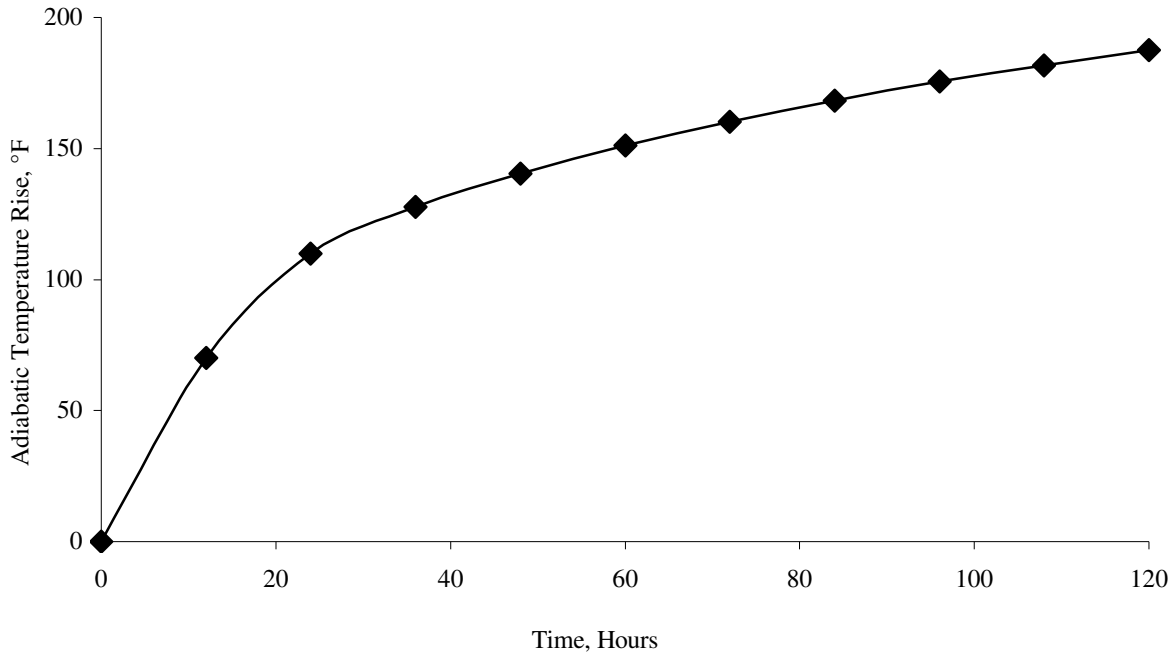

Figure 3-2 - Adiabatic Temperature Rise at center of one-meter cube concrete mix

3.2.3 Temperature Boundary Conditions for One-Meter Cube using Schmidt

The temperature boundary conditions for the one-meter cube are as follows:

- For the bottom side of the cube, the temperature rise on the outside element is half of the difference between the temperature rise at the time of placement of concrete and the surrounding temperature rise that is equal to zero at time of placement.
- For the top and sides of the cube, the temperature rise at the outside element is equal to zero at time of placement, and there is no surrounding temperature rise since the cube is in contact with air.

3.2.4 Results for One-Meter Cube using Schmidt Model

The temperature rise for the center of the one-meter cube is calculated using the Schmidt model for a period of 120 hours. Temperature rise versus time in hours are shown in Figure 3-3. It can be observed from the figure that the temperature of the sample increases rapidly by 90°F during the first 20 hours then it increased by a slower rate over the next 80 hours by an additional 76°F. Very little rise is observed after 100 hours. The total temperature rise in the concrete cube was 170°F at 120 hours.

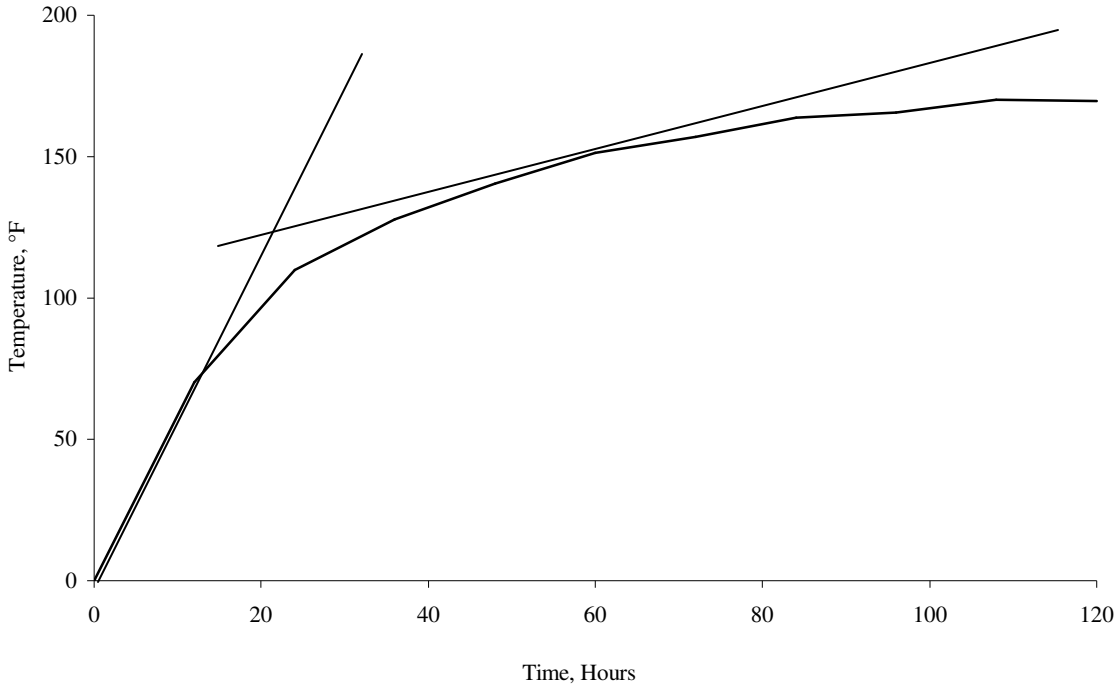

Figure 3-3 - Temperature rise at the center of the one-meter cube using the Schmidt model

3.2.5 ABAQUS Model

In the ABAQUS model, the one-meter cube was assumed to have an initial placing temperature of 18°C (64.4°F). The DC3D10 element was utilized, and the model has 7769 elements and 11751 nodes. The mesh is shown in Figure 3-4.

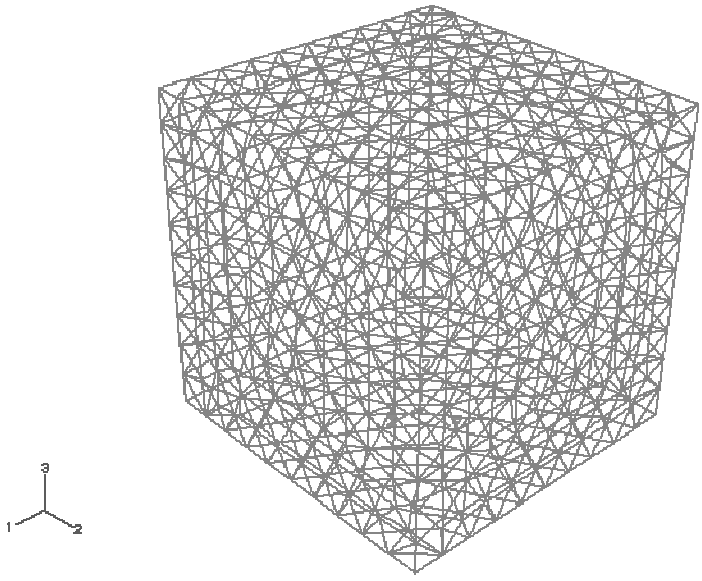

Figure 3-4 – One-Meter Cube mesh using ABAQUS

3.2.6 Material Properties for One-Meter Cube using ABAQUS

The following material properties are assumed in the analysis of the one-meter cube:

- Unit mass: 2240 Kg/m^3 (140 pcf).
- Thermal conductivity constant: 2.5 W/m/°C (1.4 Btu/ft/hr/°F).
- Coefficient of thermal expansion: 1 x 10^{-5}/°C (5.6 x 10^{-6}/°F).

- Specific heat: 922 J/Kg/°C (0.22 Btu/lb/^{o}F).

The adiabatic temperature rise as function of time is measured by the experimental test, and converted to a heat body flux for the ABAQUS finite element program as shown in Figure 3-5.

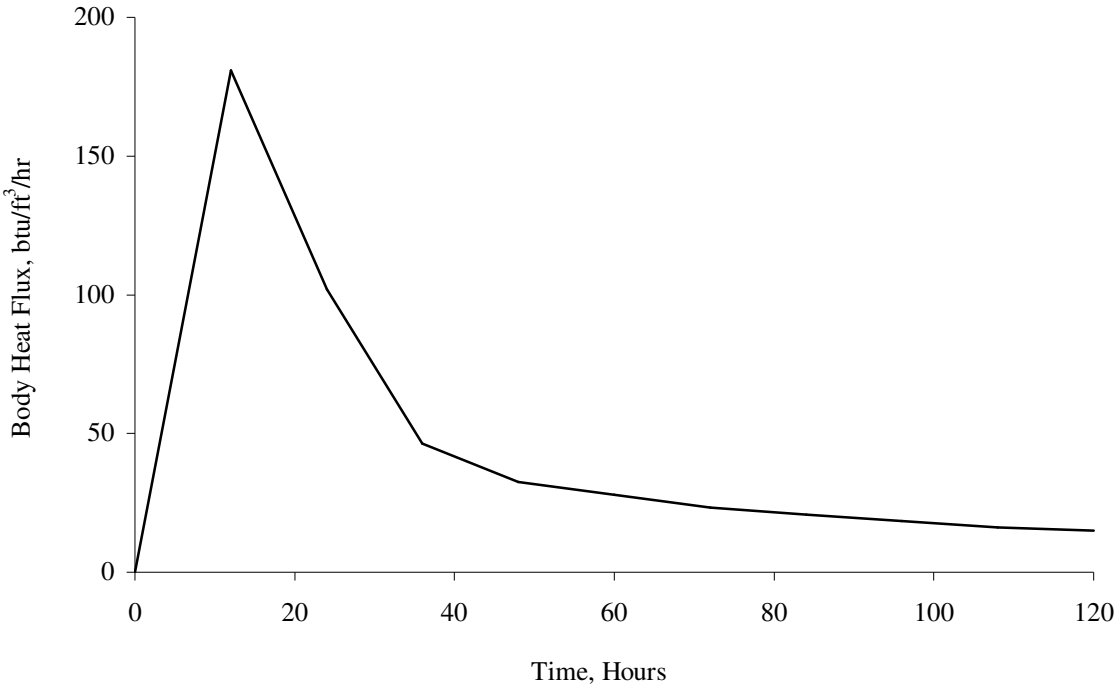

Figure 3-5 - Body Heat Flux for one-meter cube concrete mix

3.2.7 Temperature Boundary Conditions for the One-Meter Cube using ABAQUS

The temperature boundary conditions for the cube sample are as follows:

The outside temperature surrounding the bottom side of the cube was assumed to equal to 16°C (60.8 ^{o}F) at time of placement.

The ambient temperature surrounding the remaining sides of the cube varies from 7°C (44.6 ^{o}F) to 20°C (68 ^{o}F) depending on the time of the day, as shown in Figure 3-6.

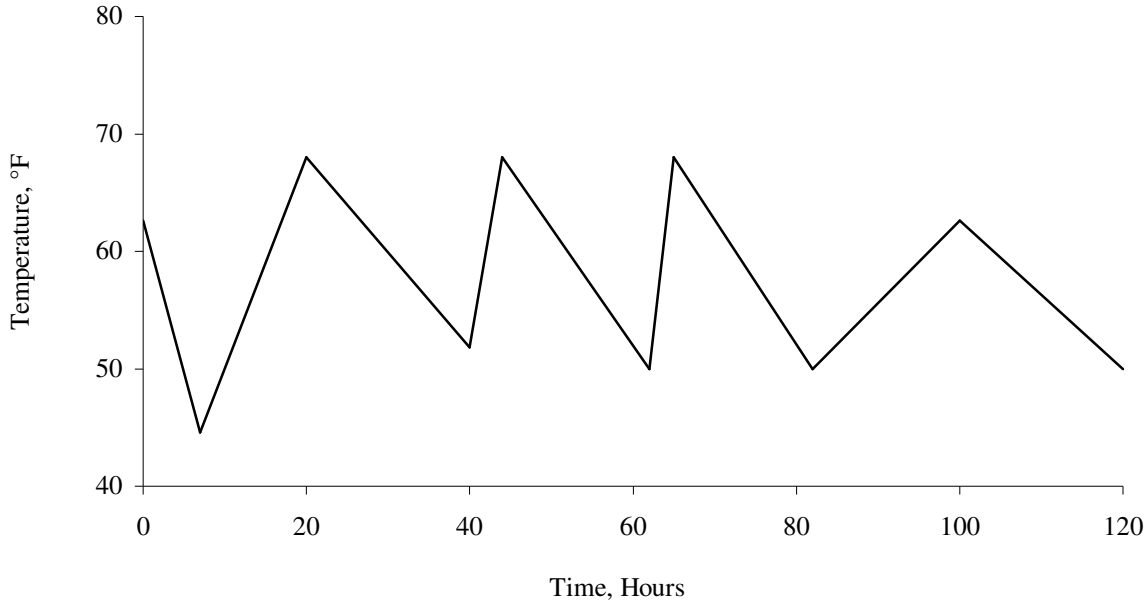

Figure 3-6 - Ambient Temperature for one-meter cube

3.2.8 Results for the One-Meter Cube using ABAQUS

The predicted temperature rise at the center element of the one-meter cube obtained from the ABAQUS model is shown in Figure 3-7. It can be observed from the figure that the peak temperature rise of the cube is reached at a maximum temperature of 45^{o}F within 24 hours, after which the temperature started to decrease to reach a stable value within 90 hours. It can also be observed that after the cube reaches its stable

condition, the temperature at the center still exhibited small decrease driven by the variations of the ambient temperature during the day.

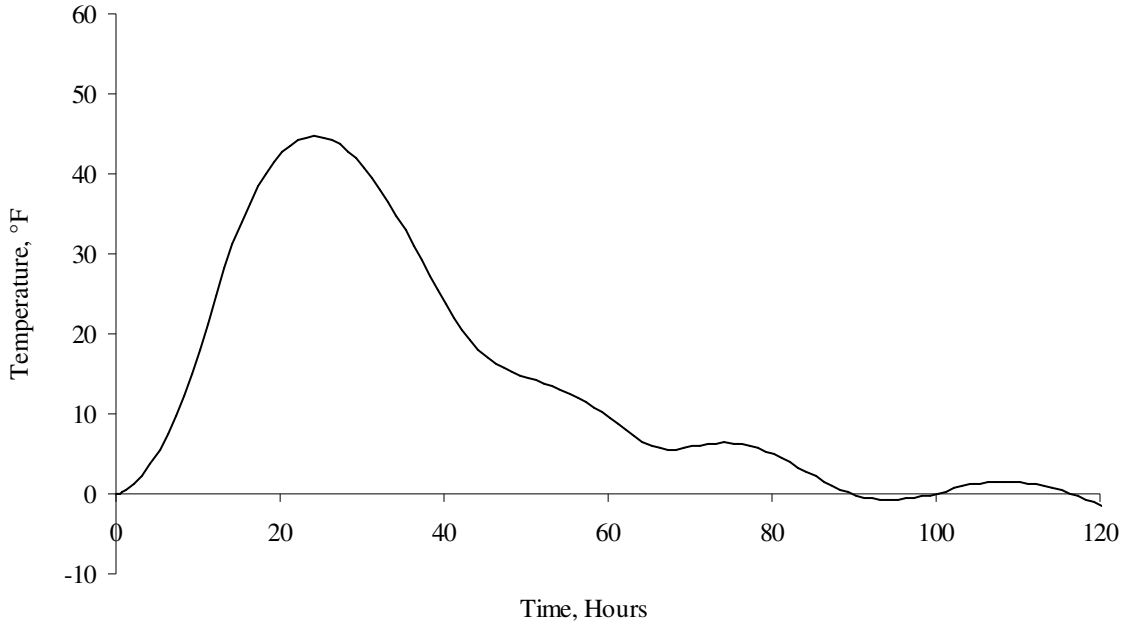

Figure 3-7 - Temperature rise at center of the concrete one-meter cube predicted by ABAQUS Model

3.2.9 Comparison between the ABAQUS and Schmidt Experimental Model

The experimental results for temperature profile at the center of the one-meter cube are compared with Schmidt and ABAQUS predictions in Figure 3-8.

It can be observed from the figure that the prediction of the ABAQUS model correlate very well to the experimental data but not the Schmidt model. Since the Schmidt model is a one-dimensional approach and is based on the principle of

superposition, its prediction overestimates the temperature rise for smaller concrete structures.

In summary, the Schmidt model is not accurate in predicting the temperature profile inside concrete cube, while the ABAQUS program predicted very well the temperature profile of the concrete cube.

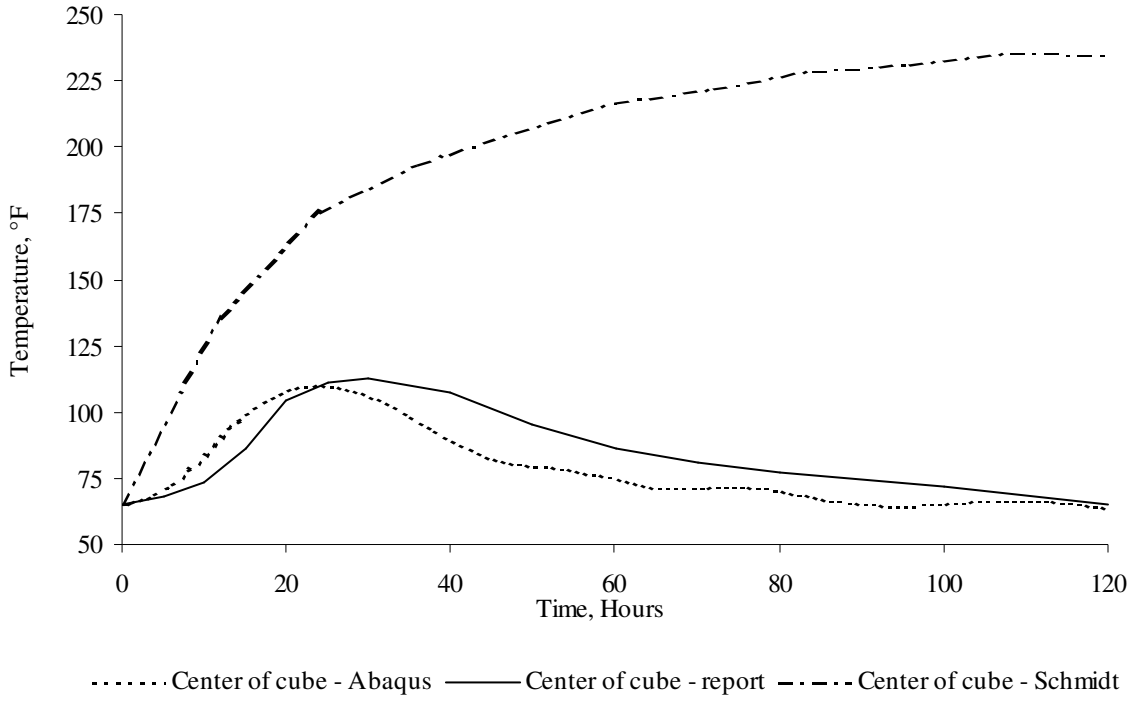

Figure 3-8 - Final Temperature at Center of One meter Cube Sample

3.3 CIDH Concrete Piles Analysis

Using the Schmidt and ABAQUS finite element model, the temperature profile for five concrete piles with diameters of 6, 8, 10, 12 and 14 ft are analyzed. For each pile diameter a study was conducted utilizing adiabatic temperature curves from experimental tests of 14 different concrete mixes. All piles were analyzed for a period of 14 days and the corresponding temperature profile for each sample is then predicted.

The mixes were divided to four series according to the quantity of the total cementitious material and they are as follows:

- Series 1: total cementitious material = 675 lb/cy.
- Series 2: total cementitious material = 591 lb/cy.
- Series 3: total cementitious material = 506 lb/cy.
- Series 4: total cementitious material = 591 lb/cy.

Series 4 differ from series 2 by the use of a retarder.

The mix proportions for the different mixes are given in Table 3-1 to Table 3-4.

Table 3-1 – Mix proportions for Series 1

Number / Lab ID	6070AA / 620	6070AB / 621	6070AC / 626	6070AD / 627
Total Cementitious, (lb/cy)	676	676	671	670
Fly Ash, (%)	15	25	35	50
Water / cementitious ratio	0.44	0.43	0.44	0.34
Cement, (lb/cy)	574	507	436	335
Cement, (Sacks)	6.1	5.4	4.6	3.6
Fly Ash, (lb/cy)	102	169	235	335
Coarse aggregate, (lb/cy)	1751	1750	1738	1736
Fine aggregate, (lb/cy)	1293	1294	1291	1394
WRDA*, (oz/cy)	27.0	27.0	26.8	51.0
Water, (lb/cy)	300.24	291.88	296.90	231.00
Air, (%)	1.4	1.5	1.2	2.3
Slump (in.)	4.00	4.00	4.00	4.75
Unit mass, (lb/ft^3)	149.1	149.1	148.9	149.7
Specific Heat, (Btu/lb/°F)	0.260	0.260	0.259	0.253

* WRDA: water reduction admixture

- Grace product WRDA 64 used for mixes 6070AA, 6070AB and 6070AC
- Adva 100 for mix 6070AD

Table 3-2 – Mix proportions for Series 2

Number / Lab ID	6070AE / 671	6070AF /672	6070AG / 664	6070AH / 665
Total Cementitious, (lb/cy)	581	580	592	590
Fly Ash, (%)	15	25	35	50
Water / cementitious ratio	0.53	0.54	0.46	0.40
Cement, (lb/cy)	493	435	385	295
Cement, (Sacks)	5.2	4.6	4.1	3.1
Fly Ash, (lb/cy)	88	145	207	295
Coarse aggregate, (lb/cy)	1723	1718	1750	1751
Fine aggregate, (lb/cy)	1369	1371	1402	1489
WRDA*, (oz/cy)	23.6	23.6	27	48
Water, (lb/cy)	310.2	310.69	275.00	233.07
Air, (%)	1.6	1.3	1.5	1.5
Slump (in.)	3.5	3.75	4	4
Unit mass, (lb/ft^3)	148.0	149.6	149.5	148.1
Specific Heat, (Btu/lb/°F)	0.260	0.260	0.257	0.251

* WRDA: water reduction admixture

- Grace product WRDA 64 used for mixes 6070AE, 6070AF and 6070AG
- Adva 100 for mix 6070AH

Table 3-3 – Mix proportions for Series 3

Number / Lab ID	6070AI / 641	6070AJ / 642	6070AK / 656	6070AL / 657
Total Cementitious, (lb/cy)	499	497	502	502
Fly Ash, (%)	15	25	35	50
Water / cementitious ratio	0.62	0.61	0.56	0.46
Cement, (lb/cy)	424	373	326	251
Cement, (Sacks)	4.5	4.0	3.5	2.7
Fly Ash, (lb/cy)	75	124	176	251
Coarse aggregate, (lb/cy)	1729	1724	1741	1733
Fine aggregate, (lb/cy)	1449	1452	1475	1559
WRDA*, (oz/cy)	20.0	19.7	19.8	44
Water, (lb/cy)	308.80	305.42	282.00	230.81
Air, (%)	1.4	1.4	1.5	2.4
Slump (in.)	4	4	4	4
Unit mass, (lb/ft^3)	148.1	147.7	148.1	148.5
Specific Heat, (Btu/lb/°F)	0.259	0.259	0.256	0.248

* WRDA: water reduction admixture

- Grace product WRDA 64 used for mixes 6070AI, 6070AJ and 6070AK
- Adva 100 for mix 6070AL

Table 3-4 – Mix proportions for Series 4

Number / Lab ID	6070AM / 683	6070AN / 684
Total Cementitious, (lb/cy)	583	581
Fly Ash, (%)	25	25
Water / cementitious ratio	0.52	0.48
Cement, (lb/cy)	437	436
Cement, (Sacks)	4.6	4.6
Fly Ash, (lb/cy)	146	145
Coarse aggregate, (lb/cy)	1726	1724
Fine aggregate, (lb/cy)	1377	1375
Retarder, (oz/cy)	25(ret*)	50(ret2*)
Water, (lb/cy)	302.96	298.00
Air, (%)	1.4	1.8
Slump (in.)	4	4
Unit mass, (lb/ft^3)	150.0	149.6
Specific Heat, (Btu/lb/°F)	0.261	0.263

*ret and ret2: Type D retarder, which known as recover and it is utilized in the concrete mixture to slow the hydration process.

3.3.1 Schmidt Model for CIDH Piles

To model the CIDH pile using the Schmidt model, a one-dimensional strip in the direction of the heat dissipation is modeled. The model is divided into 1-foot long elements throughout the pile diameter. The number of elements for each pile equal to the pile diameter. For example, Figure 3-9 shows a strip of 10 is utilized to model the 10 ft CIDH pile.

Bottom element	1ft	1ft	1ft	1ft	1ft	1ft	1ft	1ft	Top element

Figure 3-9 – One Dimensional Strip for Schmidt Model – 10 ft pile diameter

3.3.2 Material Properties for CIDH Pile using Schmidt

The material properties of concrete mix proportions for each series utilized for Schmidt model are shown in Tables 3-1 to 3-4. The adiabatic temperature rise obtained from the Q-Drum test for each mix is shown in Tables 3-5 to 3-8. The time interval of the actual experience was 4 hours. The time interval used in the Schmidt model was 0.5 days.

3.3.3 Temperature Boundary Conditions for CIDH Pile using Schmidt

The temperature boundary conditions for the piles modeled using the Schmidt are the temperature of the outside element in both sides and it is equal to the half of the first

difference in temperature rise at time of placement and the outside temperature rise is assumed zero at day of placement.

Table 3-5 - Adiabatic Temperature Rise from the QDRUM Test for Series 1

	Adiabatic Temperature Rise for series 1, °F			
Time, days	**Mix 6070AA (15% Fly Ash)**	**Mix 6070AB (25% Fly Ash)**	**Mix 6070AC (35% Fly Ash)**	**Mix 6070AD (50% Fly Ash)**
0	0	0	0	0
0.5	21.0	22.4	18.4	9.2
1	46.3	41.6	37.4	27.2
1.5	54.5	48.2	43.8	33.8
2	60.5	53.7	48.7	37.5
2.5	65.0	57.8	52.5	40.5
3	68.5	61.0	55.5	42.8
3.5	71.3	63.5	58.0	44.7
4	73.7	65.5	60.1	46.2
4.5	75.7	67.2	62.0	47.4
5	77.6	68.7	63.6	48.4
5.5	79.2	69.9	64.9	49.3
6	80.7	71.1	66.1	50.1
6.5	82.0	72.1	67.1	50.7
7	83.3	73.0	68.0	51.2
7.5	84.4	73.8	68.8	51.7
8	85.4	74.6	69.5	52.1
8.5	86.3	75.3	70.2	52.4
9	87.2	76.0	70.7	52.7
9.5	88.0	76.6	71.2	53.0
10	88.7	77.2	71.7	53.2
10.5	89.3	77.8	72.1	53.4
11	89.9	78.3	72.4	53.6
11.5	90.5	78.8	72.8	53.7
12	91.0	79.3	73.1	53.9
12.5	91.5	79.7	73.3	54.0
13	91.9	80.2	73.6	54.1
13.5	92.3	80.6	73.8	54.2
14	92.7	80.9	74.0	54.3

Table 3-6 - Adiabatic Temperature Rise from the QDRUM Test for Series 2

	Adiabatic Temperature Rise for series 2, °F			
Time, days	**Mix 6070AE (15% Fly Ash)**	**Mix 6070AF (25% Fly Ash)**	**Mix 6070AG (35% Fly Ash)**	**Mix 6070AH (50% Fly Ash)**
0	0	0	0	0
0.5	22.7	19.7	13.6	8.5
1	41.3	35.5	31.0	24.8
1.5	48.0	41.1	36.3	30.3
2	53.3	45.5	40.9	33.8
2.5	57.4	48.8	44.1	36.6
3	60.6	51.4	46.2	38.8
3.5	63.2	53.4	47.8	40.7
4	65.4	55.0	49.1	42.3
4.5	67.2	56.3	50.3	43.6
5	68.8	57.4	51.4	44.8
5.5	70.1	58.2	52.3	45.8
6	71.3	59.0	53.2	46.8
6.5	72.3	59.7	54.0	47.6
7	73.3	60.3	54.8	48.3
7.5	74.2	60.8	55.5	49.0
8	75.0	61.3	56.1	49.7
8.5	75.7	61.8	56.8	50.3
9	76.5	62.2	57.3	51.0
9.5	77.2	62.5	57.8	51.7
10	77.8	62.9	58.3	52.4
10.5	78.4	63.2	58.8	53.2
11	79.0	63.5	59.2	53.9
11.5	79.6	63.8	59.6	54.6
12	80.2	64.1	60.0	55.3
12.5	80.7	64.3	60.4	56.0
13	81.2	64.6	60.7	56.7
13.5	81.7	64.8	61.0	57.3
14	82.2	65.0	61.3	57.9

Table 3-7 - Adiabatic Temperature Rise from the QDRUM Test for Series 3

	Adiabatic Temperature Rise for series 3, °F			
Time, days	**Mix 6070AI (15% Fly Ash)**	**Mix 6070AJ (25% Fly Ash)**	**Mix 6070AK (35% Fly Ash)**	**Mix 6070AL (50% Fly Ash)**
0	0	0	0	0
0.5	19.2	16.7	10.6	10.2
1	33.9	30.2	26.8	23.3
1.5	39.3	34.7	31.7	28.7
2	43.5	38.5	35.2	31.6
2.5	46.9	41.3	38.0	33.8
3	49.7	43.3	39.8	35.9
3.5	51.8	44.8	41.5	37.7
4	53.5	46.1	42.8	39.4
4.5	54.9	47.1	43.9	40.8
5	56.2	48.1	44.8	42.0
5.5	57.3	48.9	45.6	43.0
6	58.2	49.6	46.3	43.9
6.5	59.1	50.3	47.0	44.6
7	59.9	50.9	47.7	45.3
7.5	60.6	51.5	48.3	45.8
8	61.4	52.0	48.8	46.3
8.5	62.0	52.5	49.3	46.8
9	62.7	52.9	49.7	47.1
9.5	63.3	53.3	50.1	47.5
10	64.0	53.7	50.5	47.8
10.5	64.6	54.1	50.8	48.0
11	65.3	54.4	51.1	48.3
11.5	65.9	54.8	51.4	48.5
12	66.5	55.1	51.6	48.7
12.5	67.1	55.4	51.9	48.9
13	67.7	55.6	52.1	49.0
13.5	68.3	55.9	52.3	49.2
14	68.8	56.1	52.5	49.3

Table 3-8 - Adiabatic Temperature Rise from the QDRUM Test for Series 4

	Adiabatic Temperature Rise for series 4, °F	
Time, days	**Mix 6070AM (25% Fly Ash)**	**Mix 6070AN (25% Fly Ash)**
0	0	0
0.5	13.8	10.2
1	33.4	32.1
1.5	39.5	38.4
2	44.2	43.4
2.5	47.8	47.2
3	50.8	50.1
3.5	53.1	52.3
4	55.1	53.9
4.5	56.6	55.1
5	58.0	56.0
5.5	59.1	56.8
6	60.0	57.4
6.5	60.8	57.8
7	61.6	58.4
7.5	62.3	59.0
8	63.1	59.7
8.5	63.8	60.5
9	64.6	61.2
9.5	65.3	61.7
10	66.0	62.2
10.5	66.7	62.7
11	67.3	63.0
11.5	67.9	63.3
12	68.4	63.5
12.5	68.8	63.7
13	69.2	63.8
13.5	69.6	63.9
14	69.9	64.0

3.3.4 Results for CIDH Pile using Schmidt

The final temperatures at the center element of each pile diameter from the Schmidt model calculation are shown in Figure 3-10 to Figure 3-29.

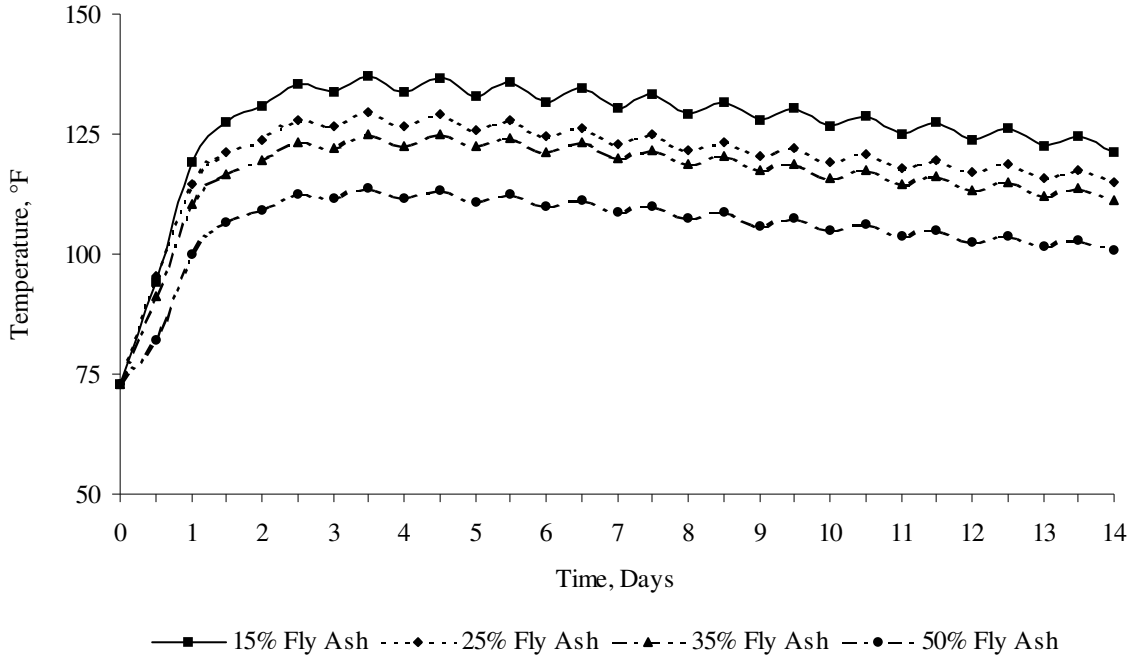

Figure 3-10 – Temperature versus Time for 6 ft Pile - Schmidt - Series 1
(Total Cementitious Materials 675 lb/cy)

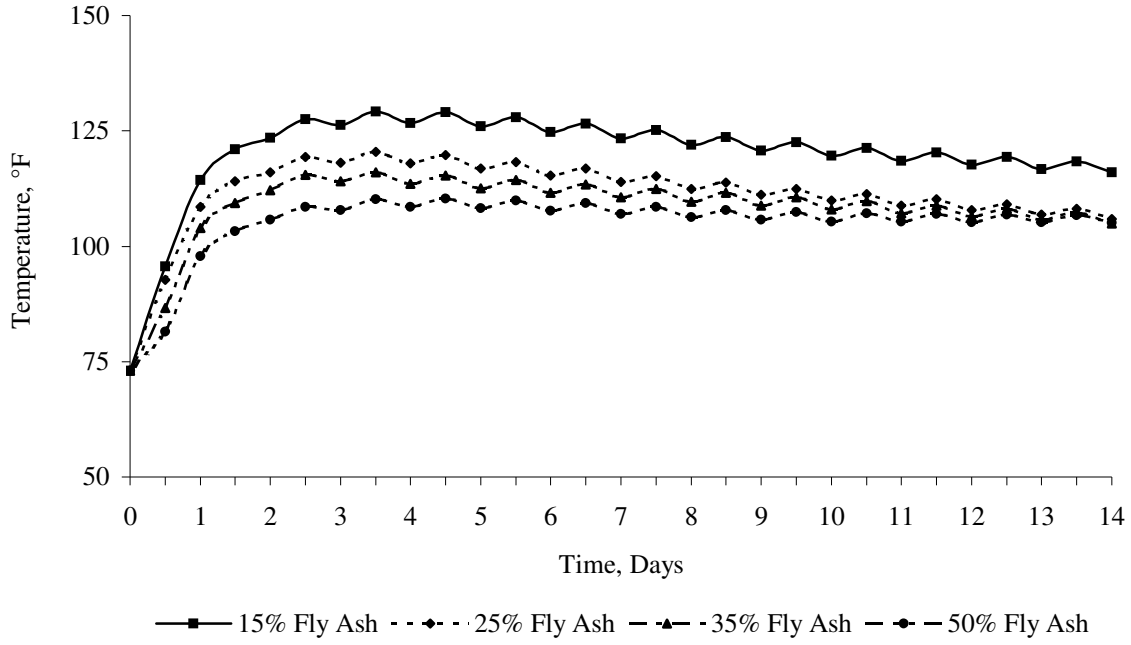

Figure 3-11 - Temperature versus Time for 6 ft Pile – Schmidt – Series 2
(Total Cementitious Materials 591 lb/cy)

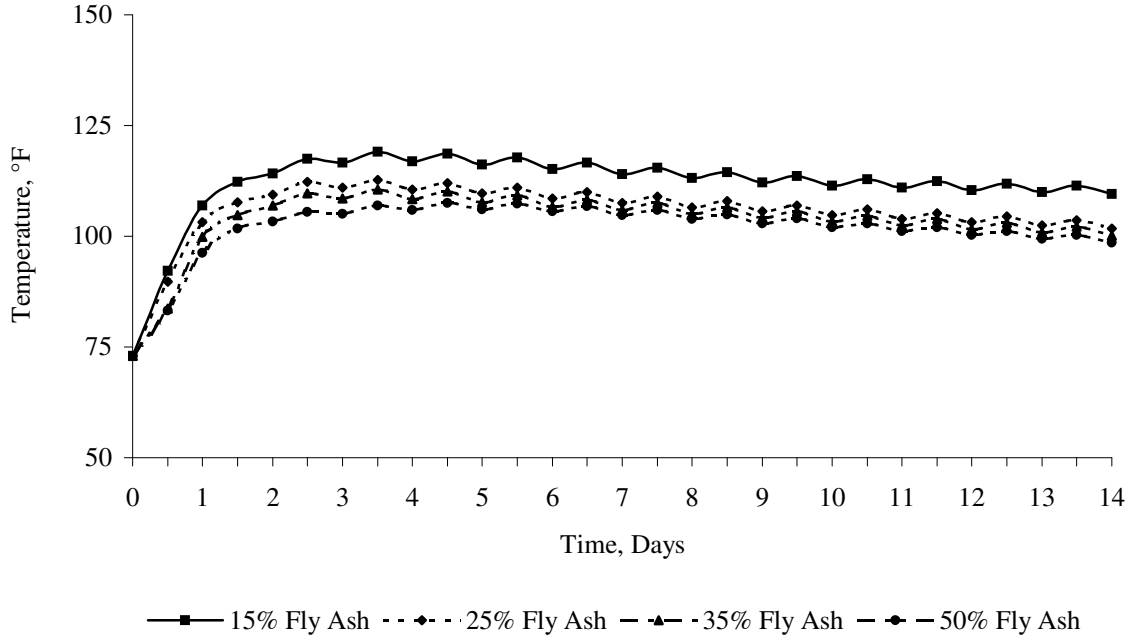

Figure 3-12 - Temperature versus Time for 6 ft Pile – Schmidt – Series 3
(Total Cementitious Materials 506 lb/cy)

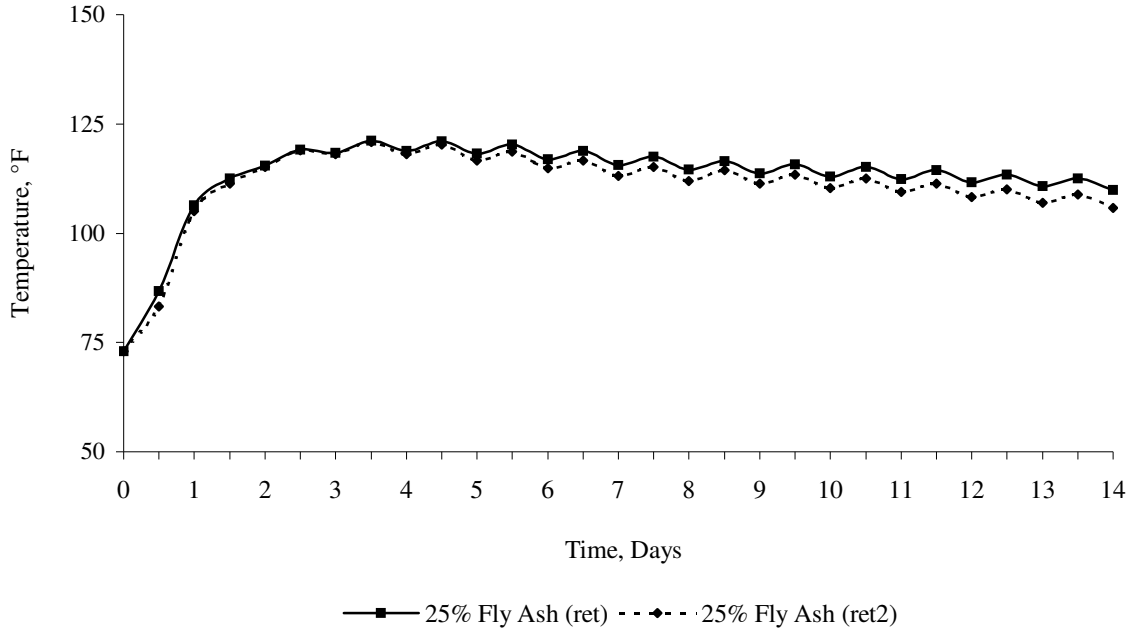

Figure 3-13 - Temperature versus Time for 6 ft Pile - Schmidt – Series 4
(Total Cementitious Materials 591 lb/cy)

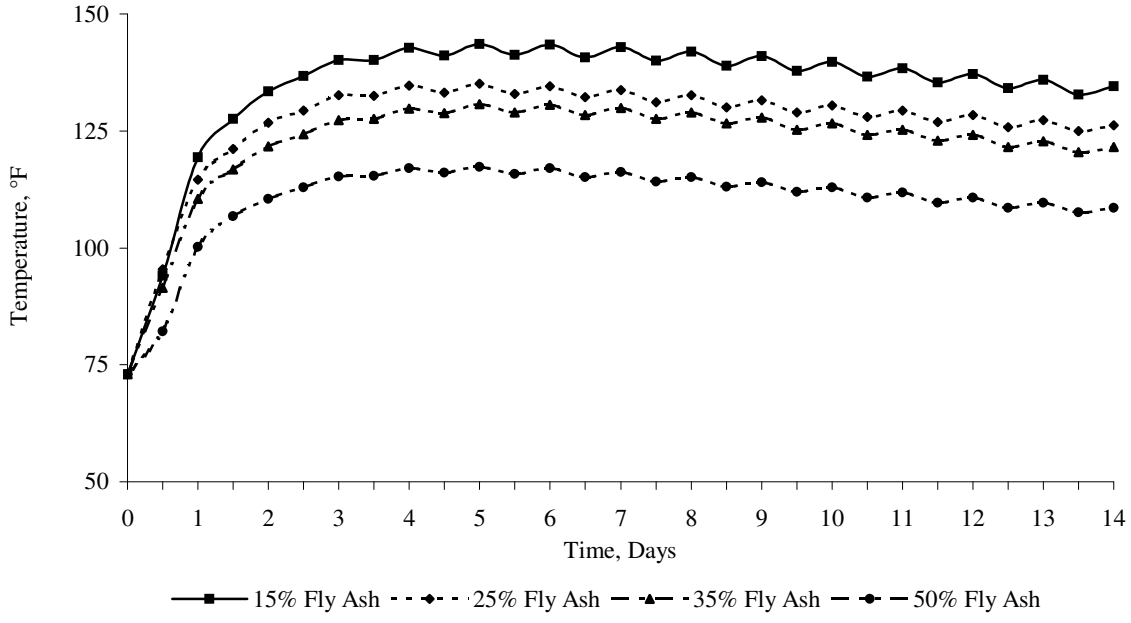

Figure 3-14 - Temperature versus Time for 8 ft Pile – Schmidt –Series 1
(Total Cementitious Materials 675 lb/cy)

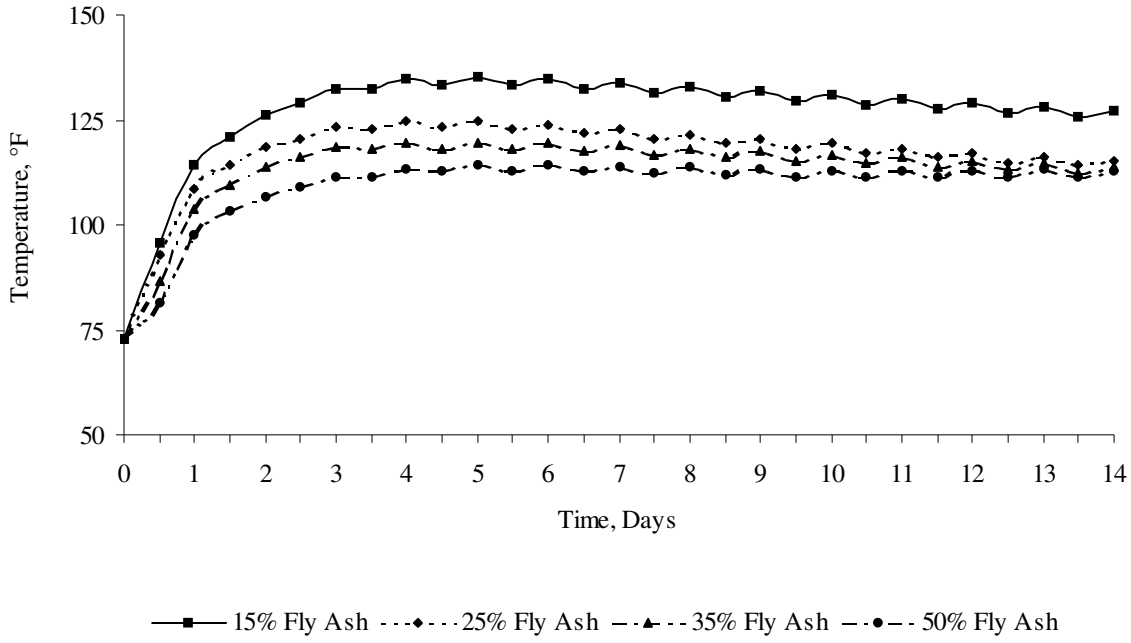

Figure 3-15 - Temperature versus Time for 8 ft Pile – Schmidt – Series 2
(Total Cementitious Materials 591 lb/cy)

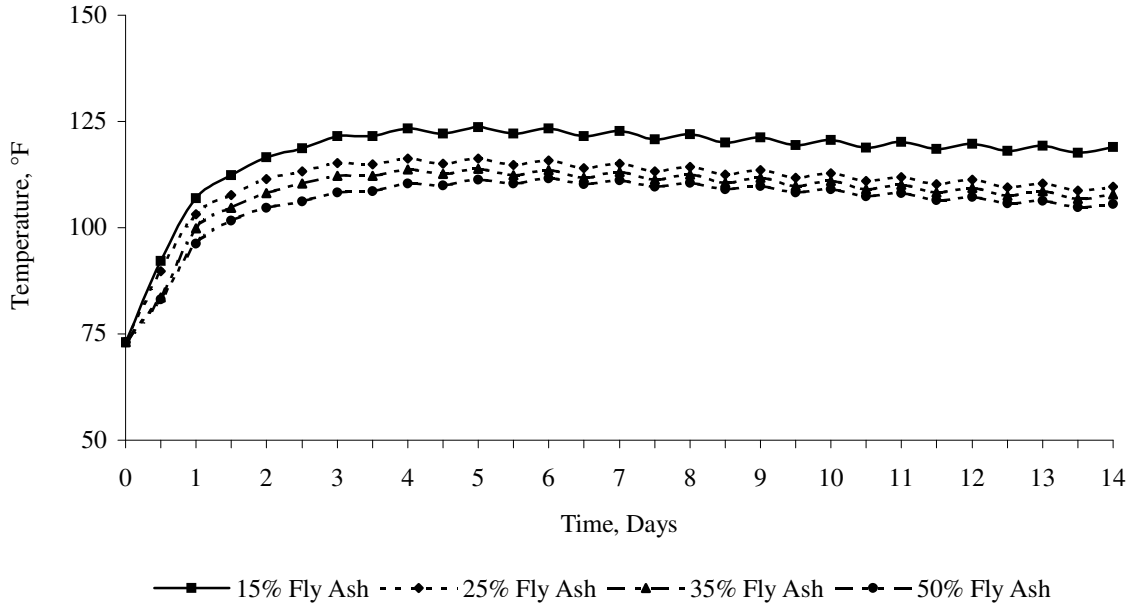

Figure 3-16 - Temperature versus Time for 8 ft Pile – Schmidt – Series 3
(Total Cementitious Materials 506 lb/cy)

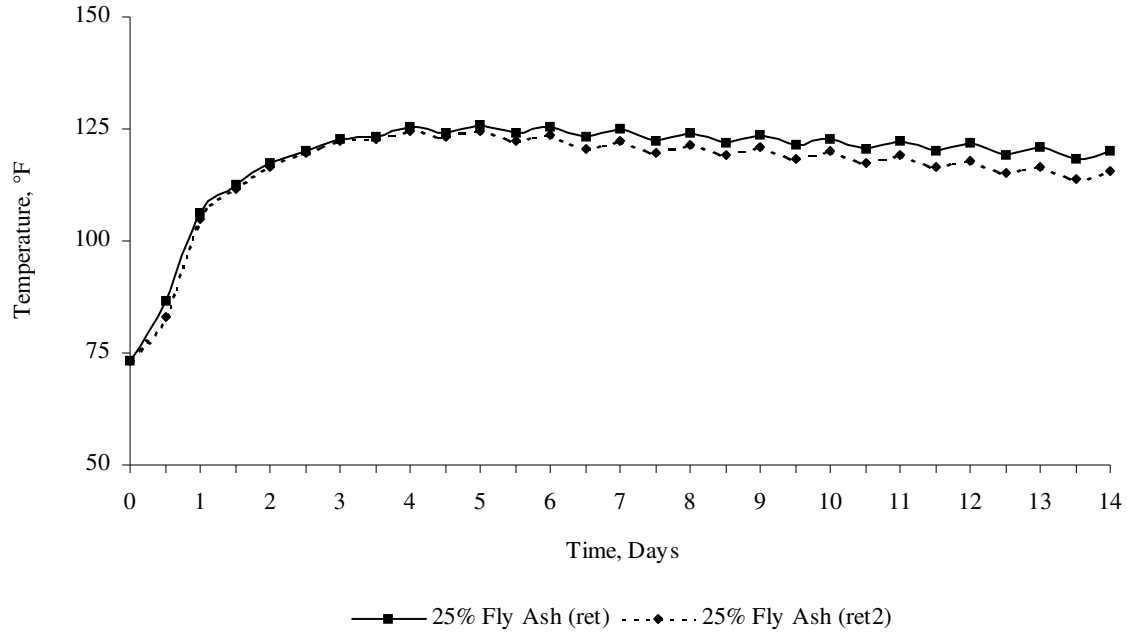

Figure 3-17 - Temperature versus Time for 8 ft Pile - Schmidt – Series 4
(Total Cementitious Materials 591 lb/cy)

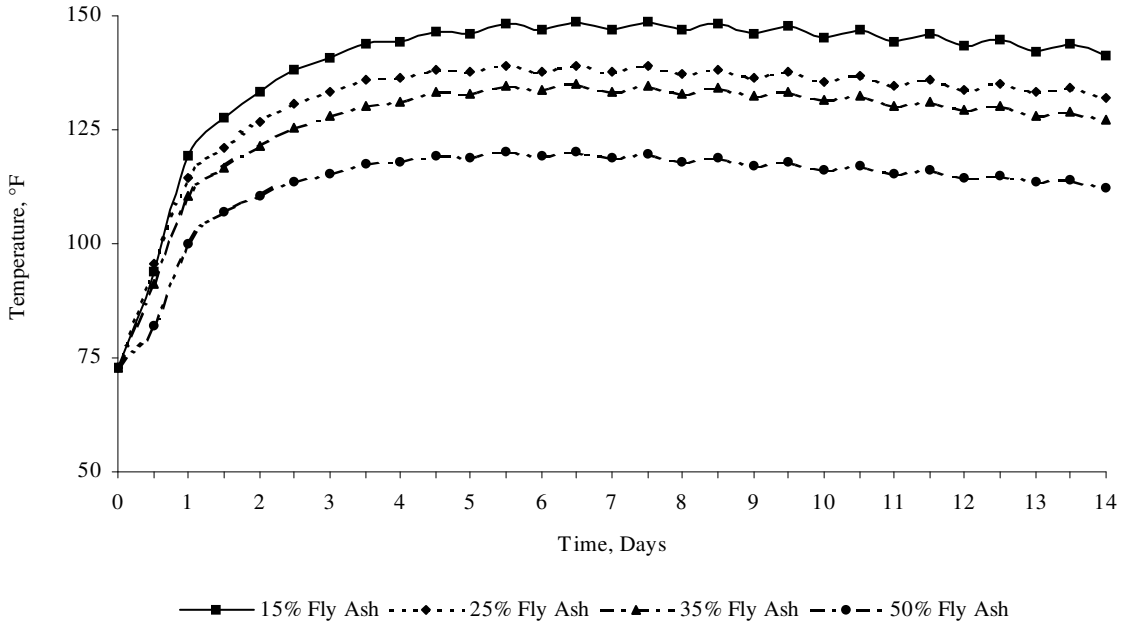

Figure 3-18 - Temperature versus Time for 10 ft Pile – Schmidt – Series 1
(Total Cementitious Materials 675 lb/cy)

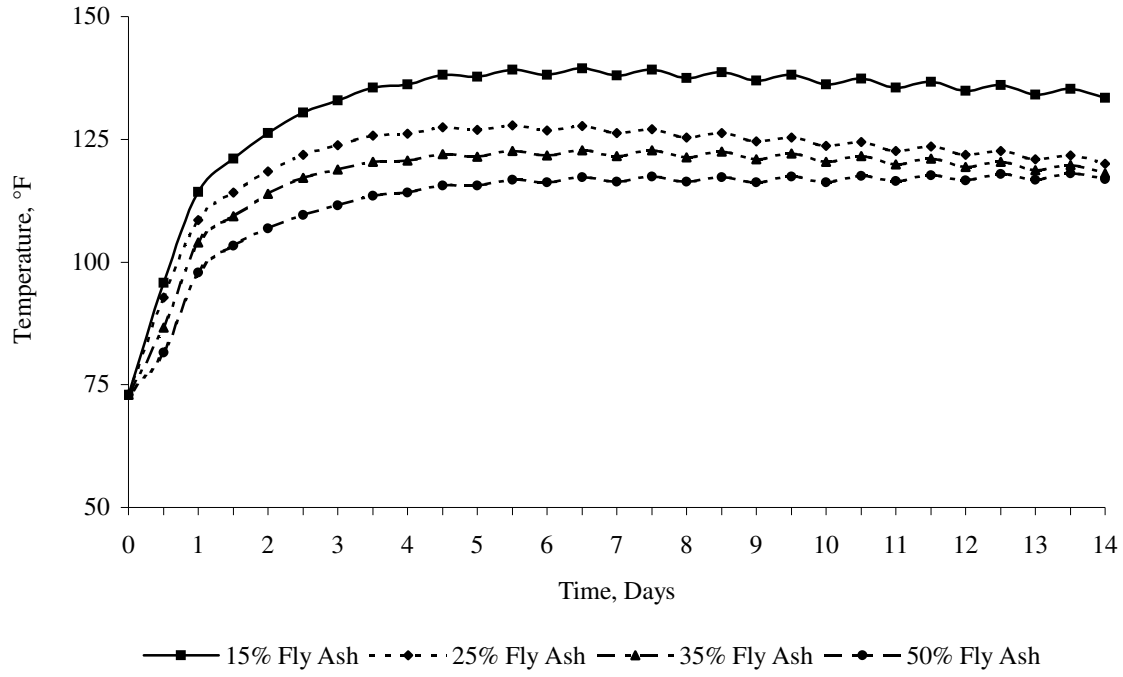

Figure 3-19 - Temperature versus Time for 10 ft ile – PSchmidt – Series 2
(Total Cementitious Materials 591 lb/cy)

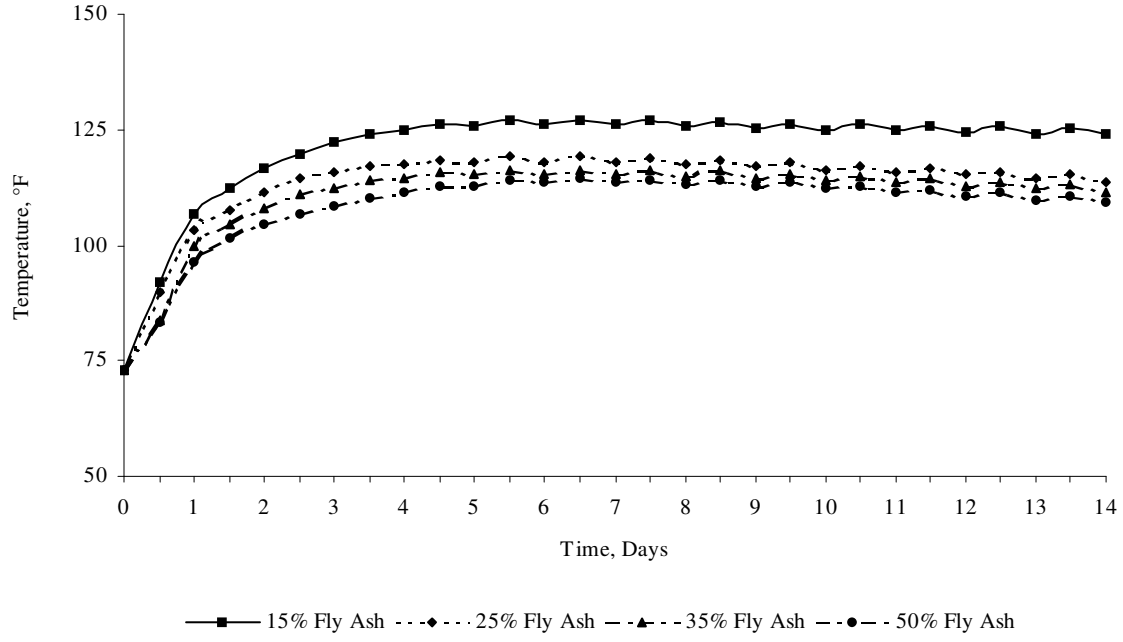

Figure 3-20 - Temperature versus Time for 10 ft Pile – Schmidt – Series 3
(Total Cementitious Materials 506 lb/cy)

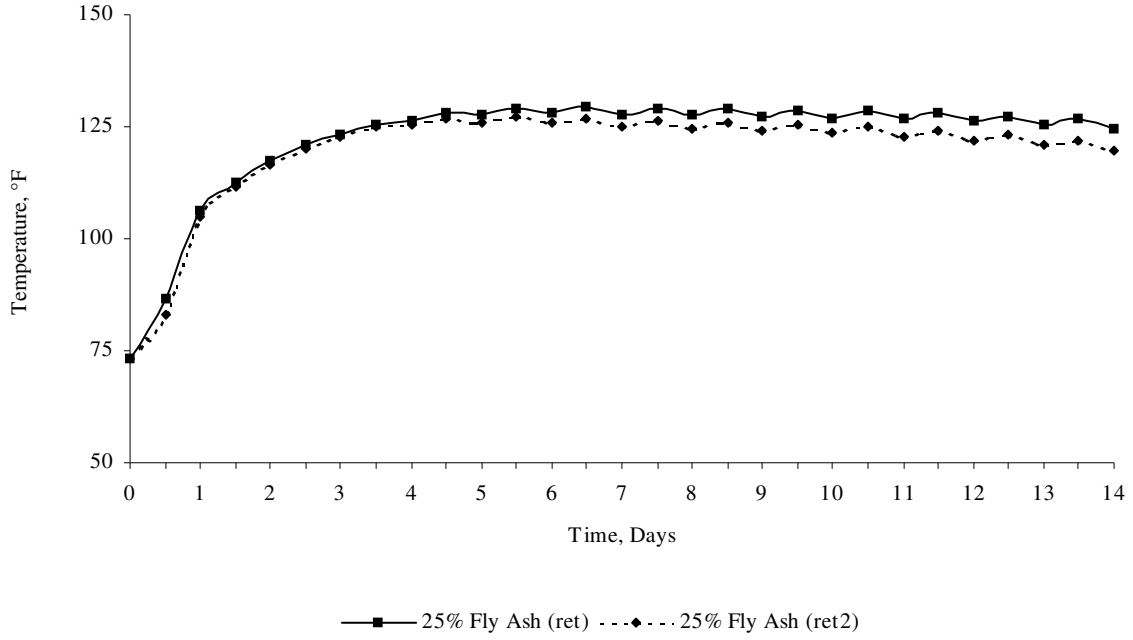

Figure 3-21 - Temperature versus Time for 10 ft Pile – Schmidt – Series 4
(Total Cementitious Materials 591 lb/cy)

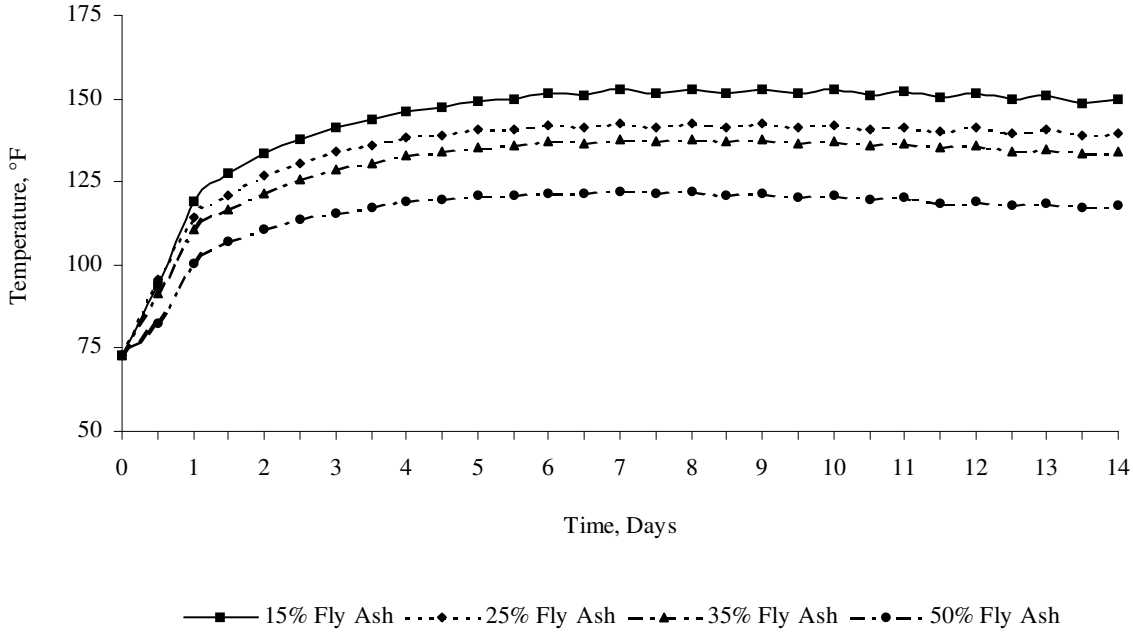

Figure 3-22 - Temperature versus Time for 12 ft Pile - Schmidt – Series 1
(Total Cementitious Materials 675 lb/cy)

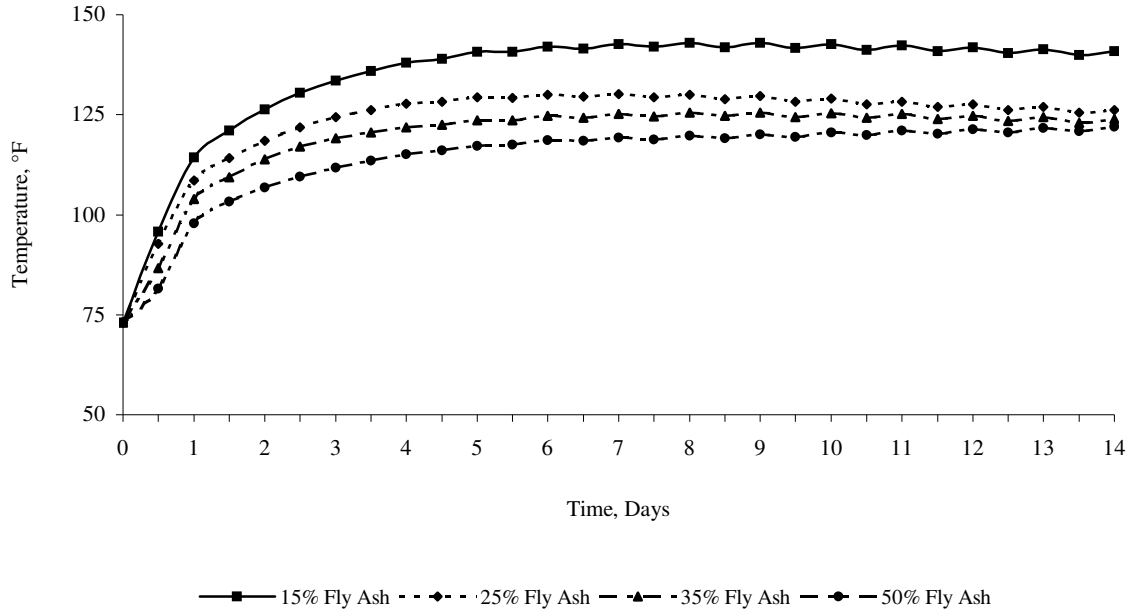

Figure 3-23 - Temperature versus Time for 12 ft Pile - Schmidt - Series 2
(Total Cementitious Materials 591 lb/cy)

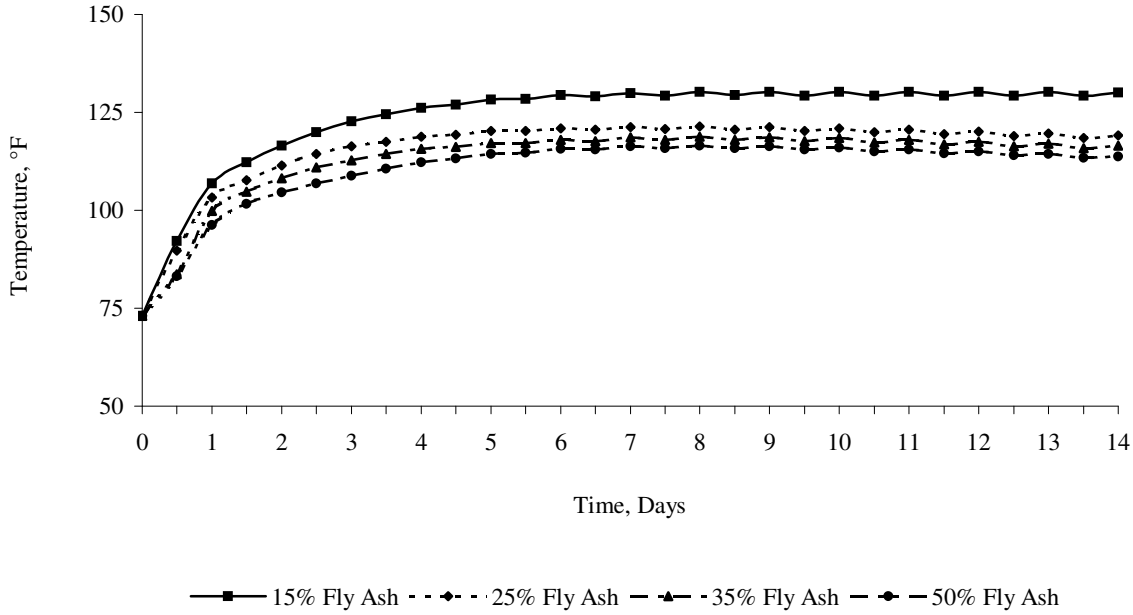

Figure 3-24 - Temperature versus Time for 12 ft Pile - Schmidt - Series 3
(Total Cementitious Materials 506 lb/cy)

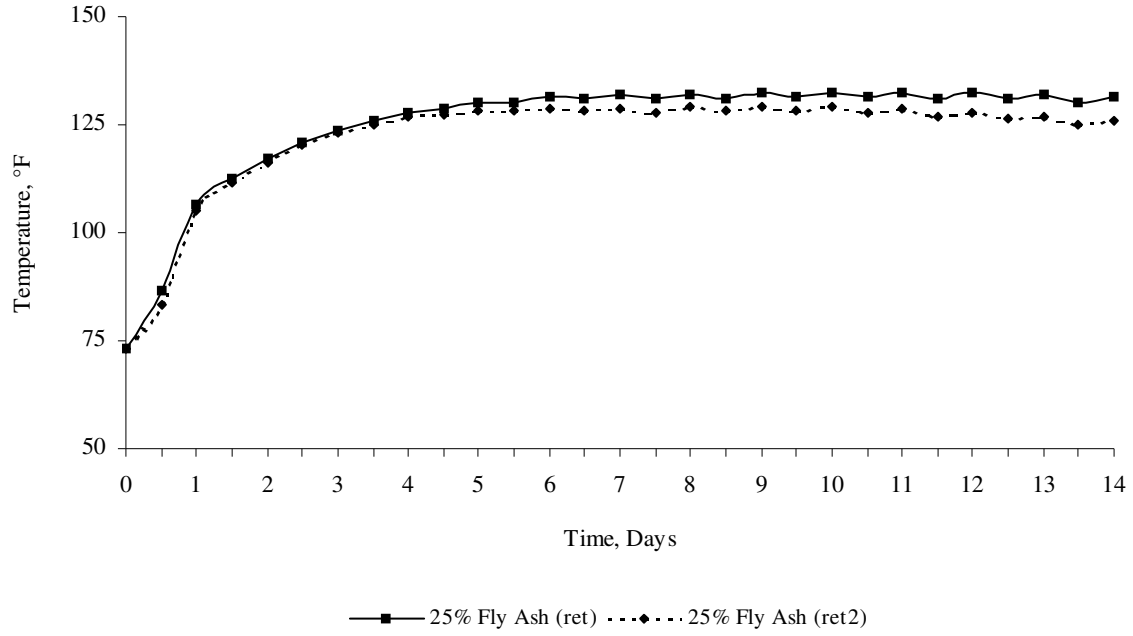

Figure 3-25 - Temperature versus Time for 12 ft Pile - Schmidt - Series 4
(Total Cementitious Materials 591 lb/cy)

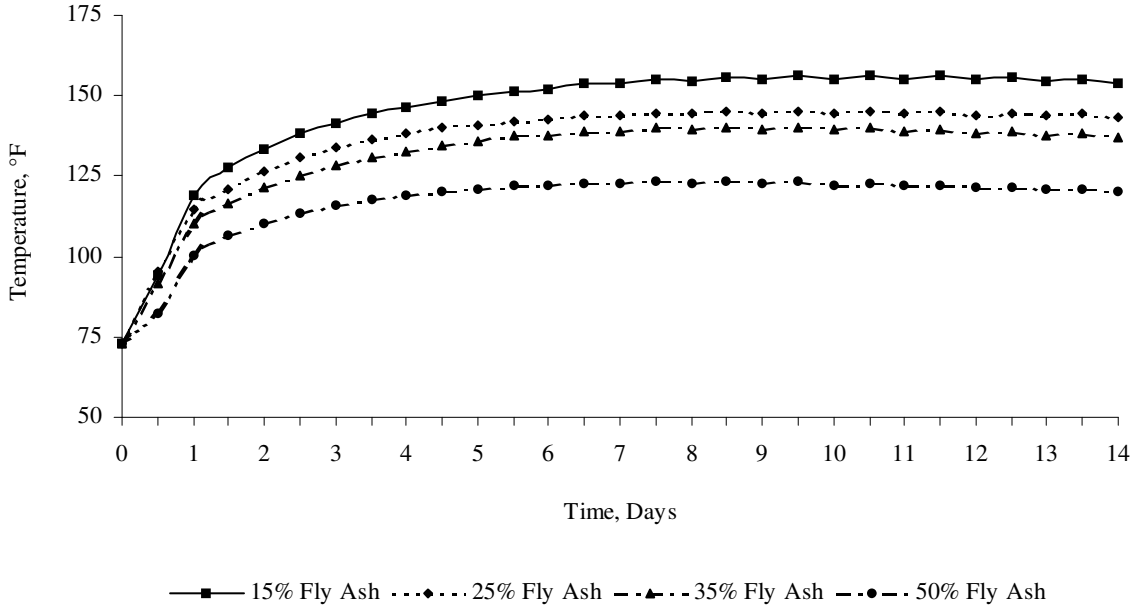

Figure 3-26 - Temperature versus Time for 14 ft Pile - Schmidt - Series 1
(Total Cementitious Materials 675 lb/cy)

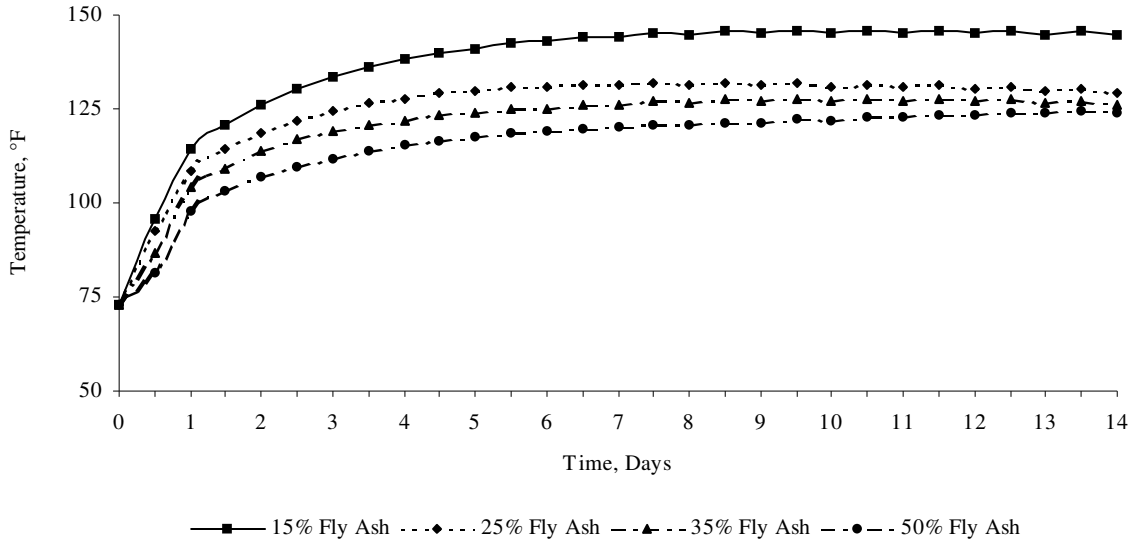

Figure 3-27 - Temperature versus Time for 14 ft Pile - Schmidt - Series 2
(Total Cementitious Materials 591 lb/cy)

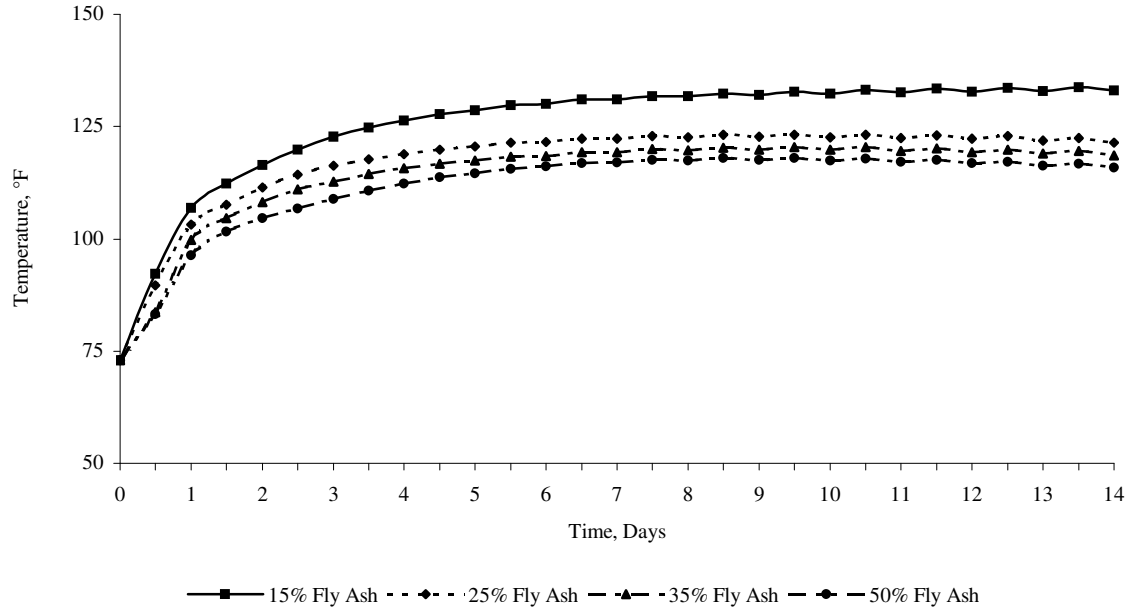

Figure 3-28 - Temperature versus Time for 14 Pile - Schmidt - Series 3
(Total Cementitious Materials 506 lb/cy)

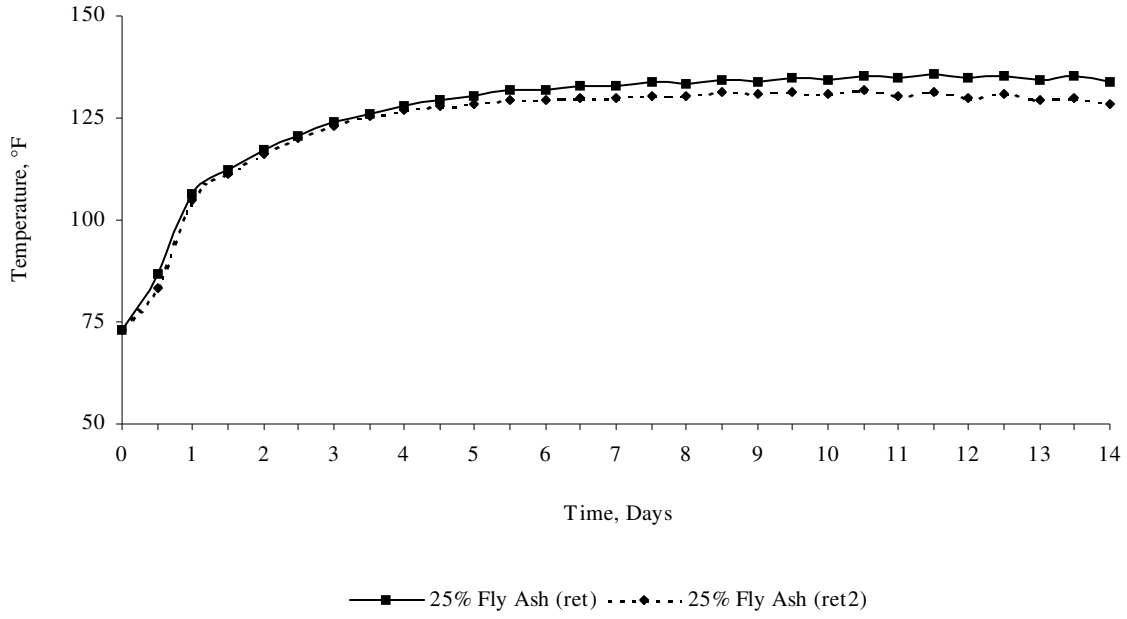

Figure 3-29 - Temperature versus Time for 14 ft Pile - Schmidt - Series 4
(Total Cementitious Materials 591 lb/cy)

The peak temperature at the center of the CIDH concrete piles with different diameters and using the Schmidt model calculation are shown in Table 3-9 to Table 3-12 and in Figure 3-30 to Figure 3-33. It can be observed that the peak temperature for all diameters is the highest at the 15% fly ash mix.

Table 3-9 - Peak Temperature for Different Pile Diameters – Schmidt – Series 1

	Temperature in center of pile for series 1 - Schmidt, °F			
Diameter, ft	**Mix 6070AA (15% Fly Ash)**	**Mix 6070AB (25% Fly Ash)**	**Mix 6070AC (35% Fly Ash)**	**Mix 6070AD (50% Fly Ash)**
6	137.1	129.6	125.1	113.7
8	143.6	135.1	130.8	117.4
10	148.8	139.2	134.9	120.0
12	153.0	142.5	138.0	122.0
14	156.4	145.4	140.4	123.4

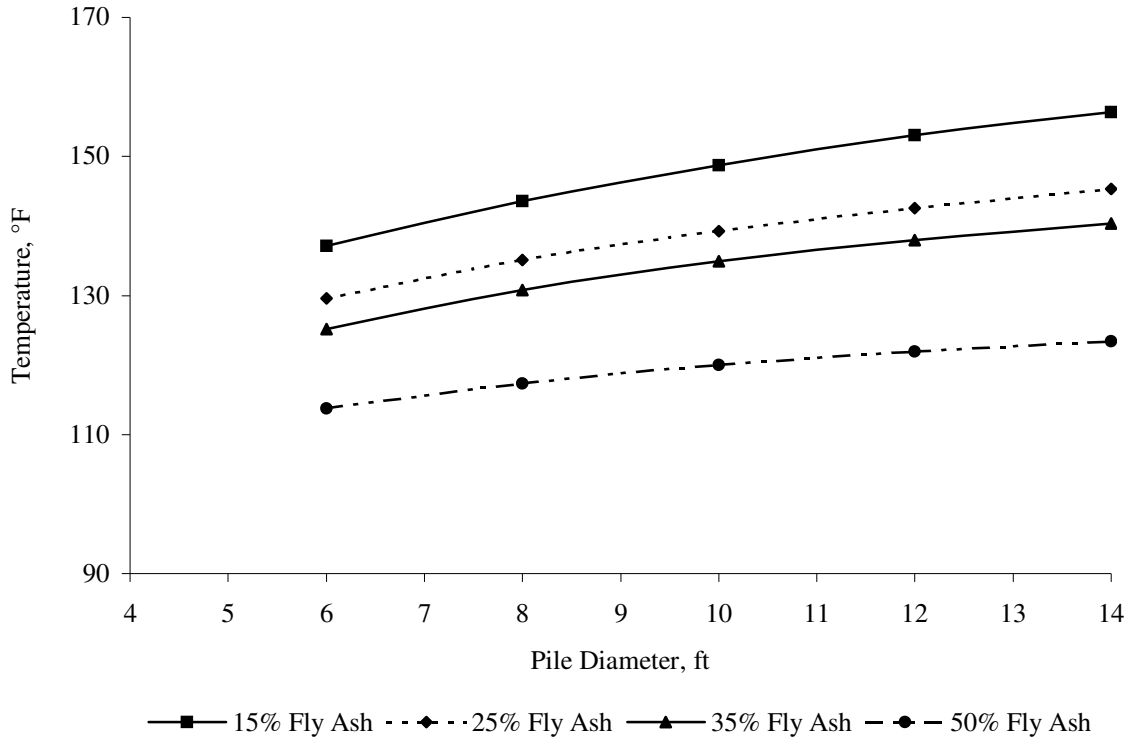

Figure 3-30 - Maximum Temperature at center of pile – Schmidt – Series 1
(Total Cementitious Materials 675 lb/cy)

Table 3-10 - Peak Temperature for Different Pile Diameters – Schmidt – Series 2

	Temperature in center of pile for series 2 - Schmidt, °F			
Diameter, ft	**Mix 6070AE (15% Fly Ash)**	**Mix 6070AF (25% Fly Ash)**	**Mix 6070AG (35% Fly Ash)**	**Mix 6070AH (50% Fly Ash)**
6	129.2	120.4	116.1	110.3
8	135.2	124.7	119.7	114.3
10	139.4	127.9	122.8	118.0
12	142.9	130.2	125.5	121.9
14	145.9	132.1	127.9	124.7

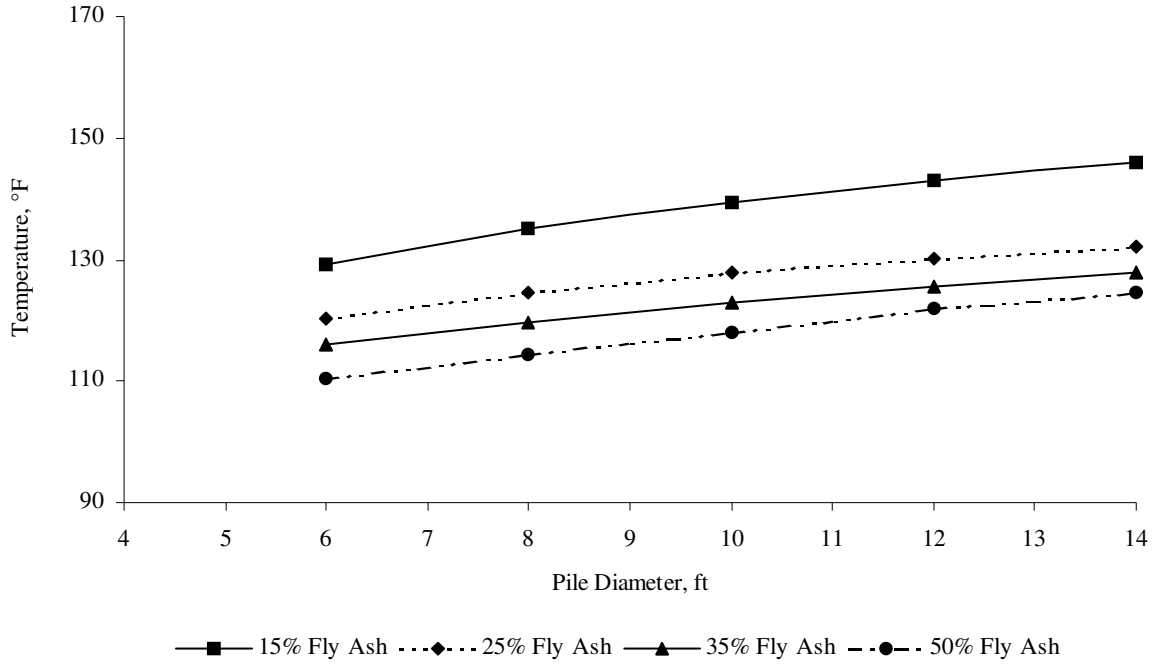

Figure 3-31 - Maximum Temperature at center of pile – Schmidt – Series 2
(Total Cementitious Materials 591 lb/cy)

Table 3-11 - Peak Temperature for Different Pile Diameters – Schmidt – Series 3

	Temperature in center of pile for series 3 - Schmidt, °F			
Diameter, ft	**Mix 6070AI (15% Fly Ash)**	**Mix 6070AJ (25% Fly Ash)**	**Mix 6070AK (35% Fly Ash)**	**Mix 6070AL (50% Fly Ash)**
6	119.0	112.7	110.6	107.6
8	123.7	116.3	113.9	111.5
10	127.2	119.1	116.4	114.3
12	130.3	121.4	118.7	116.4
14	133.8	123.2	120.5	118.1

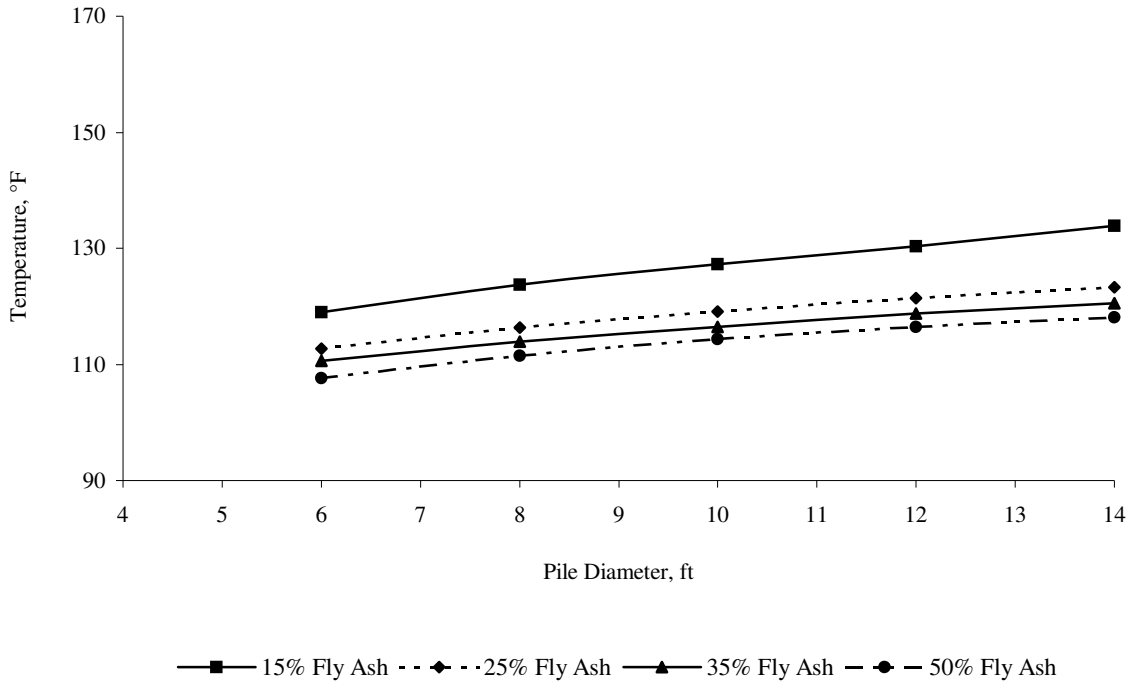

Figure 3-32 - Maximum Temperature at center of pile – Schmidt – Series 3
(Total Cementitious Materials 506 lb/cy)

Table 3-12 - Peak Temperature for Different Pile Diameters – Schmidt – Series 4

	Temperature in center of pile for series 4 - Schmidt, °F	
Diameter, ft	**Mix 6070AM (25% Fly Ash)**	**Mix 6070AN (25% Fly Ash)**
6	121.1	120.9
8	126.0	124.5
10	129.3	127.2
12	132.5	129.3
14	135.6	131.6

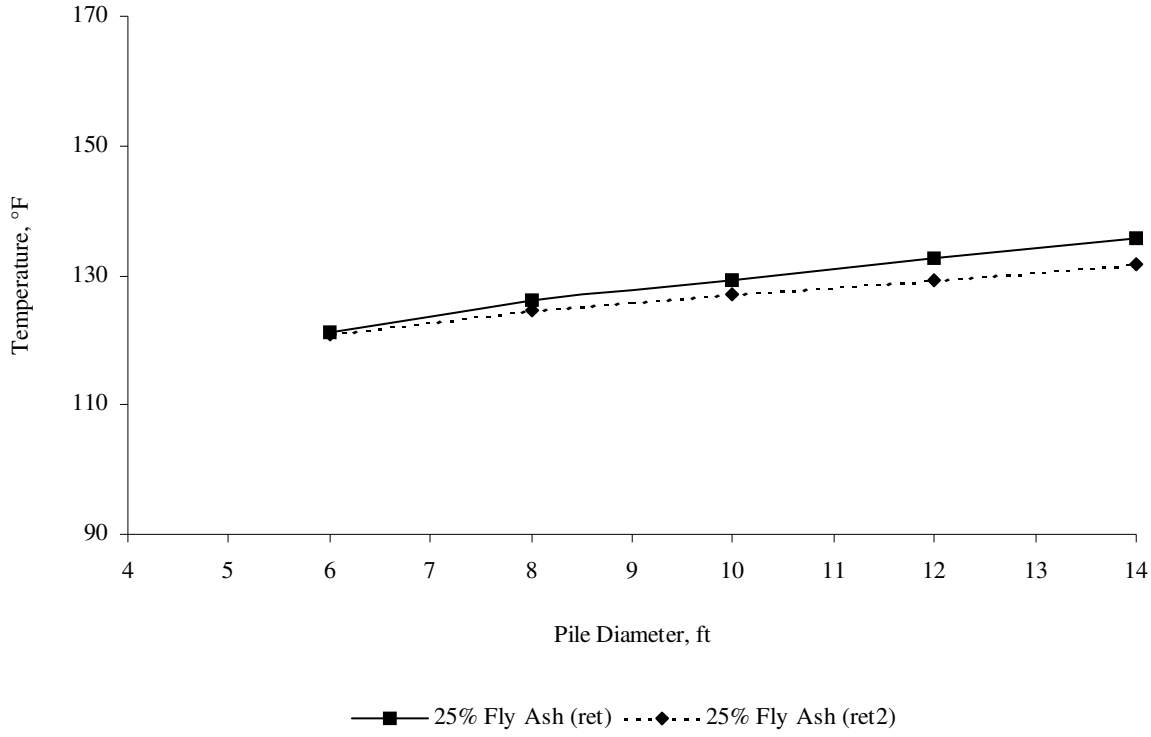

Figure 3-33 - Maximum Temperature at center of pile – Schmidt – Series 4
(Total Cementitious Materials 591 lb/cy)

3.3.5 ABAQUS Model

In order to calculate the temperature profile as function of time for the CIDH concrete piles, the ABAQUS finite element program was. The actual size of the pile modeled by a finite element mesh that represents the diameter of the pile and a 10 ft longitudinal length. The number of elements utilized for each pile was described earlier in Table 2-1. The element type for all the piles was DC3D10.

3.3.6 Material Properties for CIDH Piles using ABAQUS

The material properties utilized in the ABAQUS model to predict the peak temperature are divided into three categories. The first category is shown in Table 3-1 to Table 3-4 and includes the unit mass, the specific heat and the modulus of elasticity. The second category includes properties that are assumed constant for all analysis. These are the conductivity constant (equal to 1.4 Btu/ft/hr/°F) and the coefficient of thermal expansion (equal to $6x10^{-6}$ /°F). The third category is the adiabatic temperature rise, which are converted to body heat flux and are shown in Table 3-13 to Table 3-16. The values shown in these tables, for simplicity, are in time intervals of 0.5 days however in the ABAQUS finite element program the time intervals used were equal to 4 hours.

3.3.7 Temperature Boundary Conditions for CIDH Piles using ABAQUS

The temperature boundary conditions for the ABAQUS models are the temperature of the surrounding where the CIDH pile is placed, and it is equal to 55°F.

Table 3-13 – Body Heat Flux Calculated for Series 1

	Body Heat Flux Calculated for series 1, Btu/ft^3/hr			
Time, days	**Mix 6070AA (15% Fly Ash)**	**Mix 6070AB (25% Fly Ash)**	**Mix 6070AC (35% Fly Ash)**	**Mix 6070AD (50% Fly Ash)**
0	0.00	0.00	0.00	0.00
0.5	106.39	113.98	89.42	47.60
1	50.29	35.74	34.62	41.88
1.5	23.21	19.32	19.23	15.23
2	17.41	15.45	14.42	11.42
2.5	13.54	12.56	11.54	8.57
3	10.64	9.66	8.65	7.62
3.5	7.74	7.73	7.69	5.71
4	6.77	5.80	6.73	4.76
4.5	5.80	4.83	5.77	3.81
5	5.80	4.83	4.81	2.86
5.5	4.84	3.86	3.85	2.86
6	4.84	3.86	3.85	2.86
6.5	3.87	3.86	2.88	1.90
7	3.87	2.90	2.88	0.95
7.5	3.87	1.93	1.92	0.95
8	2.90	1.93	1.92	0.95
8.5	2.90	1.93	1.92	0.95
9	2.90	1.93	1.92	0.95
9.5	2.90	1.93	0.96	0.95
10	2.90	1.93	1.92	0.95
10.5	1.93	1.93	1.92	0.95
11	1.93	1.93	0.96	0.95
11.5	1.93	0.97	0.96	0.00
12	1.93	1.93	0.96	0.95
12.5	1.93	0.97	0.96	0.95
13	1.93	1.93	0.96	0.00
13.5	0.97	1.93	0.96	0.00
14	1.93	0.97	0.96	0.95

Table 3-14 - Body Heat Flux Calculated for Series 2

	Body Heat Flux Calculated for series 2, Btu/ft^3/hr			
Time, days	**Mix 6070AE (15% Fly Ash)**	**Mix 6070AF (25% Fly Ash)**	**Mix 6070AG (35% Fly Ash)**	**Mix 6070AH (50% Fly Ash)**
0	0.00	0.00	0.00	0.00
0.5	112.35	100.39	74.57	42.50
1	33.90	27.03	28.68	36.83
1.5	20.34	17.37	16.25	12.28
2	15.50	12.55	12.43	10.39
2.5	12.59	10.62	8.60	7.56
3	9.69	7.72	6.69	6.61
3.5	7.75	5.79	4.78	5.67
4	6.78	4.83	3.82	4.72
4.5	5.81	3.86	3.82	3.78
5	4.84	3.86	3.82	3.78
5.5	3.87	1.93	2.87	2.83
6	3.87	1.93	2.87	2.83
6.5	2.91	1.93	1.91	2.83
7	2.91	1.93	2.87	1.89
7.5	2.91	0.97	1.91	1.89
8	2.91	0.97	1.91	1.89
8.5	1.94	1.93	1.91	1.89
9	2.91	1.93	1.91	1.89
9.5	2.91	0.97	0.96	1.89
10	1.94	0.97	0.96	1.89
10.5	1.94	0.97	1.91	2.83
11	0.97	0.97	0.96	2.83
11.5	1.94	0.97	0.96	1.89
12	1.94	0.97	0.96	1.89
12.5	1.94	0.97	1.91	1.89
13	0.97	0.97	0.96	2.83
13.5	0.97	0.97	0.96	1.89
14	0.97	0.97	0.96	1.89

Table 3-15 - Body Heat Flux Calculated for Series 3

	Body Heat Flux Calculated for series 3, Btu/ft3/hr			
Time, days	**Mix 6070AI (15% Fly Ash)**	**Mix 6070AJ (25% Fly Ash)**	**Mix 6070AK (35% Fly Ash)**	**Mix 6070AL (50% Fly Ash)**
0	0.00	0.00	0.00	0.00
0.5	91.41	79.65	58.01	54.12
1	26.94	22.07	28.53	29.86
1.5	15.39	13.43	13.31	12.13
2	11.55	11.52	10.46	7.46
2.5	10.58	7.68	8.56	6.53
3	8.66	5.76	4.76	6.53
3.5	5.77	3.84	5.71	5.60
4	4.81	3.84	3.80	5.60
4.5	3.85	2.88	3.80	4.67
5	3.85	2.88	2.85	3.73
5.5	3.85	2.88	2.85	2.80
6	2.89	1.92	1.90	2.80
6.5	2.89	1.92	1.90	1.87
7	2.89	1.92	1.90	1.87
7.5	1.92	1.92	1.90	0.93
8	2.89	1.92	1.90	0.93
8.5	1.92	1.92	1.90	1.87
9	1.92	0.96	0.95	0.93
9.5	1.92	0.96	0.95	0.93
10	1.92	0.96	0.95	0.93
10.5	1.92	0.96	0.95	0.93
11	2.89	0.96	0.95	0.93
11.5	1.92	0.96	0.95	0.93
12	1.92	0.96	0.00	0.93
12.5	1.92	0.96	0.95	0.93
13	1.92	0.96	0.95	0.00
13.5	1.92	0.96	0.95	0.93
14	1.92	0.96	0.95	0.00

Table 3-16 - Body Heat Flux Calculated for Series 4

	Body Heat Flux Calculated for series 4, Btu/ft^3/hr	
Time, days	**Mix 6070AM (25% Fly Ash)**	**Mix 6070AN (25% Fly Ash)**
0	0.00	0.00
0.5	77.41	64.27
1	36.77	41.87
1.5	18.39	18.50
2	13.55	14.61
2.5	10.64	11.69
3	8.71	8.76
3.5	6.77	6.82
4	5.81	4.87
4.5	3.87	3.90
5	4.84	1.95
5.5	3.87	2.92
6	2.90	1.95
6.5	2.90	0.97
7	2.90	1.95
7.5	1.94	1.95
8	2.90	1.95
8.5	1.94	2.92
9	2.90	2.92
9.5	1.94	0.97
10	1.94	0.97
10.5	1.94	1.95
11	1.94	0.97
11.5	1.94	0.97
12	1.94	0.97
12.5	0.97	0.97
13	0.97	0.00
13.5	0.97	0.00
14	0.97	0.00

3.3.8 Results for CIDH Piles using ABAQUS

The final temperatures at the center element of each pile diameter are shown in Figure 3-34 to Figure 3-51.

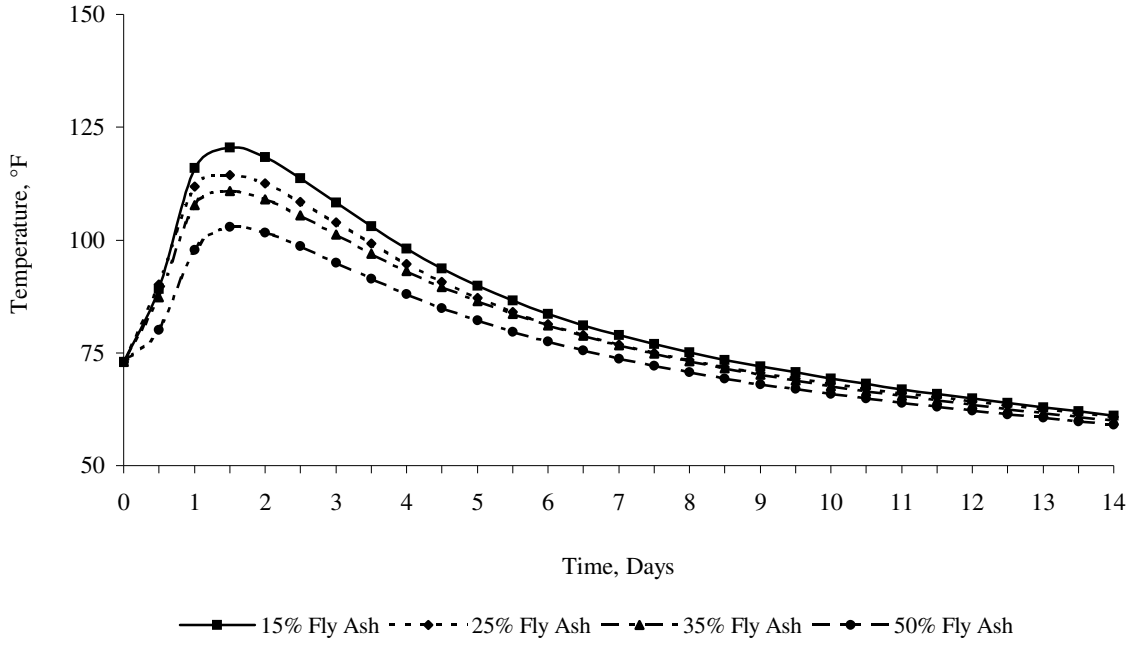

Figure 3-34 - Temperature versus Time for 6ft Pile – ABAQUS – Series 1
(Total Cementitious Materials 675 lb/cy)

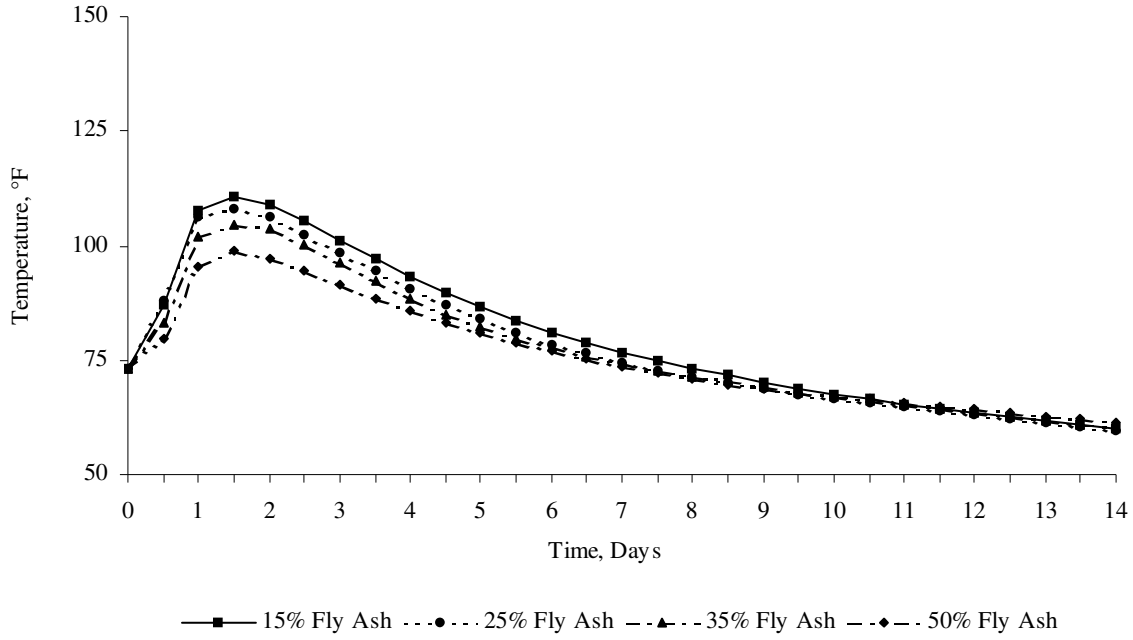

Figure 3-35 - Temperature versus Time for 6ft Pile – ABAQUS – Series 2
(Total Cementitious Materials 591 lb/cy)

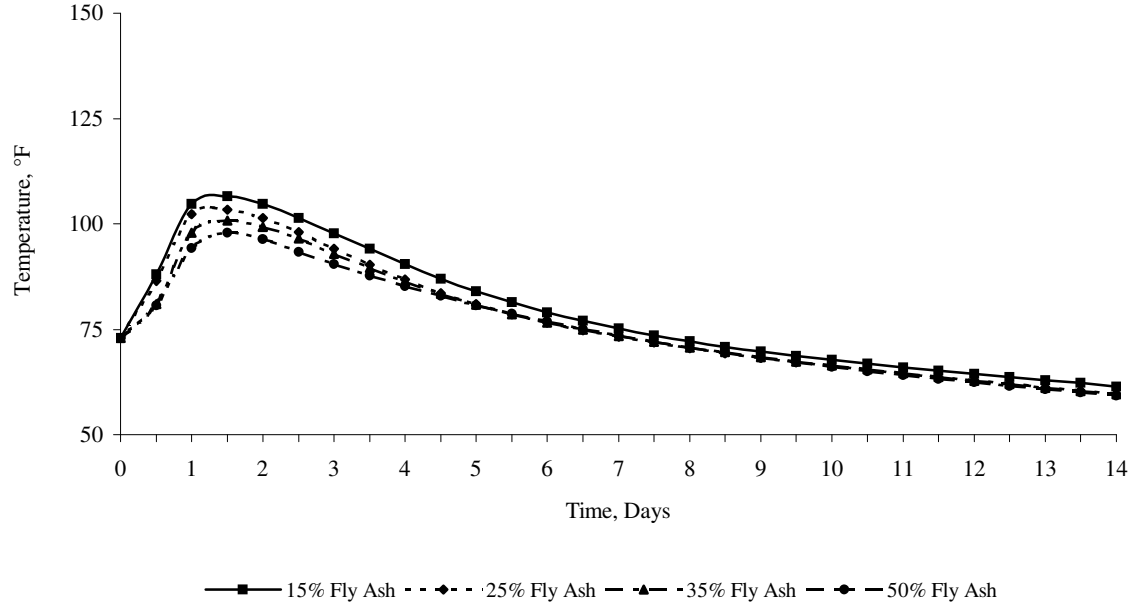

Figure 3-36 - Temperature versus Time for 6ft Pile – ABAQUS – Series 3
(Total Cementitious Materials 506 lb/cy)

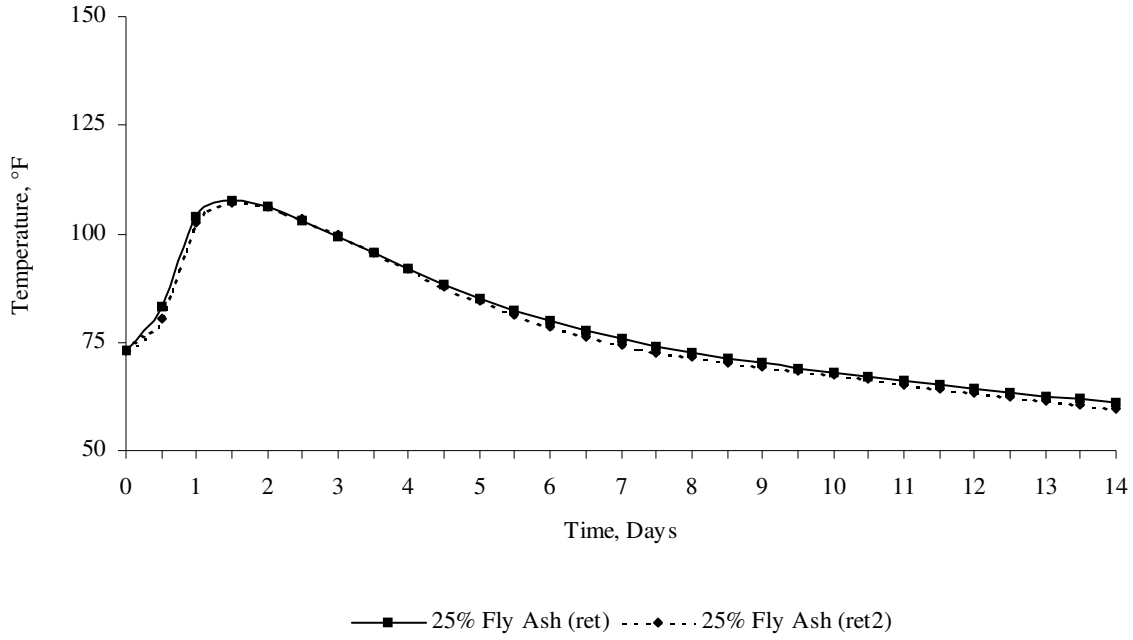

Figure 3-37 - Temperature versus Time for 6ft Pile - ABAQUS – Series 4
(Total Cementitious Materials 591 lb/cy)

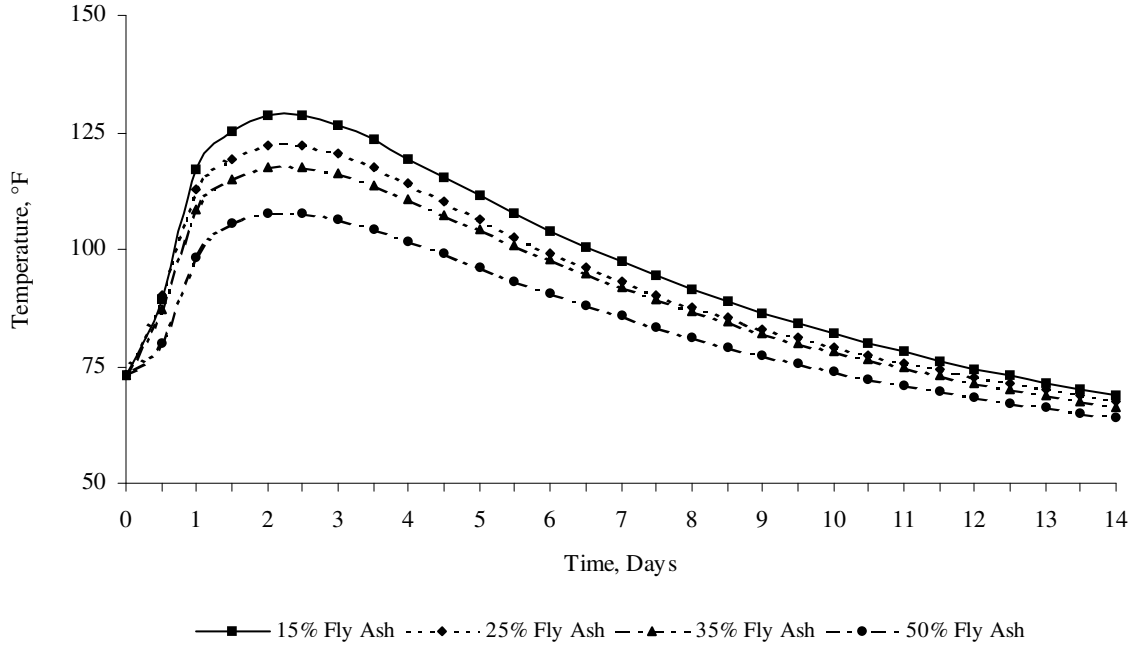

Figure 3-38 – Temperature versus Time for 8ft Pile - ABAQUS – Series 1
(Total Cementitious Materials 675 lb/cy)

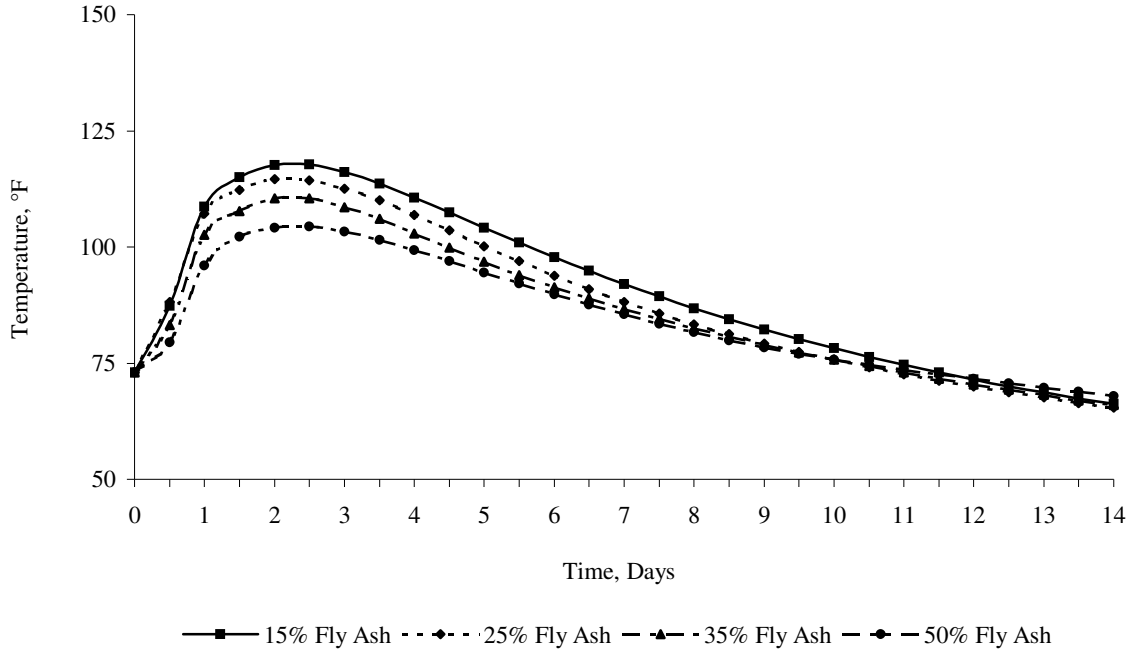

Figure 3-39 –Temperature versus Time for 8ft Pile – ABAQUS – Series 2
(Total Cementitious Materials 591 lb/cy)

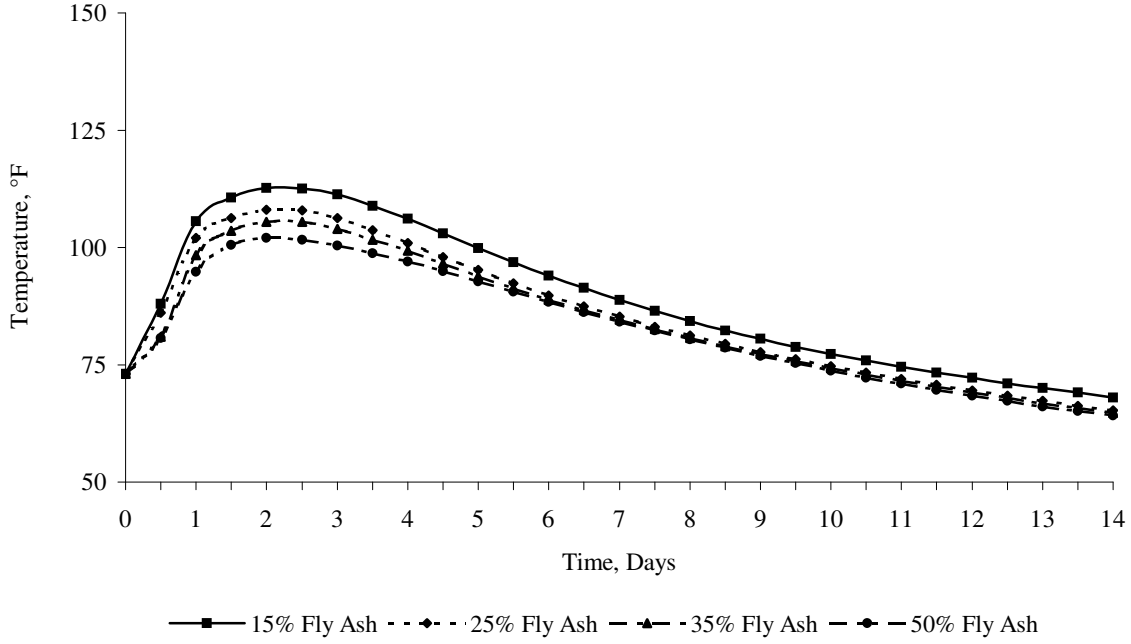

Figure 3-40 –Temperature versus Time for 8ft Pile – ABAQUS – Series 3
(Total Cementitious Materials 506 lb/cy)

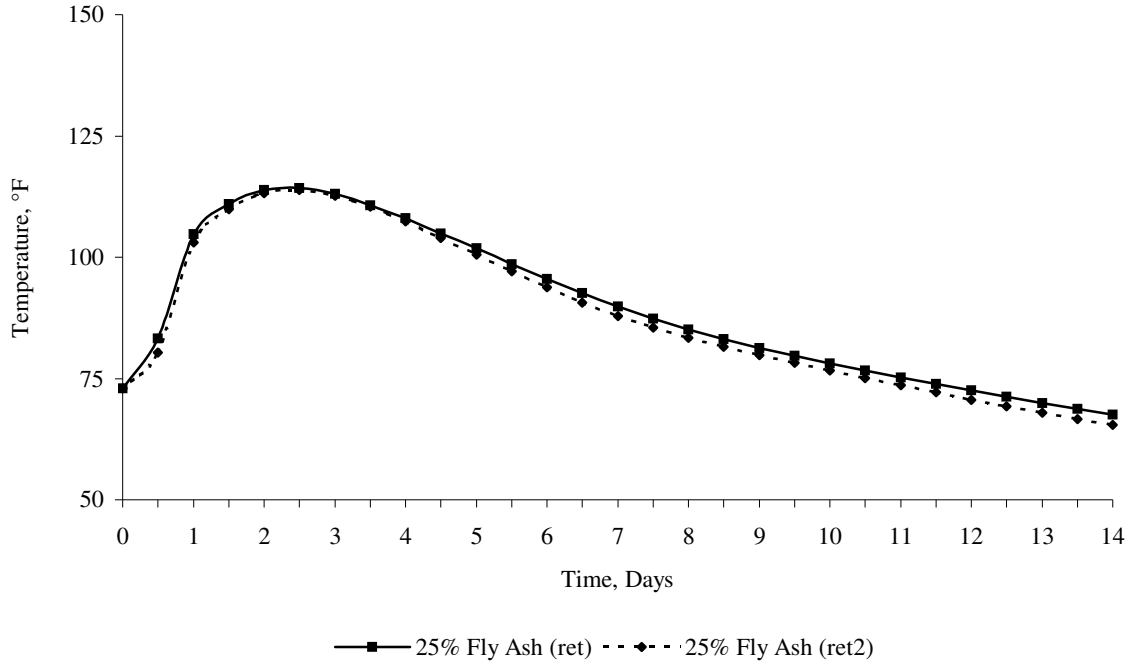

Figure 3-41 –Temperature versus Time for 8ft Pile - ABAQUS – Series 4
(Total Cementitious Materials 591 lb/cy)

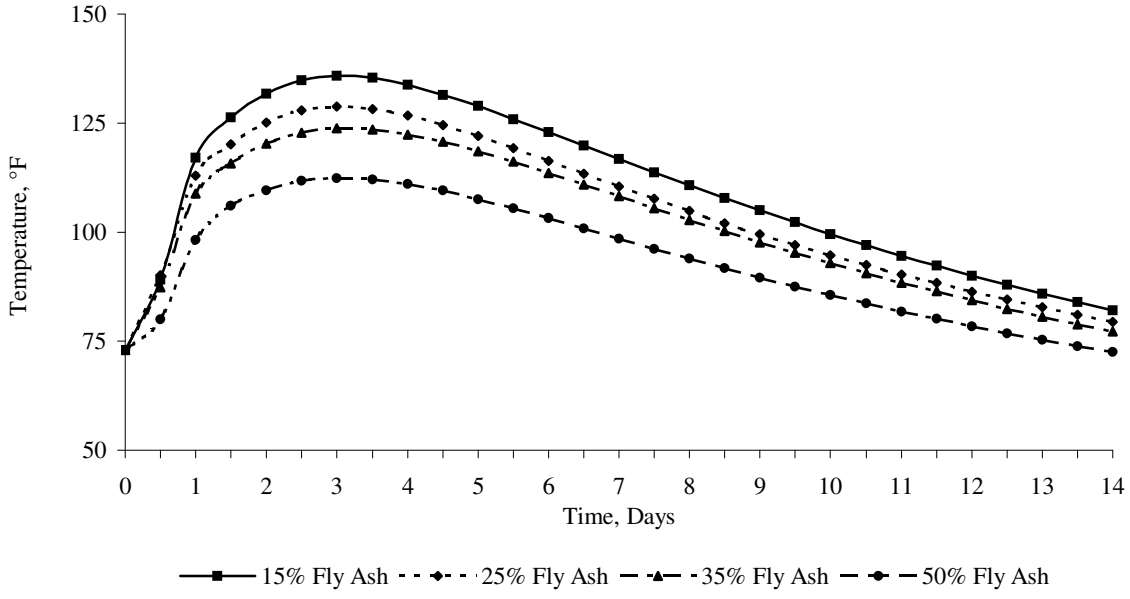

Figure 3-42 –Temperature versus Time for 10ft Pile – ABAQUS – Series 1
(Total Cementitious Materials 675 lb/cy)

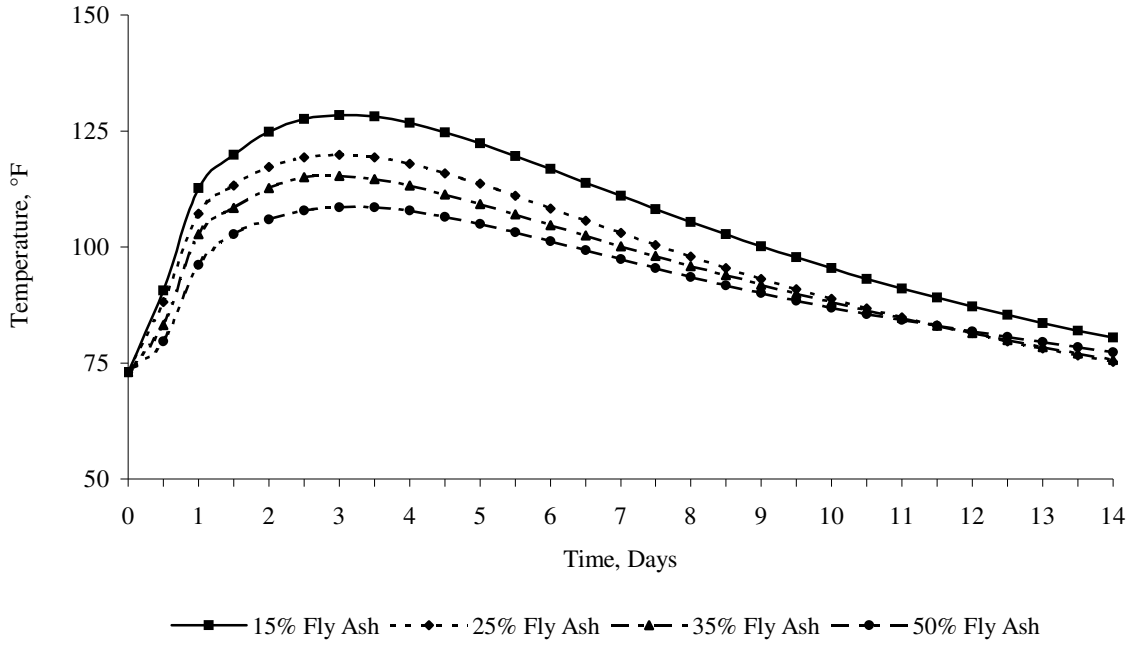

Figure 3-43 –Temperature versus Time for 10ft Pile – ABAQUS – Series 2
(Total Cementitious Materials 591 lb/cy)

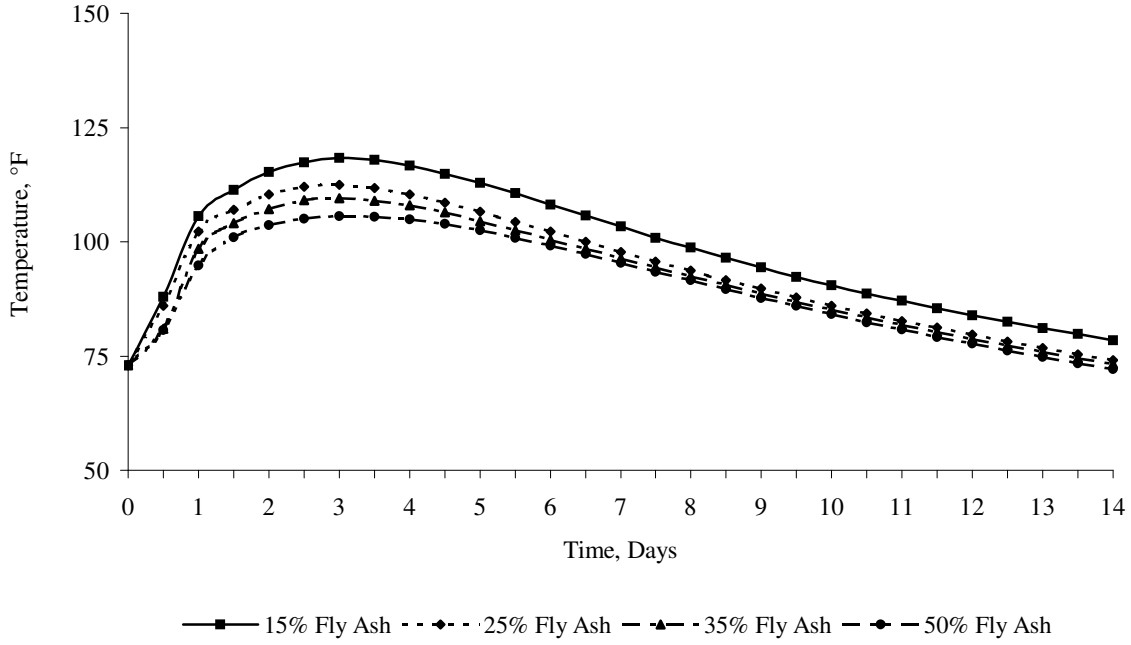

Figure 3-44 – Temperature versus Time for 10ft Pile – ABAQUS – Series 3
(Total Cementitious Materials 506 lb/cy)

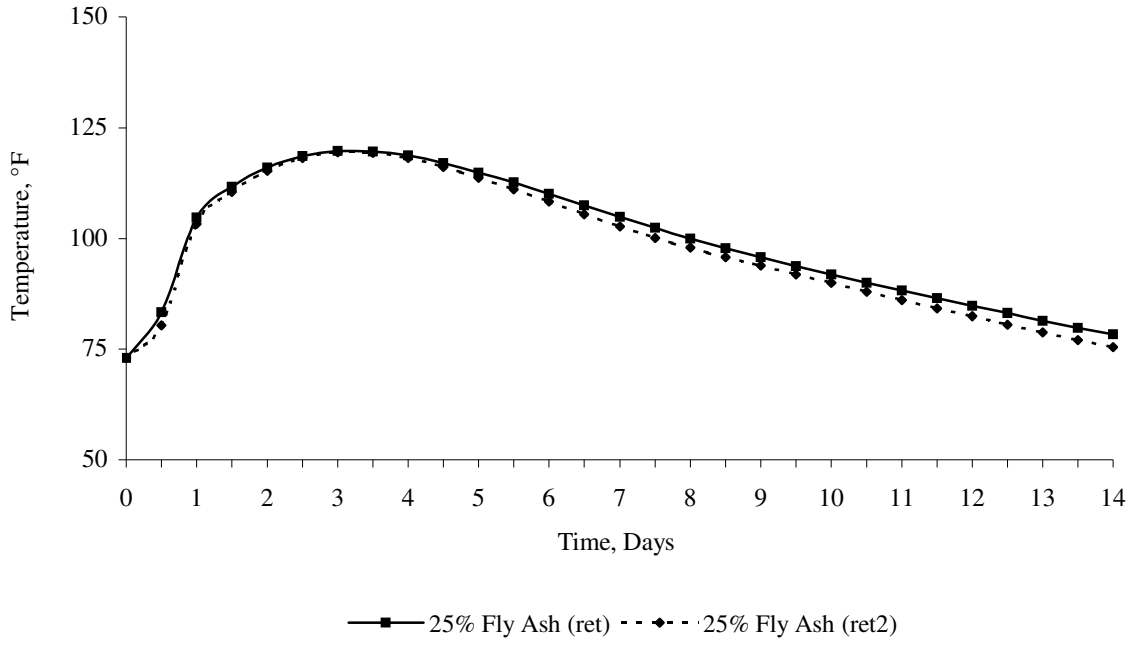

Figure 3-45 – Temperature versus Time for 10ft Pile – ABAQUS – Series 4
(Total Cementitious Materials 591 lb/cy)

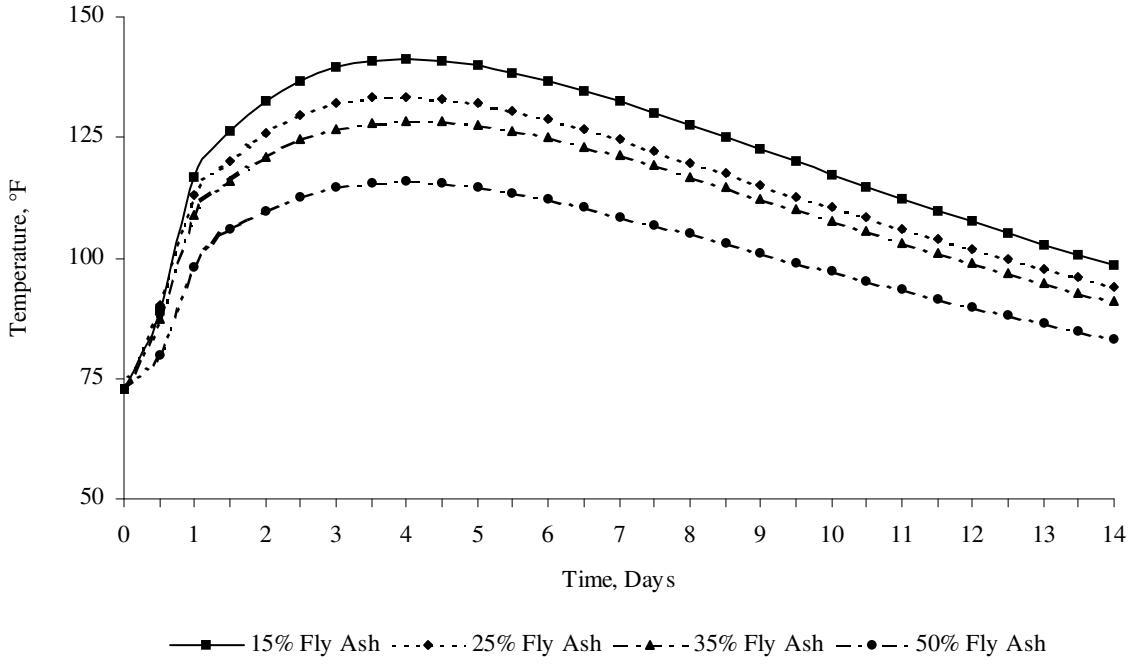

Figure 3-46 – Temperature versus Time for 12ft Pile – ABAQUS – Series 1
(Total Cementitious Materials 675 lb/cy)

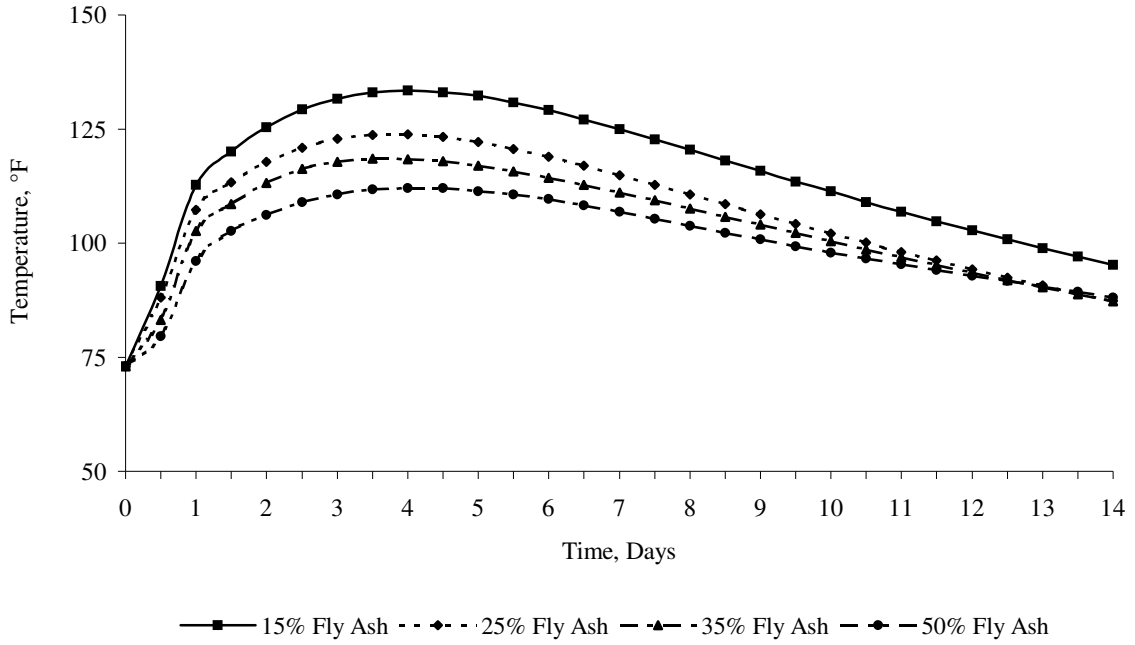

Figure 3-47 – Temperature versus Time for 12ft Pile – ABAQUS – Series 2
(Total Cementitious Materials 591 lb/cy)

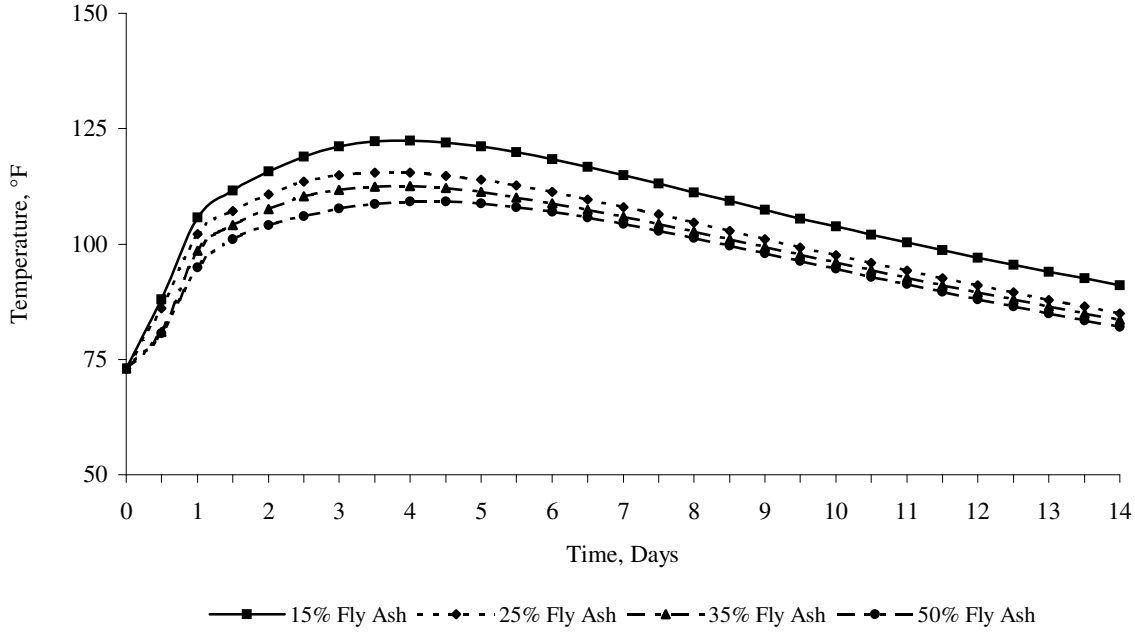

Figure 3-48 – Temperature versus Time for 12ft Pile – ABAQUS – Series 3
(Total Cementitious Materials 506 lb/cy)

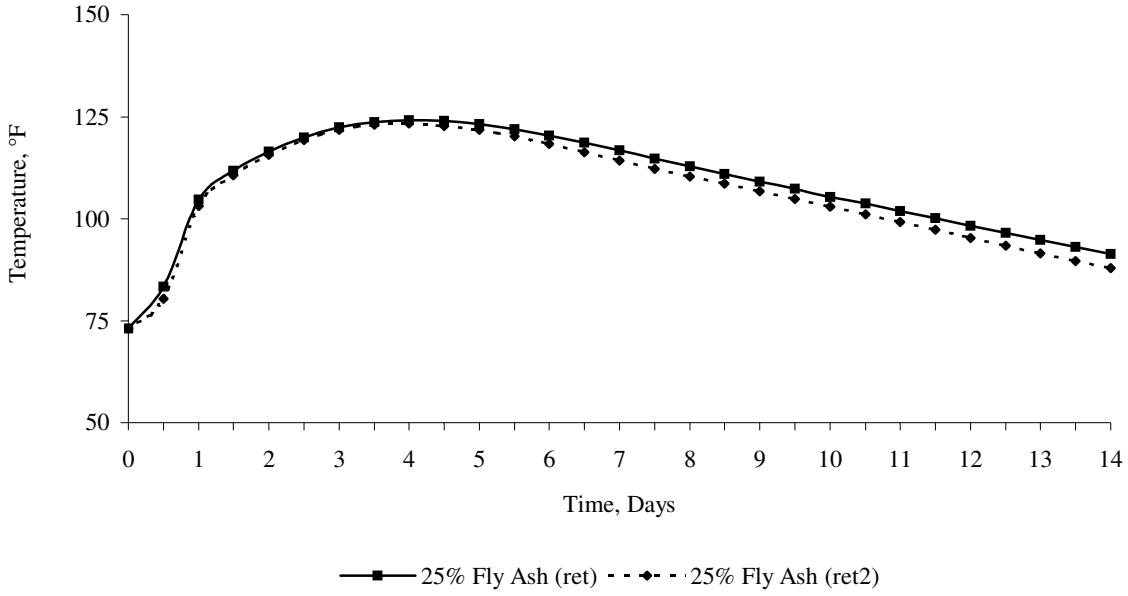

Figure 3-49 – Temperature versus Time for 12ft Pile – ABAQUS – Series 4
(Total Cementitious Materials 591 lb/cy)

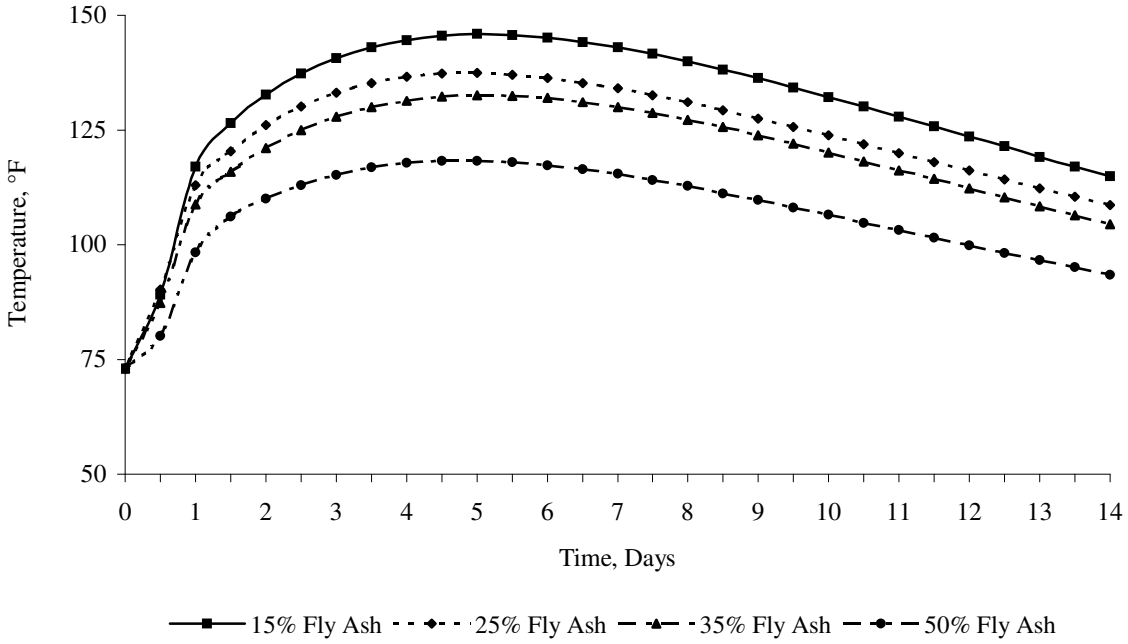

Figure 3-50 – Temperature versus Time for 14ft Pile – ABAQUS – Series 1
(Total Cementitious Materials 675 lb/cy)

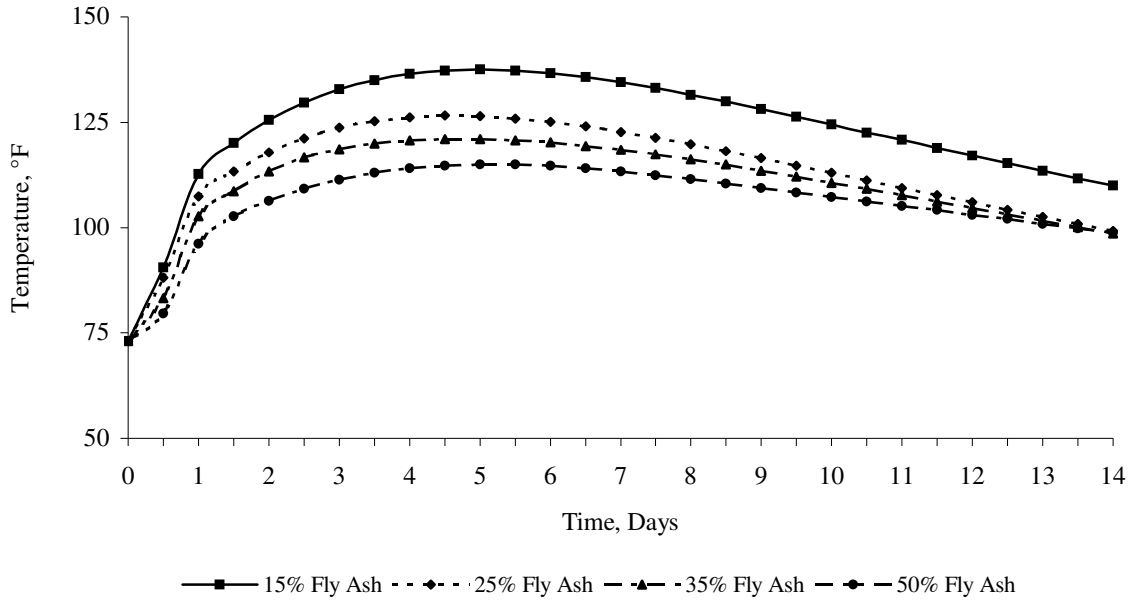

Figure 3-51 – Temperature versus Time for 14ft Pile – ABAQUS – Series 2
(Total Cementitious Materials 591 lb/cy)

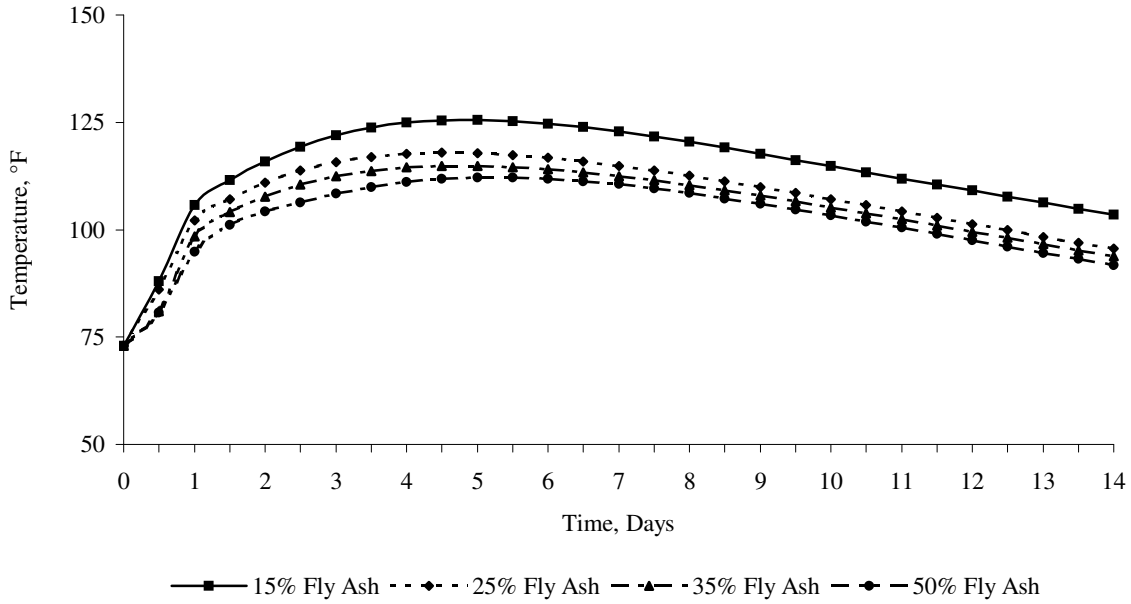

Figure 3-52 – Temperature versus Time for 14ft Pile – ABAQUS – Series 3
(Total Cementitious Materials 506 lb/cy)

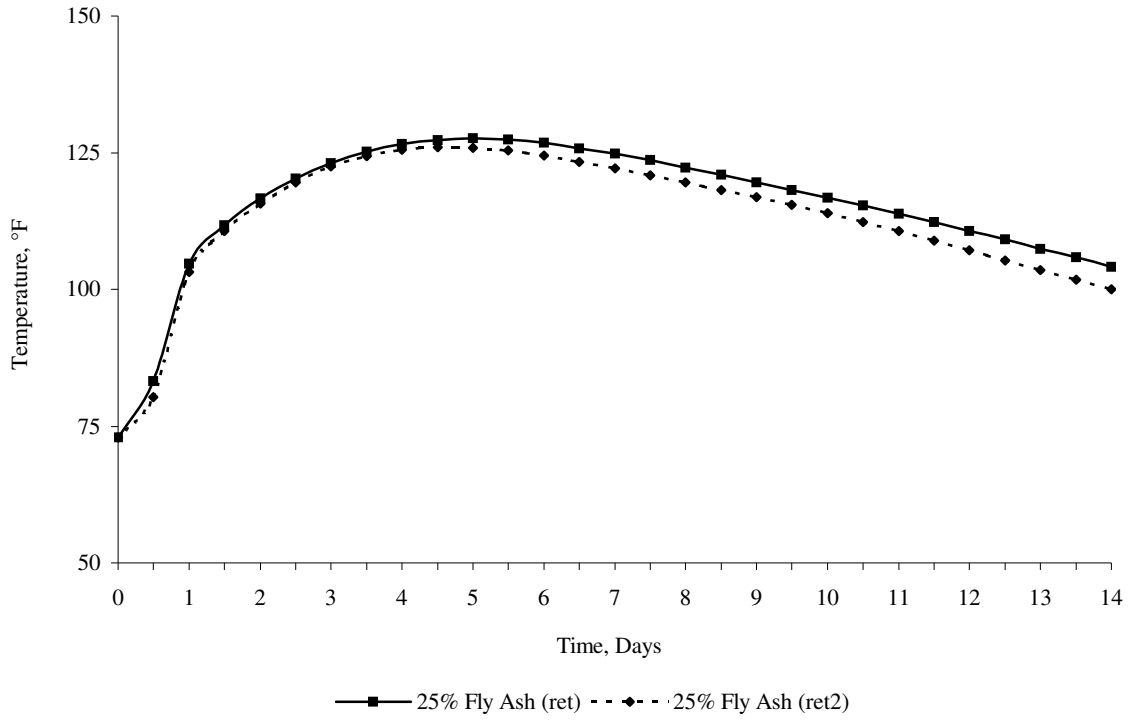

Figure 3-53 – Temperature versus Time for 14ft Pile – ABAQUS – Series 4
(Total Cementitious Materials 591 lb/cy)

The peak temperature at the center of the CIDH concrete piles with different diameters and using the ABAQUS finite element model are shown in Table 3-17 to Table 3-20 and in Figure 3-54 to Figure 3-57. It can be observed that the peak temperature for all diameters is the highest at the 15% fly ash mix.

Table 3-17 - Peak Temperature for Different Pile Diameters – ABAQUS – Series 1

	Temperature in center of pile for series 1 - ABAQUS, °F			
Diameter, ft	**Mix 6070AA (15% Fly Ash)**	**Mix 6070AB (25% Fly Ash)**	**Mix 6070AC (35% Fly Ash)**	**Mix 6070AD (50% Fly Ash)**
6	120.5	114.4	110.8	102.9
8	128.7	122.2	117.7	107.9
10	135.9	128.8	123.8	112.4
12	141.4	133.6	128.6	115.9
14	145.9	137.4	132.6	118.2

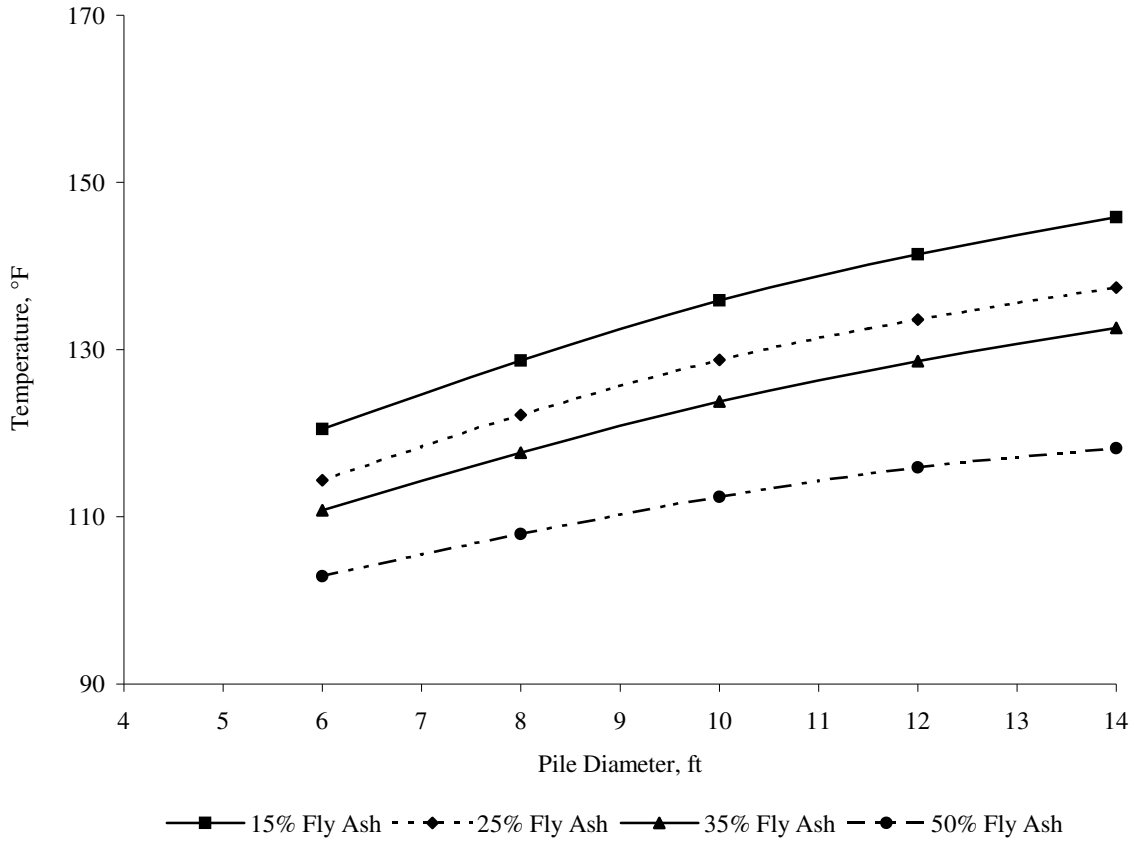

Figure 3-54 - Maximum Temperature at center of pile – ABAQUS – Series 1
(Total Cementitious Materials 675 lb/cy)

Table 3-18 - Peak Temperature for Different Pile Diameters – ABAQUS – Series 2

	Temperature in center of pile for series 2 - ABAQUS, °F			
Diameter, ft	**Mix 6070AE (15% Fly Ash)**	**Mix 6070AF (25% Fly Ash)**	**Mix 6070AG (35% Fly Ash)**	**Mix 6070AH (50% Fly Ash)**
6	110.8	108.2	104.5	98.8
8	117.7	114.6	110.5	104.4
10	128.4	119.9	115.3	108.6
12	133.5	123.8	118.5	112.1
14	137.6	126.6	121.0	115.0

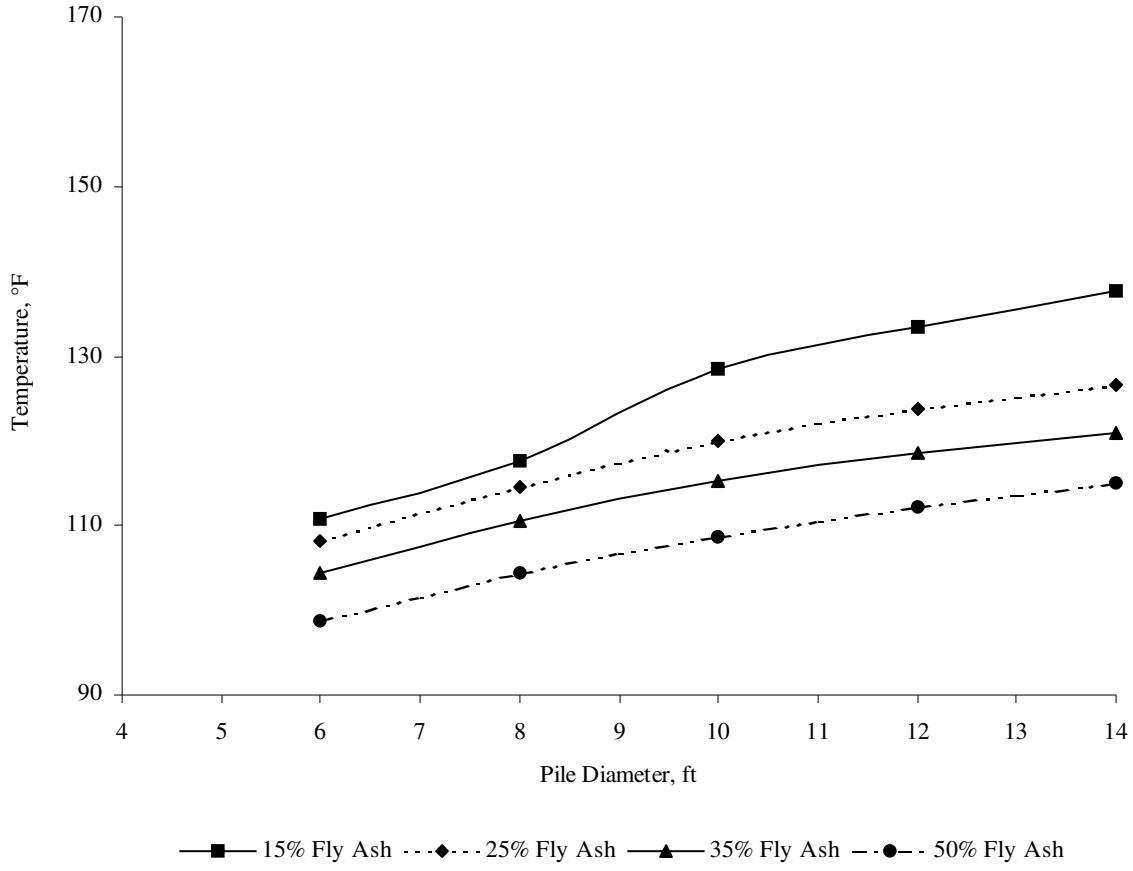

Figure 3-55 - Maximum Temperature at center of pile – ABAQUS – Series 2
(Total Cementitious Materials 591 lb/cy)

Table 3-19 - Peak Temperature for Different Pile Diameters – ABAQUS – Series 3

	Temperature in center of pile for series 3 - ABAQUS,°F			
Diameter, ft	**Mix 6070AI (15% Fly Ash)**	**Mix 6070AJ (25% Fly Ash)**	**Mix 6070AK (35% Fly Ash)**	**Mix 6070AL (50% Fly Ash)**
6	106.6	103.3	100.7	97.8
8	112.7	108.1	105.4	102.0
10	118.3	112.4	109.5	105.6
12	122.4	115.5	112.5	109.2
14	125.6	117.9	114.9	112.2

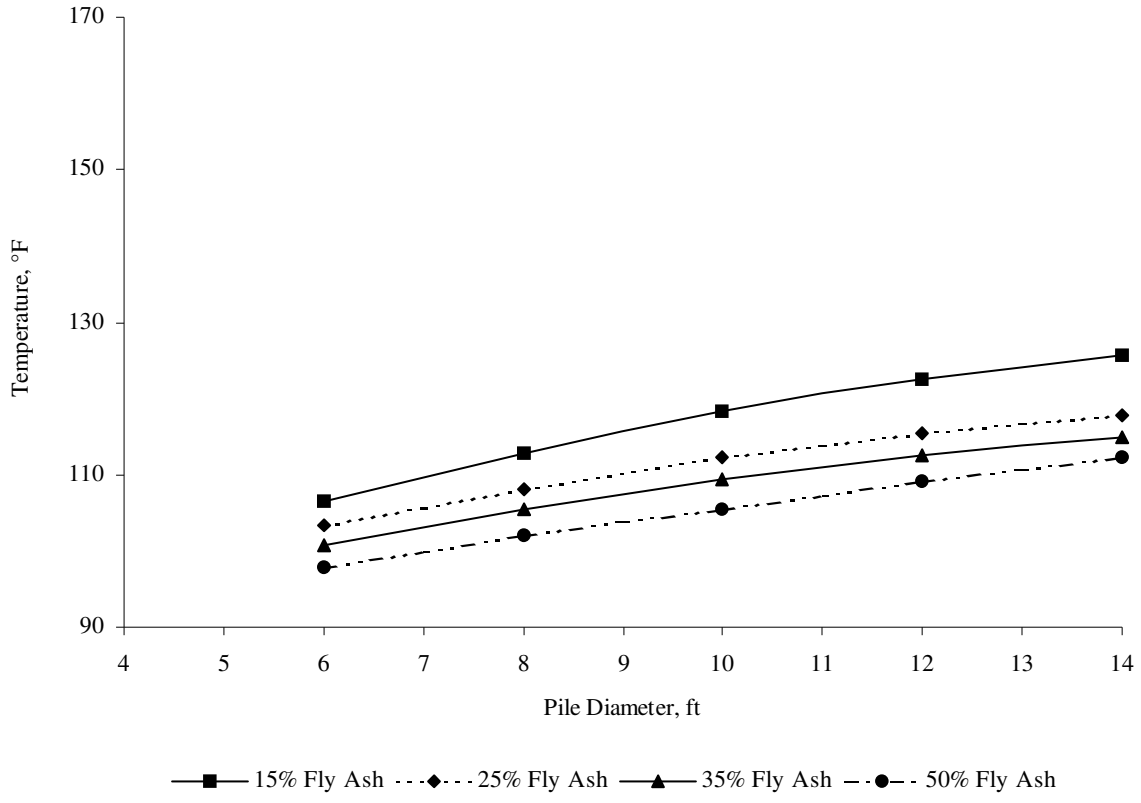

Figure 3-56 - Maximum Temperature at center of pile – ABAQUS – Series 3
(Total Cementitious Materials 506 lb/cy)

Table 3-20 - Peak Temperature for Different Pile Diameters – ABAQUS – Series 4

	Temperature in center of pile for series 4 - ABAQUS, °F	
Diameter, ft	**Mix 6070AM (25% Fly Ash)**	**Mix 6070AN (25% Fly Ash)**
6	107.6	107.1
8	114.2	113.8
10	119.8	119.4
12	124.2	123.3
14	127.6	126.0

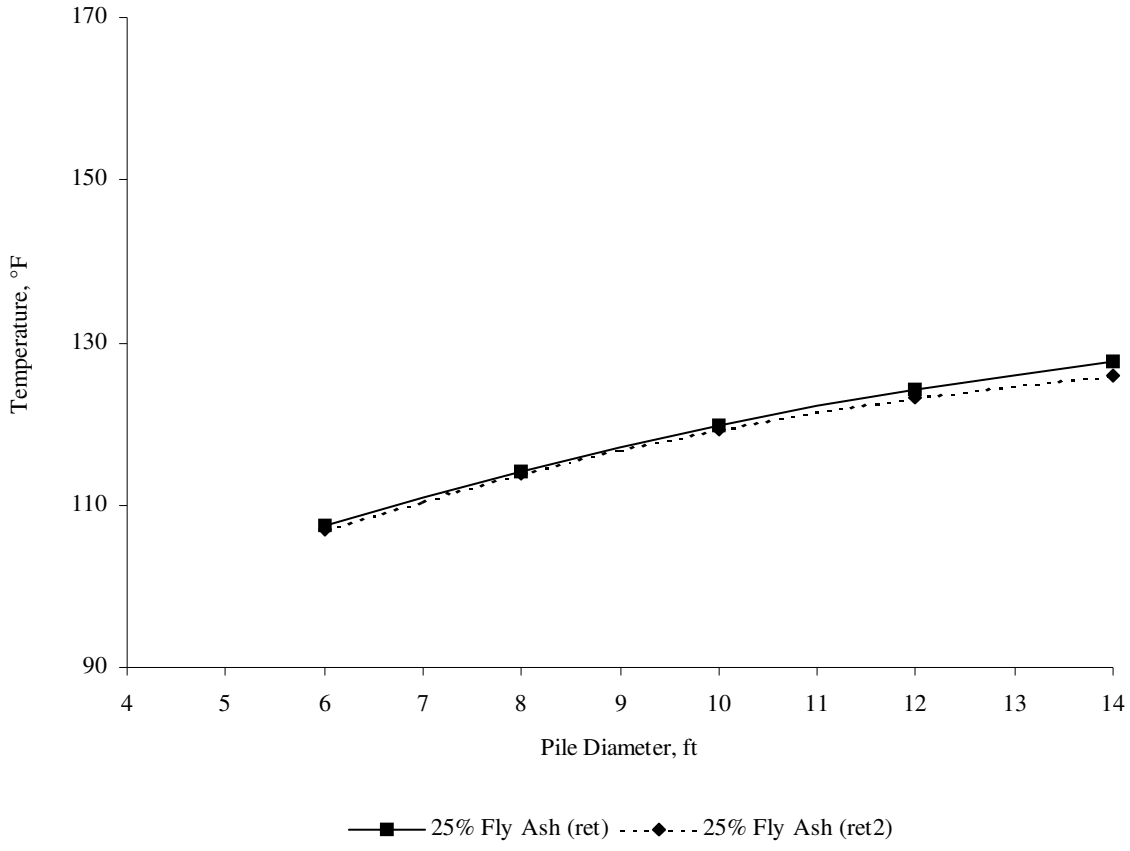

Figure 3-57 - Maximum Temperature at center of pile – ABAQUS – Series 4
(Total Cementitious Materials 591 lb/cy)

3.3.9 Discussion of Results

The peak temperature at the center of the CIDH piles from the ABAQUS and the Schmidt are shown in Figure3-58 to Figure 3-61. It can be observed from these figures that the Schmidt model predicts higher peak temperatures at the center of the CIDH concrete piles than the ABAQUS. The reasons are shown in Table 3-21.

Table 3-21 – Difference between Schmidt and ABAQUS Models

Schmidt model	**ABAQUS Model**
One dimensional - 1D	Three dimensional – 3D
Step-by-step computation	Finite element computation

The percentage difference between the ABAQUS model and the Schmidt model for the peak temperature at the center of the CIDH concrete piles is shown in Table 3-22 to Table 3-25. The difference in percent is calculated from:

$$\% \text{ difference} = \frac{\text{Peak temperature at time } t_1 \text{ (Schmidt)} - \text{Peak temperature at time } t_2 \text{ (ABAQUS)}}{\text{Peak temperature at time } t_1 \text{ (Schmidt)}}$$

Where:

t_1 = time at which peak temperature of the Schmidt is observed

t_2 = time at which peak temperature of the ABAQUS is observed

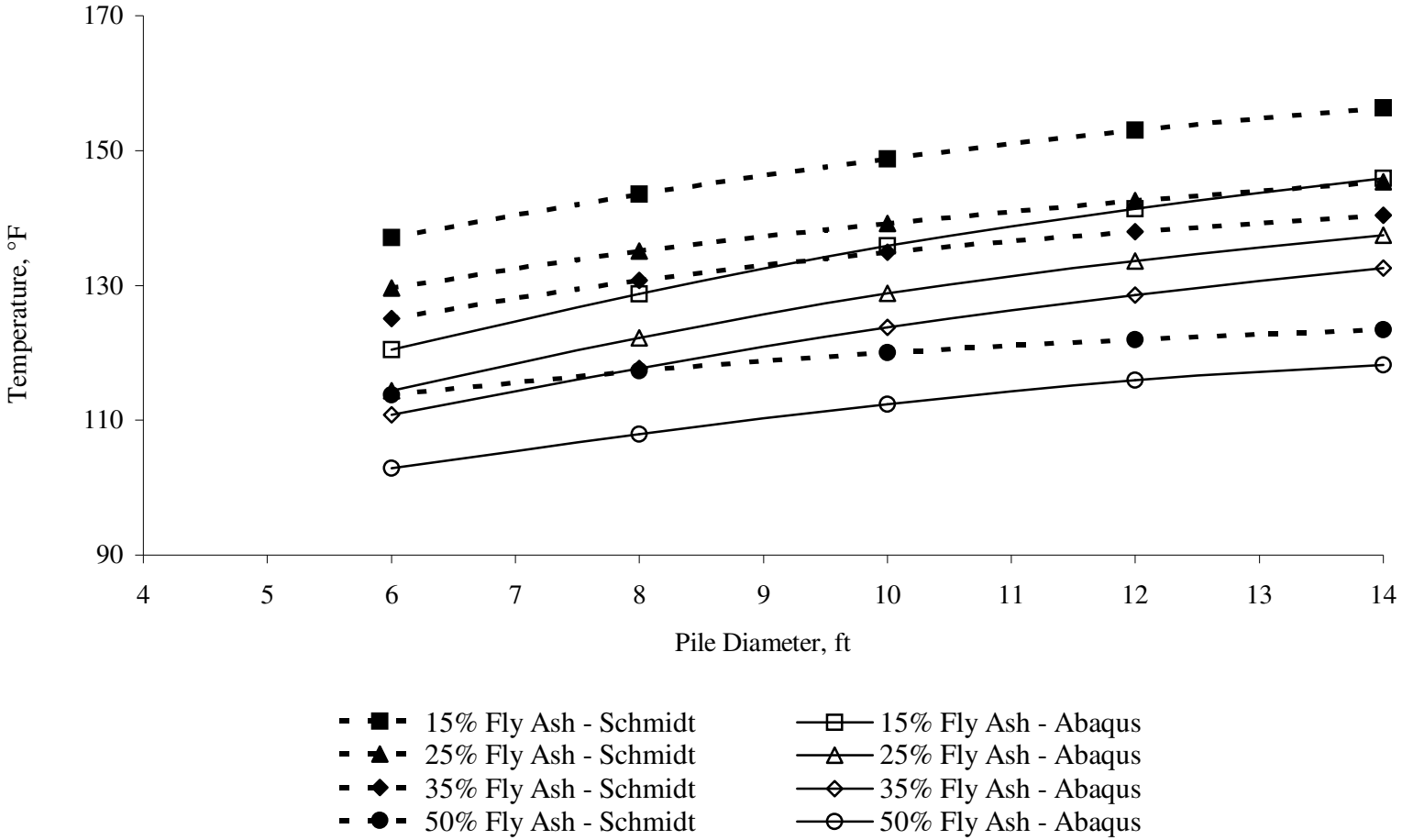

Figure 3-58 - Maximum Temperature – Schmidt versus ABAQUS – Series 1
(Total Cementitious Materials 675 lb/cy)

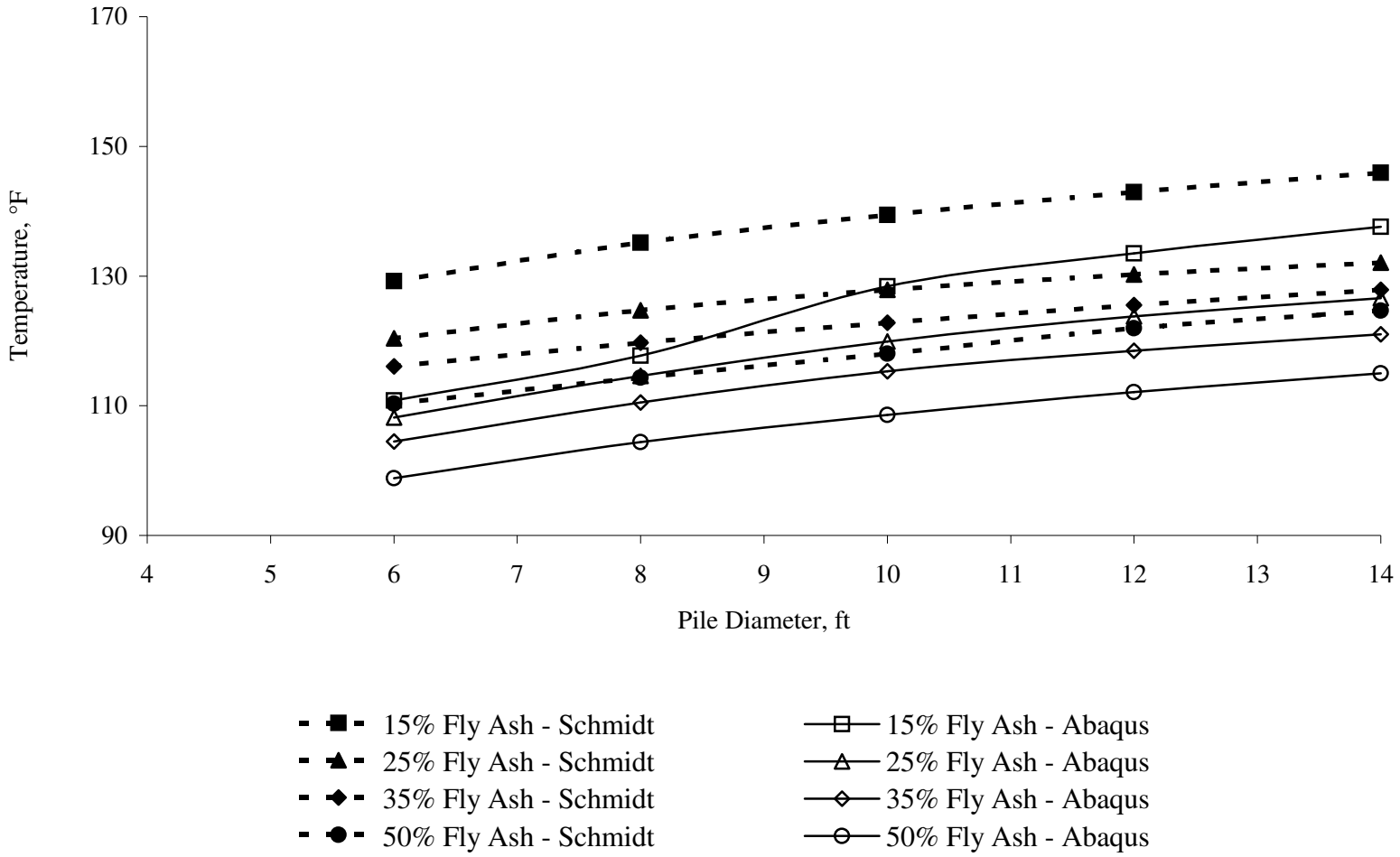

Figure 3-59 - Maximum Temperature – Schmidt versus ABAQUS – Series 2
(Total Cementitious Materials 591 lb/cy)

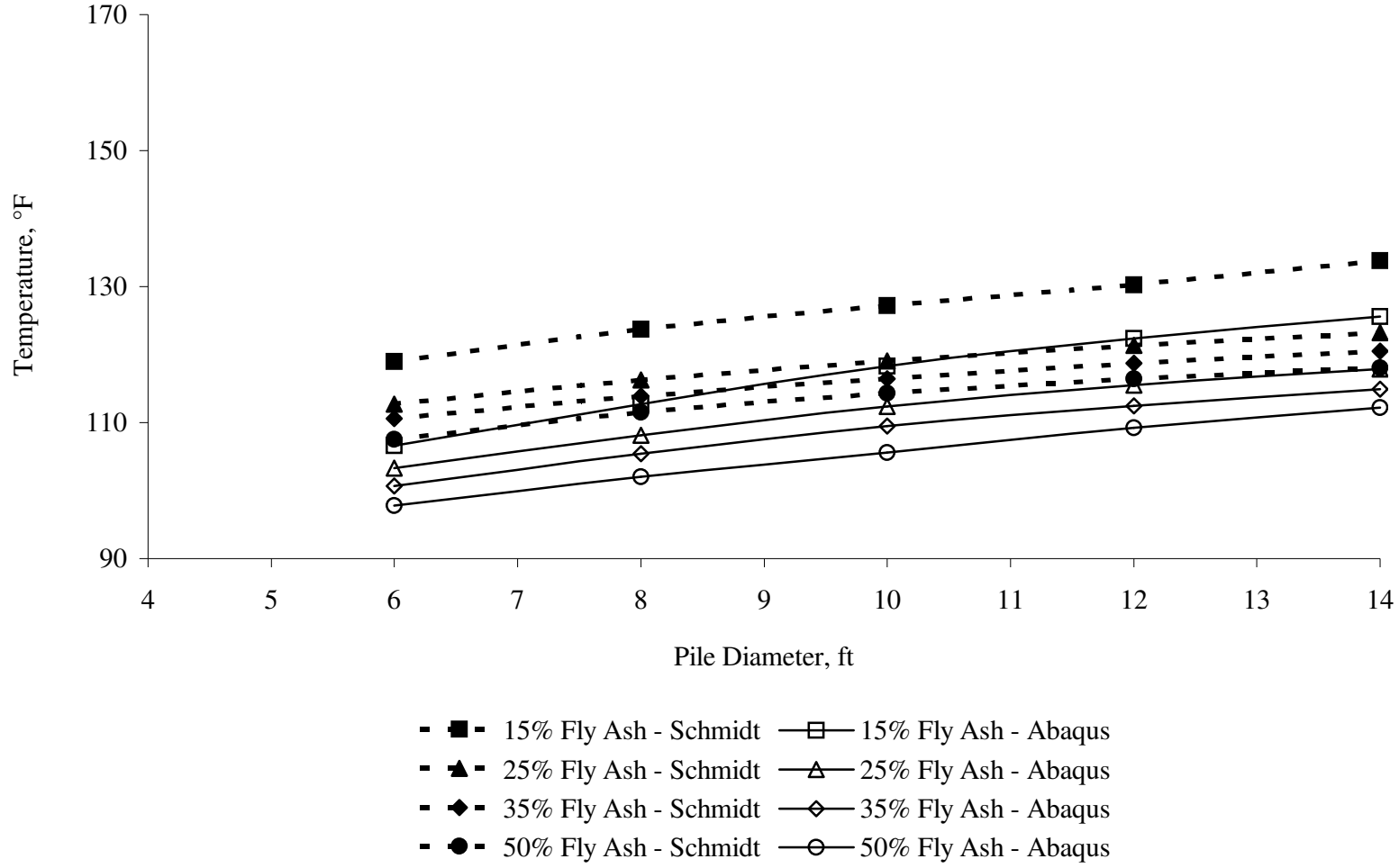

Figure 3-60 - Maximum Temperature – Schmidt versus ABAQUS – Series 3
(Total Cementitious Materials 506 lb/cy)

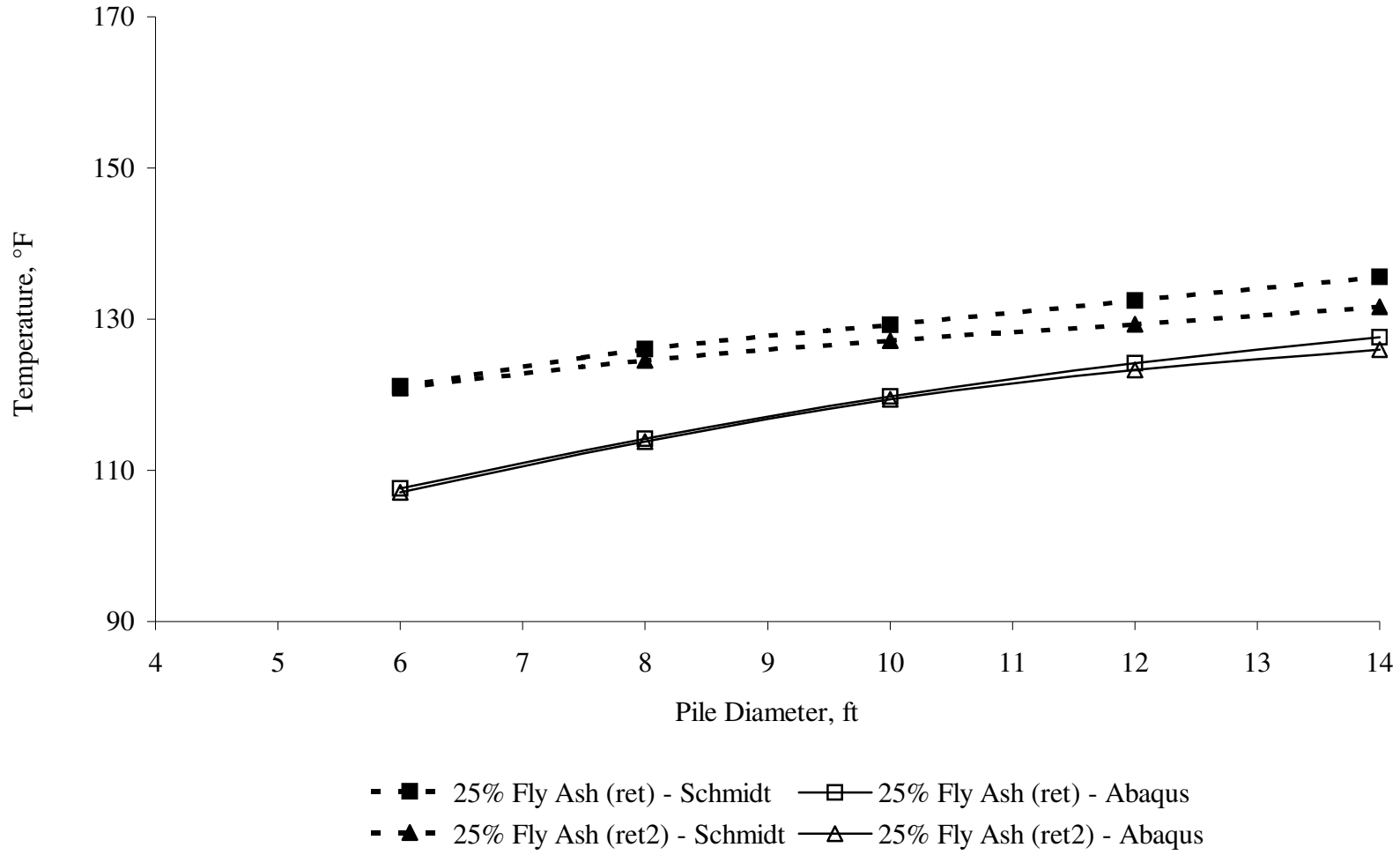

Figure 3-61 - Maximum Temperature – Schmidt versus ABAQUS – Series 4
(Total Cementitious Materials 591 lb/cy)

Table 3-22 – Temperature Percentage Difference - Schmidt vs. ABAQUS – Series 1
(Total Cementitious Materials 675 lb/cy)

	Temperature percentage difference in center of pile for series 1 – Schmidt versus ABAQUS			
Diameter, ft	**Mix 6070AA (15% Fly Ash)**	**Mix 6070AB (25% Fly Ash)**	**Mix 6070AC (35% Fly Ash)**	**Mix 6070AD (50% Fly Ash)**
6	12%	12%	11%	10%
8	10%	10%	10%	8%
10	9%	7%	8%	6%
12	8%	6%	7%	5%
14	7%	5%	6%	4%

Table 3-23 – Temperature Percentage Difference - Schmidt vs. ABAQUS – Series 2
(Total Cementitious Materials 591 lb/cy)

	Temperature percentage difference in center of pile for series 2 – Schmidt versus ABAQUS			
Diameter, ft	**Mix 6070AE (15% Fly Ash)**	**Mix 6070AF (25% Fly Ash)**	**Mix 6070AG (35% Fly Ash)**	**Mix 6070AH (50% Fly Ash)**
6	14%	10%	10%	10%
8	13%	8%	8%	9%
10	8%	6%	6%	8%
12	7%	5%	6%	8%
14	6%	4%	5%	8%

Table 3-24 **–** Temperature Percentage Difference - Schmidt vs. ABAQUS – Series 3 (Total Cementitious Materials 506 lb/cy)

	Temperature percentage difference in center of pile for series 3 – Schmidt versus ABAQUS			
Diameter, ft	**Mix 6070AI (15% Fly Ash)**	**Mix 6070AJ (25% Fly Ash)**	**Mix 6070AK (35% Fly Ash)**	**Mix 6070AL (50% Fly Ash)**
6	10%	8%	9%	9%
8	9%	7%	7%	9%
10	7%	6%	6%	8%
12	6%	5%	5%	6%
14	6%	4%	5%	5%

Table 3-25 - Temperature Percentage Difference - Schmidt vs. ABAQUS – Series 4 (Total Cementitious Materials 591 lb/cy)

	Temperature percentage difference in center of pile for series 4 –- Schmidt versus ABAQUS	
Diameter, ft	**Mix 6070AM (25% Fly Ash) (ret)**	**Mix 6070AN (25% Fly Ash) (ret2)**
6	11%	11%
8	9%	9%
10	7%	6%
12	6%	5%
14	6%	4%

For the 6, 8, 10, 12 and 14 ft piles, the percent difference was 10.5 %, 9.0 %, 7.0 %, 6.1 % and 5.4 % respectively.

Figure 3-62 to Figure 3-66 show temperature versus time comparison between the Schmidt and the ABAQUS for the mix 6070AA from series 1. These graphs show the peak temperature of each pile and highlight the differences between the two models. As shown from these figures, the ABAQUS and the Schmidt predict similar peak temperatures for the large 14 ft diameter pile, but the error becomes significantly higher for the smaller 6 ft diameter pile.

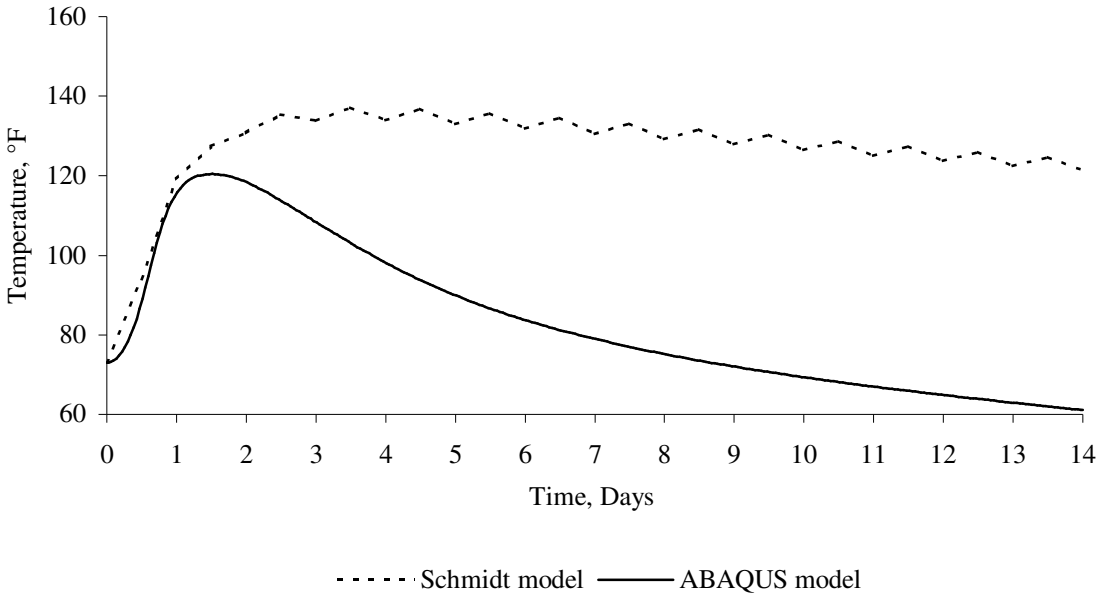

Figure 3-62 – Temperature versus Time for 6 ft Pile – 15% Fly Ash - Series1

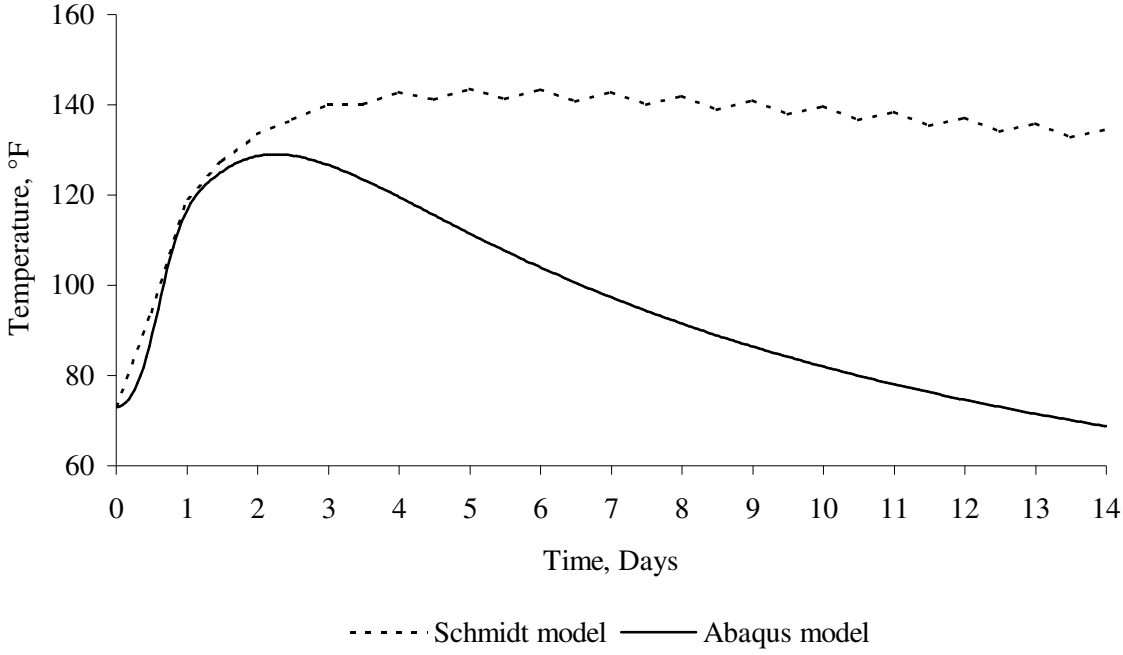

Figure 3-63 – Temperature versus Time for 8 ft Pile – 15% Fly Ash - Series1

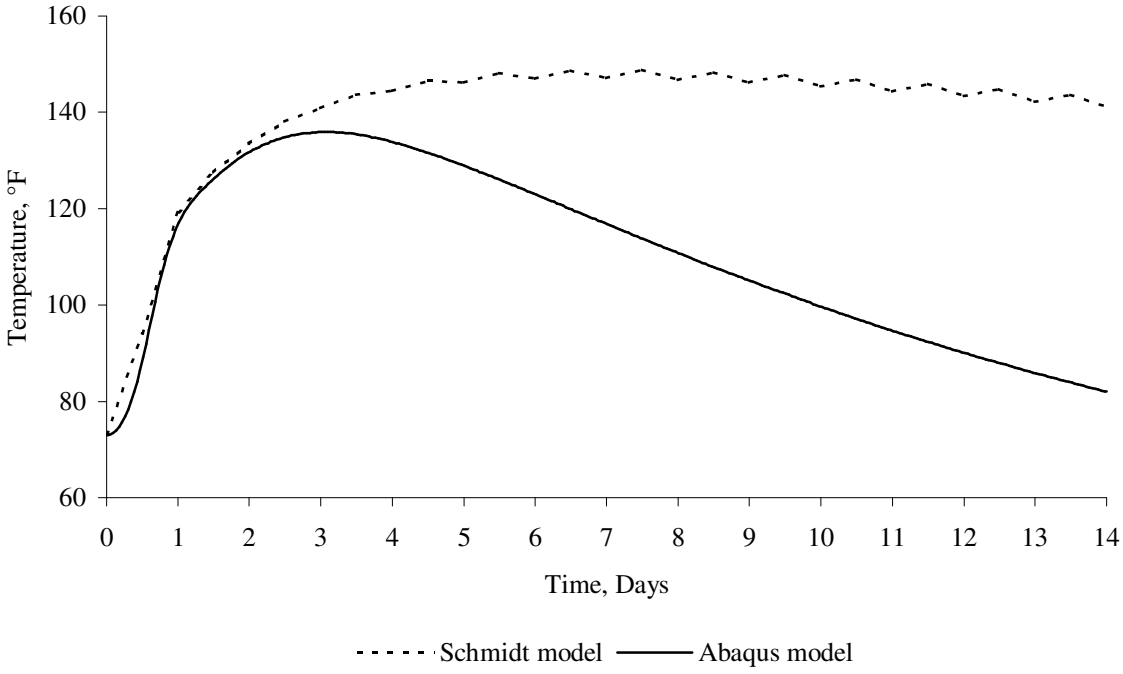

Figure 3-64 – Temperature versus Time for 10 ft Pile – 15% Fly Ash - Series1

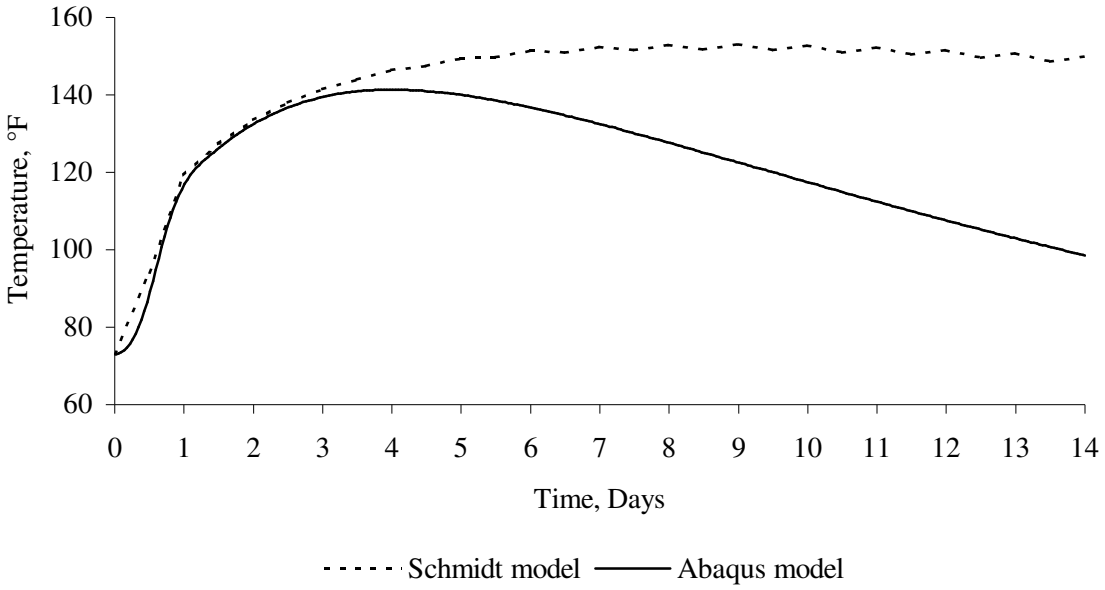

Figure 3-65 – Temperature versus Time for 12 ft Pile – 15% Fly Ash - Series1

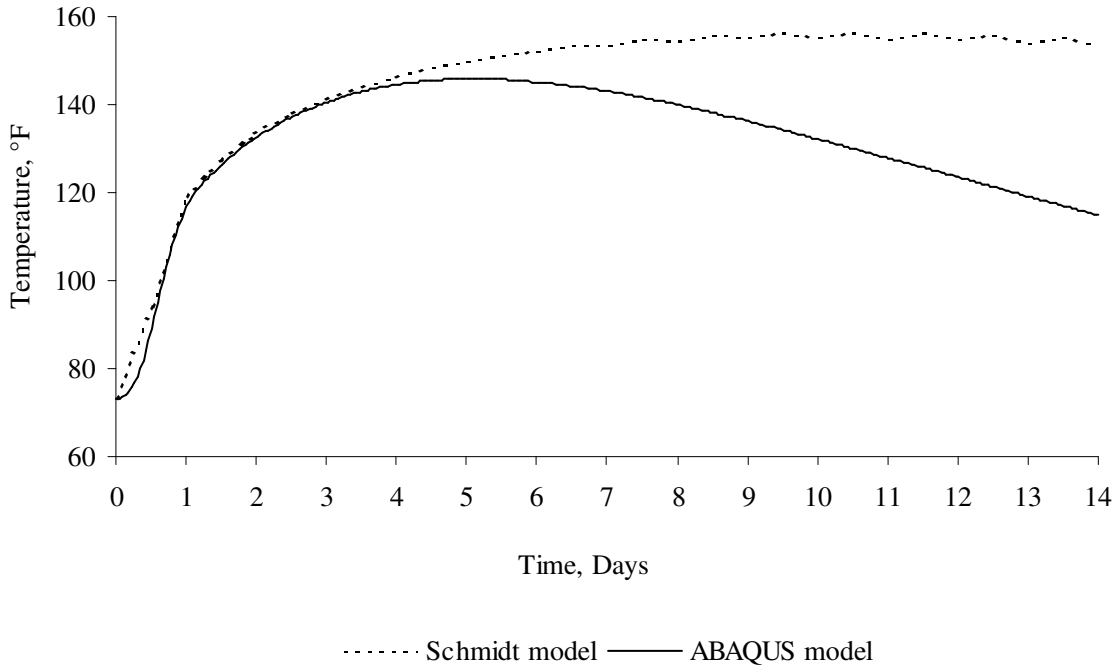

Figure 3-66 – Temperature versus Time for 14 ft Pile – 15% Fly Ash - Series1

CHAPTER 4 CONCLUSIONS AND RECOMMENDATIONS

4.1 Summary

This study used two guidelines, the ACI (Schmidt model) and the finite element program (ABAQUS), to determine the heat of hydration of mass concrete pile and to find the peak temperature that a pile can reach. An acceptable design criteria for mass concrete for CIDH piles is provided.

Data from Schmidt model, shown in Tables 3-11, 3-12, 3-13 and 3-14, are summarized in Table 4-1. Data from ABAQUS model, shown in Tables 3-20, 3-21, 3-22, and 3-23, are summarized in Table 4-2. It can be observed from Tables 4-1 and 4-2 that the Schmidt model predicts higher peak temperatures the ABAQUS model.

4.2 Conclusions

Using ABAQUS finite element program and the ACI 207 Schmidt model, the peak temperature can be predicted for various CIDH concrete piles. The study shows that ABAQUS can be an effective tool to predict the percentage of Fly Ash that can be used effectively to reduce the peak temperatures of a concrete structure.

The ABAQUS model delivers a more accurate result than the Schmidt model, and is considered more reliable in predicting the peak temperature of concrete structures.

The ABAQUS and the Schmidt model predict similar peak temperatures for large diameter piles, but their results differ significantly for smaller diameter piles.

For a peak temperature of 140^{o}F in CIDH concrete piles with varying diameters between 6 and 14 foot, the mixes that are acceptable in term of cement contents are given in Table 4-3.

4.3 Future Recommendations

The followings recommendations are proposed for future studies:

- Conducting an experimental study to compare the experimental results to the finite element model results for the CIDH concrete piles.
- Conducting a study to determine the positions and widths of cracks, resulting from heat of hydration of concrete piles.

Table 4-1 – Peak Temperature at center of CIDH piles using Schmidt

	SERIES 1				SERIES 2				SERIES 3				SERIES 4	
Toatal Cementitious Materials, lb/cy	**675**				**591**				**506**				**591**	
Fly Ash, %	**15**	**25**	**35**	**50**	**15**	**25**	**35**	**50**	**15**	**25**	**35**	**50**	**25 (ret)***	**25 (ret2)**
Cement, sacks	**6.1**	**5.4**	**4.7**	**3.6**	**5.2**	**4.6**	**4.1**	**3.1**	**4.5**	**4.0**	**3.5**	**2.7**	**4.6**	**4.6**
6ft diameter	137.1	129.6	125.1	113.7	129.2	120.4	116.1	110.3	119.0	112.7	110.6	107.6	121.1	120.9
8ft diameter	143.6	135.1	130.8	117.4	135.2	124.7	119.7	114.3	123.7	116.3	113.9	111.5	126.0	124.5
10ft diameter	148.8	139.2	134.9	120.0	139.4	127.9	122.8	118.0	127.2	119.1	116.4	114.3	129.3	127.2
12ft diameter	153.0	142.5	138.0	122.0	142.9	130.2	125.5	121.9	130.3	121.4	118.7	116.4	132.5	129.3
14ft diameter	156.4	145.4	140.4	123.4	145.9	132.1	127.9	124.7	133.8	123.2	120.5	118.1	135.6	131.6

*ret: Retarder type D

Table 4-2 – Peak Temperature at center of CIDH piles using ABAQUS

	SERIES 1				SERIES 2				SERIES 3				SERIES 4	
Toatal Cementitious Materials, lb/cy	**675**				**591**				**506**				**591**	
Fly Ash, %	**15**	**25**	**35**	**50**	**15**	**25**	**35**	**50**	**15**	**25**	**35**	**50**	**25 (ret)***	**25 (ret2)**
Cement, sacks	**6.1**	**5.4**	**4.7**	**3.6**	**5.2**	**4.6**	**4.1**	**3.1**	**4.5**	**4.0**	**3.5**	**2.7**	**4.6**	**4.6**
6ft diameter	120.5	114.4	110.8	102.9	110.8	108.2	104.5	98.8	106.6	103.3	100.7	97.8	107.6	107.1
8ft diameter	128.7	122.2	117.7	107.9	117.7	114.6	110.5	104.4	112.7	108.1	105.4	102.0	114.2	113.8
10ft diameter	135.9	128.8	123.8	112.4	128.4	119.9	115.3	108.6	118.3	112.4	109.5	105.6	119.8	119.4
12ft diameter	141.4	133.6	128.6	115.9	133.5	123.8	118.5	112.1	122.4	115.5	112.5	109.2	124.2	123.3
14ft diameter	145.9	137.4	132.6	118.2	137.6	126.6	121.0	115.0	125.6	117.9	114.9	112.2	127.6	126.0

*ret: Retarder type D

Table 4-3 – Mixes Acceptable for CIDH piles for a temperature less than 140^{o}F

	Quantity of Portland Cement measured in sacks should be equal or less than:	
Diameter, ft	**Schmidt Model**	**ABAQUS Model**
6	6.1 with FA* ≥ 15%	6.1 with FA ≥ 15%
8	5.4 with FA ≥ 25%	6.1 with FA ≥ 15%
10	4.7 with FA ≥ 35%	6.1 with FA ≥ 15%
12	4.7 with FA ≥ 35%	5.4 with FA ≥ 25%
14	4.6 with FA ≥ 50%	5.4 with FA ≥ 25%

*FA: Fly Ash

CHAPTER 5 THERMAL SPECIFICATION FOR CONCRETE PILING

5.1 Assumptions

The assumptions made to compute max temperatures for the preparation of this specification are as follows:

1. The computed max temperature in both the Schmidt and ABAQUS models is based upon a starting concrete temperature of 73^{o}F.
2. Models are assumed to be adiabatic systems used to compute thermal properties of the pilings independent of the ambient conditions. This assumption allows the scaling of initial and final internal temperatures using the temperature differences computed by the models.
3. The boundary temperature of 55^{o}F for the outside of the piling is independent of the initial concrete temperature.
4. Maximum allowable internal temperature of the concrete is 140^{o}F. This is the basis for development of this specification. This temperature is generally accepted as the max temperature that can be reached without danger of DEF formation.
5. The temperature limit on maximum differential is related to crack formation and requires specific knowledge of the concrete thermal expansion properties. The limit of 140^{o}F max is assumed to be low enough that differential temperature is

not a factor. Using the maximum predicted temperature to develop the specification is relatively straightforward. Further work is required if the specification were to be based upon crack potential since these computations requires much more detailed information about the thermal expansion properties of the concrete.

6. Although results from both models are show in the tables, the ABAQUS results are used to develop the specification limits.

5.2 Procedure

Maximum temperatures computed in the models were scaled to show the deviation from the 140^{o}F limit and the predicted temperatures for various initial concrete casting temperatures. Table 5-1 shows the deviations for casting temperature of 75 F used in the model.

5.3 Observations

1. 90 Degree F casting temperature
    a. At cement contents at 590 lb/cy or higher temperatures with 15% Fly ash are approaching the heat limit for all pilings (Schmidt Model). Since most of the concrete used in pilings will have a 25% replacement for ASR (Alkali-Silica reaction) purposes it simplifies the thermal specification if the minimum fly ash content is set at 25%.

b. At cement contents of 505 lb/cy piling up to 14 ft in diameter at 15% fly ash and higher replacement values will not exceed 140°F.

c. At cement contents of 675 lb/cy (400 kg/m^3) pilings larger than 8 ft diameter will exceed 140°F.

2. 85 Degree F casting temperature

   a. At cement contents 590 lb/cy and lower the temperature will be below 140°F for all diameters up to 14 ft.

   b. At cement contents 650 lb/cy and lower pilings 10 ft diameter and smaller will not exceed 140°F.

3. 80 degree F casting temperature

   a. Predicted by Abacus, piling up to 14 ft diameter cement contents 650 and lower should not significantly exceed 140°F.

4. 75 degree F casting temperature

   a. Predicted by Schmidt, piling up to 14 ft diameter cement contents 650 and lower should not significantly exceed 140°F.

5.4 Specification Development

Under current Caltrans standard specifications the use of 25% minimum cement replacement is, in most cases, required. Development of a specification with 35% replacement might be appropriate for large sections; it has very little significance for piling up to 14 ft diameter. The experimental data shows that there is no significant thermal change when the concrete is retarded. It appears from this study that a standard

specification for the majority of Caltrans projects can be written to limit the maximum internal temperature by addressing cement contents, casting temperature and piling diameter. The most versatile approach is to make it the responsibility of the contractor to provide a thermal control plan and then give him some limits where computations and extensive materials testing is not required.

5.5 Cast Piling Thermal Specification

It is the responsibility of the contractor to submit a thermal control plan outlining means and methods for limiting the maximum internal temperature of concrete pilings to 140^{o}F. Computations will not be required if the following conditions are met.

Minimum fly ash replacement shall be no less than 25% for the cement content listed in Table 5-1. Maximum cement contents shall not exceed those listed for the maximum casting temperature and piling diameter shown.

Table 5-1 – Maximum Allowable Cement Content

Piling Diameter	**Maximum Allowable Cement Content**
90 Degree F Maximum Casting Temperature	
8 ft and less	675 lb/cy (400 kg/m^3)
Larger than 8 ft to 14 ft	590 lb/cy (350 kg/m^3)
Larger than 14 ft	Thermal Computations required
85 Degree F Maximum Casting Temperature	
8 ft and less	675 lb/cy (400 kg/m^3)
12 ft to 14 ft	590 lb/cy (350 kg/m^3)
Larger than 14 ft	Thermal Computations required
85 Degree F Maximum Casting Temperature	
14 ft or less	675 lb/cy (400 kg/m^3)
Larger than 14 ft	Thermal Computations required

APPENDIX A LITERATURE REVIEW

A.1 Introduction

Mass Concrete is defined by ACI 207 as "any volume of concrete with dimensions large enough to require that measures and be taken to cope with generation of heat from hydration of the cement and attendant volume change to minimize cracking." [11]

When hydraulic cement is mixed with water, chemical reactions will occur causing a temperature rise in the concrete mass. The heat generated due to this temperature rise is called the heat of hydration. Several factors affecting the hydration process and the interactions of all these factors are quite complex. Most factors influencing the hydration process will also influence the rate of heat development and need to be accounted for in any mechanistic modeling procedure. The factors influencing temperature rise include the amount and type of cement and admixtures used, the water content, the construction conditions, the thermal properties of the concrete, the geometry of the structure, and the surrounding environmental conditions.

After placement of concrete, the temperature within the structure reach its peak within a period varying from few days to weeks then the concrete cools to a final stable temperature. When the internal temperature of the concrete exceeds a critical value, the chemical reaction allows the potential for delayed ettringite formations (DEF) during curing. The DEF is an internal form of concrete deterioration. However, the change in volume occurs proportionally to the temperature change and the coefficient of thermal expansion of the concrete. If the volume change is restrained during cooling period of

the mass, then sufficient tensile strain can develop causing internal cracks and self-deterioration.

Several studies have been conducted to simulate the thermal behavior of a concrete structure. Different analytical and numerical methods are available. Most of these methods yield approximate but conservative prediction. Among these different methods, the finite element model has been proven to accurately predict the temperature variation in mass concrete across a given time and size. Another method, the Schmidt model provided by the ACI 207.1R, which is a fast approach since it can be solved with computer spreadsheets, but the accuracy of the results vary by the size of the structure being modeled.

In the following sections, different experimental, numerical, and analytical methods are summarized. The experimental methods measure the adiabatic temperature rise of different mixes. The analytical methods use measured heat of hydration values to estimate temperature profile in a structure foe a given time.

A.2 Experimental Methods

There are two main experimental methods used to measure the heat of hydration of concrete. These two methods are: the Adiabatic Calorimetry and Isothermal Calorimetry known as Conduction Calorimetry.

A.2.1 Adiabatic Calorimetry

This method allows the determination of the total heat and the rate of heat generation in the sample. In this method, there is no heat transfer between the test sample and its surrounding. This method is described in more details in Appendix B.

A.2.2 Isothermal Calorimetry

This method often called conduction calorimetry. It allows the measurement of thermal power under constant temperature conditions from a hydrating cementitious paste sample. The difference between this method and the Adiabatic Calorimetry method is that the isothermal method uses a Dewar or thermos flask to prevent heat loss instead of an adiabatic control system. The hydration process will be affected because of the difficulty of determining the heat loss from the flask. This method does not allow the sample to reach the temperatures that it would in a concrete mix since the rate of hydration is dependant on temperature and then the true condition is not simulated.

A.3 Numerical Methods

There have been numerous methods developed to predict the temperature of a mass concrete using software and models. The results from these numerical methods are often compared to the experimental work. Among the various numerical methods that exist, four of them are discussed in the following sections. These methods are: Construction Technology Laboratories, Bentz and Associates, Ballim, and Swaddiwudhipong and Associates.

A.3.1 Construction Technology Laboratories

While working at the Construction Technology Laboratories (CTL), Gadja developed a program that uses the Schmidt method to analyze a one, two or three-dimensional concrete element. This program is capable of predicting the maximum concrete temperature for any concrete mix proportion in various placement conditions.[12]

A.3.2 Bentz and Associates

Bentz and Associates developed a three-dimensional microstructural model to predict the adiabatic temperature rise in a concrete structure. The results from this model correlates well with the corresponding experimental results.[13]

A.3.3 Ballim

A two-dimensional finite model was developed by Ballim to predict the temperature profiles across time in mass concrete. Based on Ballim reports, the accuracy of this model is within 3.6°F throughout the specified temperature range.[14]

A.3.4 Swaddiwudhipong and Associates

Swaddiwudhipong and Associates developed a numerical model to predict the process of hydration of the cement and the rise of temperature in the mass concrete. Their conclusion was: "Compared with other empirical methods, the proposed model serves as a more reasonable and effective tool to predict the evolution of heat of hydration, the degree of hydration and the temperature rise in concrete mixtures". [15]

A.4 Analytical Methods for Temperature Calculation

For thermal studies, the computation of temperature distribution and the boundary conditions is required in a structure, and the complexity of this computation varies widely depending on the method used. The methods provided by ACI 207.1R are fast and simple and yield an approximate evaluation. Other methods, including Schmidt and finite element, are also used to compute the temperature distribution, depending on the complexity of the analysis.

The Schmidt method is a step-by-step integration technique adaptable to spreadsheets. It is suitable for computing temperature gradients where one dimensional heat flow with simple boundary conditions is assumed. Analysis of more complex models requires use of finite element computations. In the following four sections, different calculation methods are presented.

A.4.1 Simple Maximum Temperature Method

This method is used to compute the peak and the final stable temperature in the mass concrete structure. The results obtained by using this method are approximate and predict a conservative peak temperature defined as the sum of the placing temperature, the adiabatic temperature rise of concrete mixture, and a correction of heat lost or gained due to ambient conditions.

A.4.2 Heat Dissipation Method

This method consists of using the heat loss charts provided by the ACI 207.1R, to compute the time needed for a structure to cool down from a peak temperature to a specific stable temperature. It is worthwhile mentioning that this method does not compute the peak temperature. It simply takes the peak temperature as an input and predicts the final stable temperature.

A.4.3 The Schmidt Method

This method is also provided by the ACI 207.1R and is one of the earliest incremental methods used to compute the temperature distribution in a structure. The Schmidt method can be adapted to computer spreadsheet computations to calculate the peak temperature of a structure.

A.4.4 Finite Element Method

The finite element method is a more recent method for computing temperatures in mass concrete. This method is described as a numerical technique for determining the distribution of temperature or stress in a structure. To use this method, a finite element model must be prepared.

In this method, the actual structure is mathematically replaced by finite number of elements connected to a finite number of nodes where behavior is governed by mathematical relationships. Computations are made for the model after applying the boundary conditions including the material thermal properties and ambient temperature.

The global stiffness matrix of the structure is obtained by combining the individual stiffness matrices of all the elements in the proper manner. If conditions of equilibrium are applied at every node of the idealized structure, a set of simultaneous equations can be formed and solved to give all nodal temperatures of the structure at different times.

ABAQUS, a finite element program, was used in this study to calculate the temperature variation as a function of time and size for CIDH concrete piles.

APPENDIX B – QUADREL IQDRUM CALORIMETERS

B.1 Q-Drum Description

Q-Drum calorimeters automatically measure the Adiabatic Heat Signature (i.e. the cumulative heat of hydration and its rate versus the maturity curing age).

Adiabatic calorimetry, shown in Figure B-1, is performed by computerized monitoring of a concrete sample's heat loss and temperature in a well insulated environment. Q-Drums measure the Heat Signature during a 1 to 7-day period. [16]

Figure B-1 – Q-Drum calorimeter

B.2 Q-Drum Capabilities and Specifications

Q-Drum calorimeters provide a unique non-destructive testing method. It provides a unique means for gathering accurate heat signature or heat of hydration data. For quality assuring materials or for new product development, Quadrel iQdrums can provide a way to quickly test different admixture and cement combinations to determine the expected performance of a concrete mix containing them. [16]

The Q-Drum specifications are shown in Figure B-1.

Table B-1 – Q-Drum Specifications

GENERAL	
Application	Concrete
Model	QiL 300-6X
Sample mold used	6in. x 12 in. Cylinder or 4 in. x 8 in.
Requires	Quadrel iService software application
Test repeatability	Within 1% to 3%
Dimensions	30.75 in. (Height) x 15 in. (Diameter)
OPERATION	
Sampling rate	15 minutes interval
Operating range	Ambient ± 10 °F (± 5 °C)

APPENDIX C - CALCULATION OF THE BODY HEAT FLUX

Given the density, the specific heat and the adiabatic temperature rise as function of time; the body heat flux can be calculated as follow:

1. Find the difference between adiabatic temperature rise between two time periods.

   For example in Table C-1:

   6.9 (at time 8 hours) = [10 (at time 8 hours)] – [3.1 (at time 4 hours)]

2. Calculating the heat of hydration between two time periods.

   Heat of Hydration = adiabatic temperature rise difference x unit mass x specific heat

   For example in Table C-1:

   266.95 (at time 8 hours) = [6.9 (at time 8 hours)] x [148.8 lb/ft^3] x [0.26 btu/lb/°F]

3. Calculating the time difference in hours between two periods.

   For example in Table C-1: the difference in time should be in seconds:

   4 (at time 8 hours) = [8 (at time 8 hours) – 4 (at time 4 hours)]

4. Calculating the body heat flux between two time periods.

   Body Heat Flux = Heat of Hydration / time difference

   For example in Table C-1:

   66.74 (at time 8 hours) = [266.95 (at time 8 hours)] / [4 (at time 8 hours)]

Example of body heat flux calculation for the 15% Fly Ash for series 1 is shown in Table C-1.

Table C-1 – Body Heat Flux for concrete containing 15% Fly Ash - series 1

Time, hours	Adiabatic Temperature Rise, °F	Difference of Adiabatic Temperature Rise, °F	Heat of Hydration, Btu/ft^3	Time Difference, hours	Body Heat Flux, Btu/ft^3/hr
0	0.0	0.0	0.00	0	0.00
4	3.1	3.1	119.93	4	29.98
8	10	6.9	266.95	4	66.74
12	21	11	425.57	4	106.39
16	32.8	11.8	456.52	4	114.13
20	41.1	8.3	321.11	4	80.28
24	46.3	5.2	201.18	4	50.29
28	49.6	3.3	127.67	4	31.92
32	52.1	2.5	96.72	4	24.18
36	54.5	2.4	92.85	4	23.21
40	56.7	2.2	85.11	4	21.28
44	58.7	2	77.38	4	19.34
48	60.5	1.8	69.64	4	17.41
52	62.1	1.6	61.90	4	15.48
56	63.6	1.5	58.03	4	14.51
60	65	1.4	54.16	4	13.54
64	66.2	1.2	46.43	4	11.61
68	67.4	1.2	46.43	4	11.61
72	68.5	1.1	42.56	4	10.64
76	69.5	1	38.69	4	9.67
80	70.5	1	38.69	4	9.67
84	71.3	0.8	30.95	4	7.74
88	72.2	0.9	34.82	4	8.70
92	73	0.8	30.95	4	7.74
96	73.7	0.7	27.08	4	6.77
100	74.4	0.7	27.08	4	6.77
104	75.1	0.7	27.08	4	6.77
108	75.7	0.6	23.21	4	5.80
112	76.4	0.7	27.08	4	6.77
116	77	0.6	23.21	4	5.80
120	77.6	0.6	23.21	4	5.80

Unit Mass = 148.8 lb/ft^3
Specific Heat = 0.26 btu/lb/^{o}F

REFERENCES

1. Lu, H.R., Swaddiwudhipong, S and Wee, T.H., "Evaluation of Thermal Crack by a probabilistic Model Using the Tensile Strain Capacity," Magazine of Concrete Research, Vol. 53, No.1, pp. 25-30, 2001.
2. U.S. Army Corps of Engineers Washington, DC, (USACE), "Engineering and Design - Gravity Dam Design," EM 1110-2-2200, chapter 6, 1995.
3. U.S. Army Corps of Engineers Washington, DC, (USACE), "Engineering and Design – Thermal Studies of Mass Concrete Structures," ETL 1110-2-542, Appendix A, 1997.
4. Abdol R. Chini and Arash Parham, "Adiabatic Temperature Rise of Mass Concrete in Florida," Florida Department of Transportation: Contract No. BD 29, February 2005.
5. American Concrete Institute Committee 207, Mass Concrete, ACI 207.2R-95, 2005.
6. American Concrete Institute Committee 207, Mass Concrete, ACI 207.1R-96, 2006.
7. ABAQUS, "ABAQUS Product Overview," http://www.hks.com/products/products_overview.html.
8. ABAQUS, "Analysis User's Manual," volume IV – Elements, version 6.6, chapter 22.

9. Schindler, A.K. and Folliard, K.J. “Influence of Supplementary Cementing on the Heat of hydration of Concrete,” Advances in Cement and Concrete IX Conference, August 2003.

10. Maggenti, R., “Mass Concrete Report - San Francisco-Oakland Bay Bridge East Spans Safety Project: Skyway Structure,” 04-Ala/SF-80-Var, E.A. 04-12021, January 2001.

11. American Concrete Institute Committee 207, Mass Concrete, ACI 207.1R-96, 2006.

12. Gajda John and VanGeem Martha, “Controlling temperatures in Mass Concrete,” Concrete International, pp. 59 – 62, January 2002.

13. Bentz, D..P., Waller, V. and De Larrard F., “Prediction of Adiabatic Temperature Rise in Conventional and High-Performance Concrete using a 3-D Microstructural Model,” Cement and Concrete research, Vol. 28, No.2, pp. 285 – 297, 1998.

14. Ballim Y., “A Numerical Model and Associated Calorimeter for Predicting temperature Profiles in Mass Concrete,” Cement and Concrete Composites, Vol. 26, pp. 695 – 703, 2004.

15. Swaddiwudhipong,S., Chen, D., and Zhang, M.H., “Simulation of the Exothermic Hydration Process of Portland Cement,” Advances in Cement Research, Vol. 14, No.2, pp. 61 - 69, April 2002.

16. Quadrel iService, Products, Quadrel iTesting trechnologies, http://www.quadreliservice.com/products_sc21.html.